

# Nuclear Fragmentation Measurements for Particle Therapy and Beyond

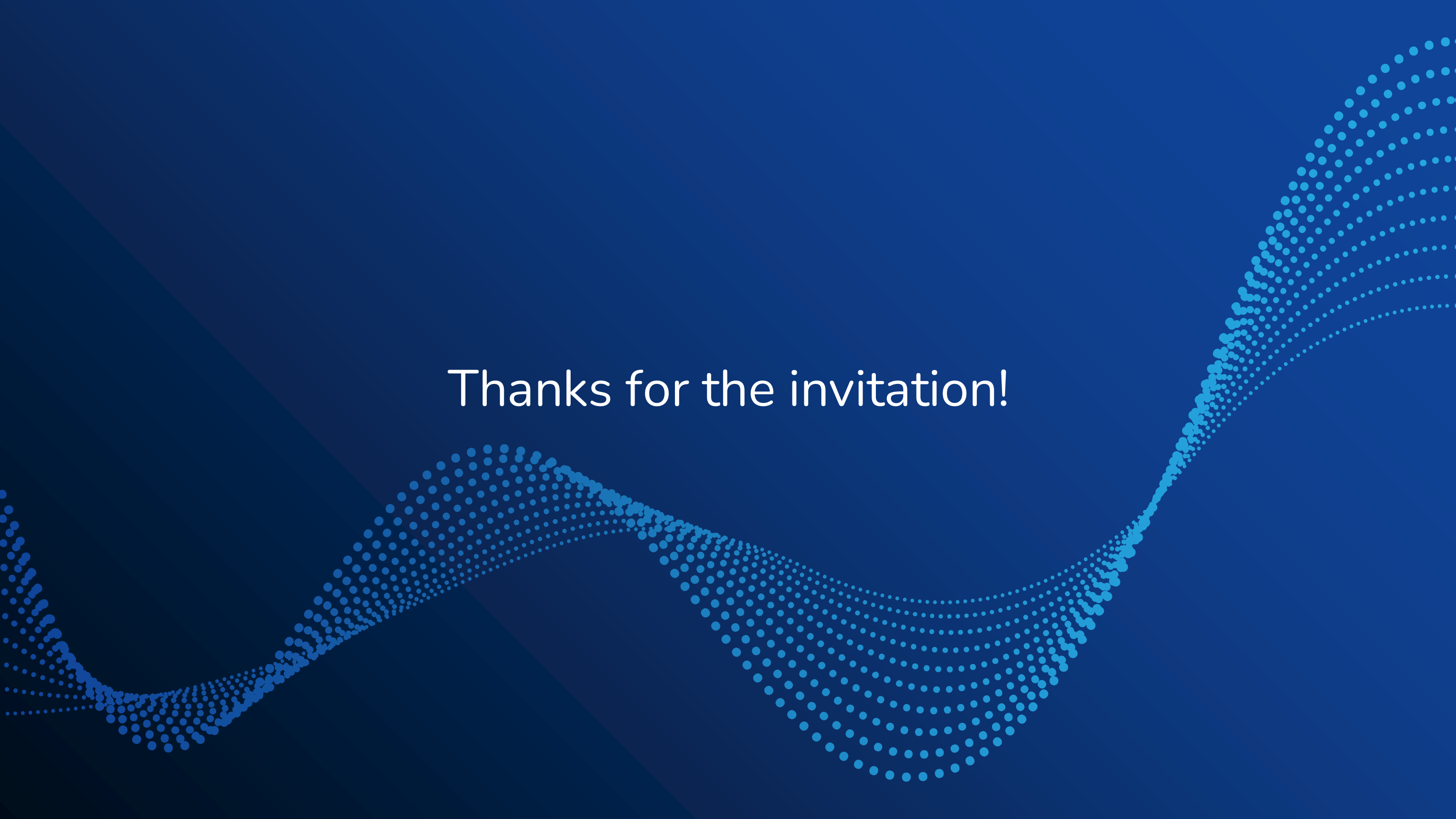
Aafke Kraan

National Institute for Nuclear Physics (INFN), Pisa, Italy

Warsaw, 19 march 2026



Thanks for the invitation!

The background is a solid dark blue color. A decorative element consists of multiple parallel, wavy lines of small, light blue dots that flow from the bottom left towards the top right. Additionally, a diagonal stripe of a slightly darker blue shade runs from the top left towards the bottom right, crossing the wavy dot pattern.

# Introduction

Physics motivation



# The FOOT experiment

Battistoni et al, Measuring the Impact of Nuclear Interaction in Particle Therapy and in Radio Protection in Space: the FOOT Experiment, Front. Phys., 08 February 2021, Sec. Radiation Detectors and Imaging

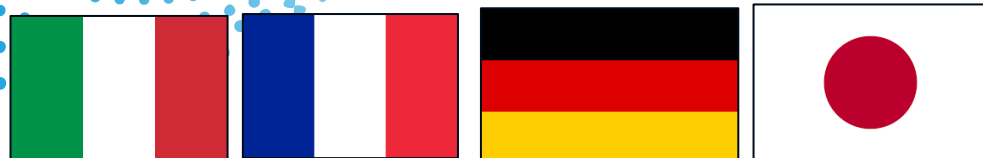


**FOOT**=FragmentatiOn Of Target

**FOOT is an applied nuclear physics experiment** that aims at measuring the double differential fragmentation cross-section for ions at energies and materials of interest for hadron therapy and radioprotection in space

- Italy:
  - 10 INFN sections/labs
  - CNAO (Centro Nazionale di Adroterapia Oncologica)
- Germany: GSI
- France: IPHC Strasbourg
- Japan: Nagoya University
- Collaborating since recently with India
- ~95 researchers

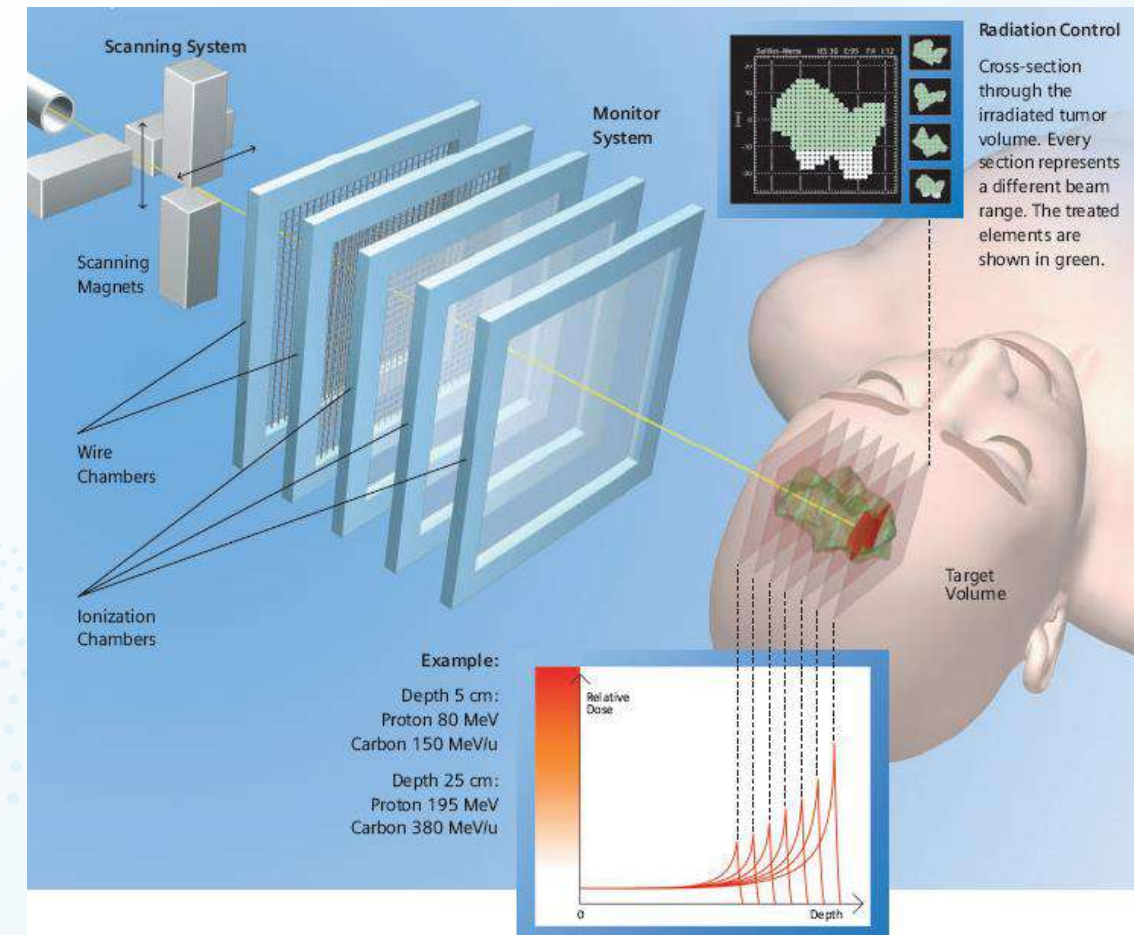
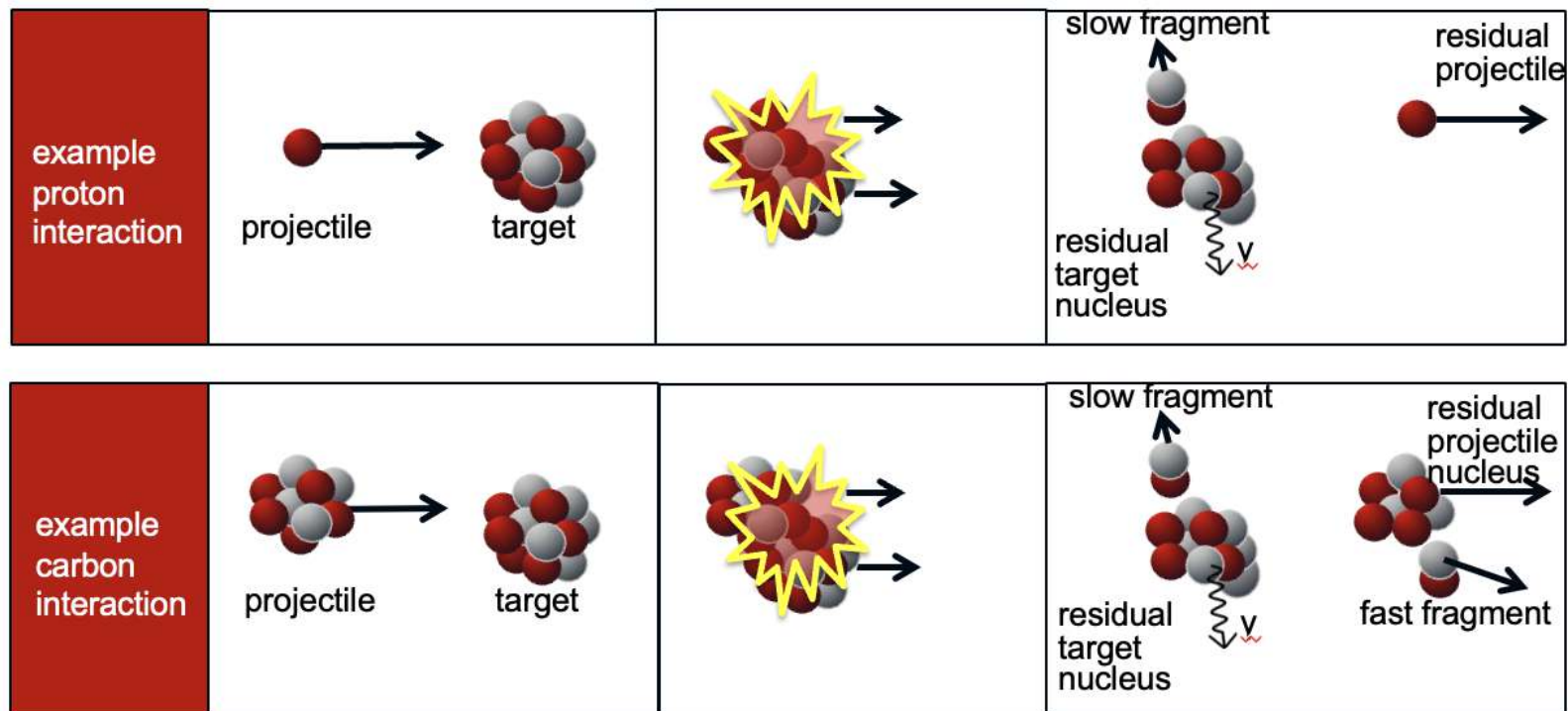
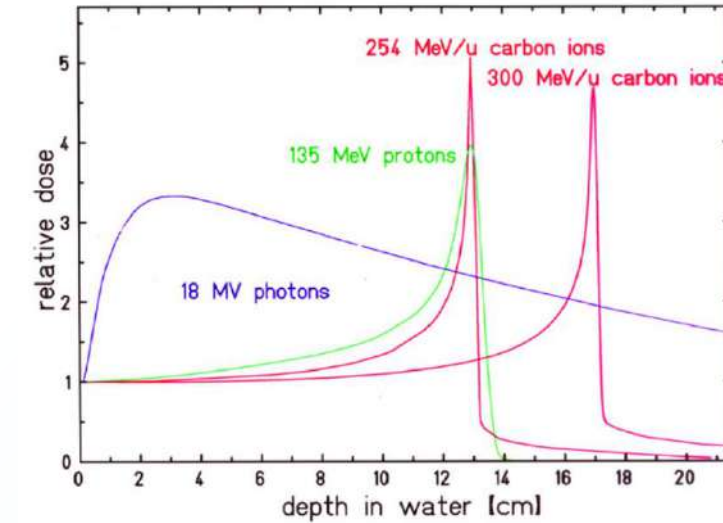
**Construction almost completed**



# Motivation: particle therapy

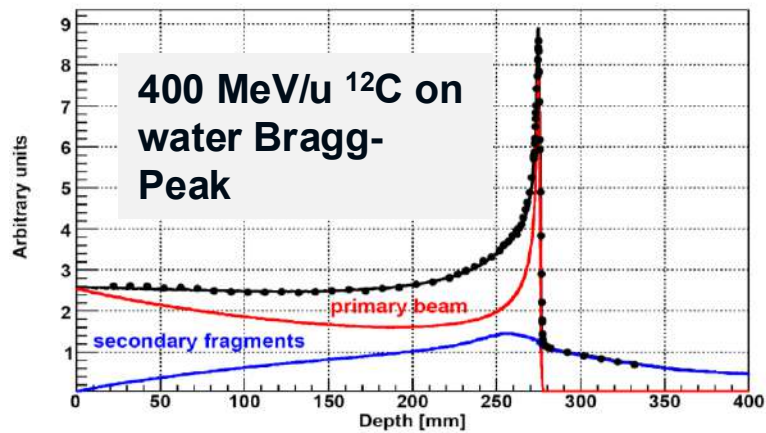


- Particle therapy: radiotherapy with charged particles: protons, carbon, but being explored is also helium, oxygen
  - Energy range 50-250 MeV (p), 100- 450 MeV/u (carbon)
- Depth-dose profile distributions of protons and carbon ions are characterized by a small entrance dose and a distinct narrow peak dose (**Bragg peak**) → precise dose
- The fragmentation of the tissue (and projectile in case of carbon ions) leads to production of secondaries.



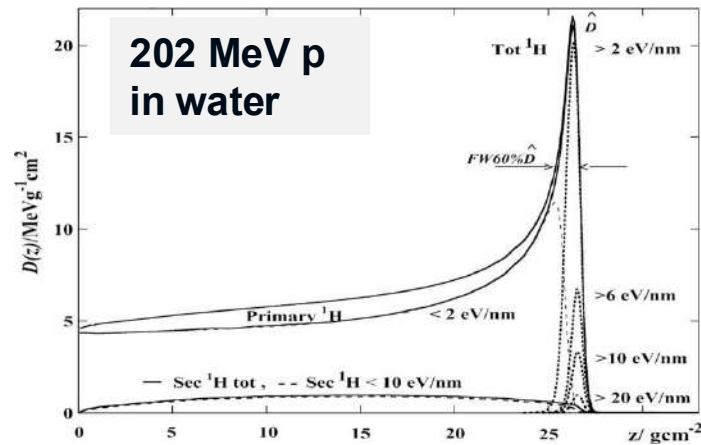
# Motivation: particle therapy

**Carbon** therapy: ~40% of absorbed (physics) dose in entrance channel is due to secondary fragments! Bohlen, et al, Phys Med Biol. (2010). 55:5833–47.



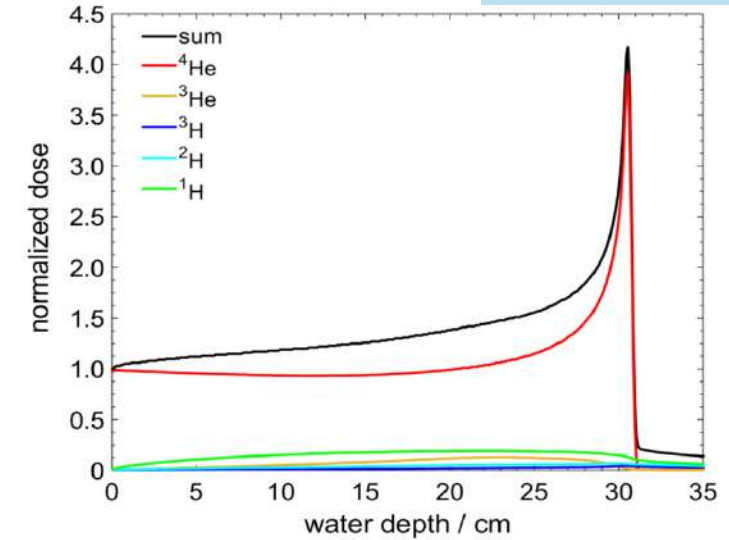
**Proton** therapy: ~10%

J. Kempe et al, Med. Phys. 34, 1 2007



**Helium** therapy: ~20%

F.Horst, MCMA2017



- Secondaries have high Linear Energy Transfer (LET) and a high Relative Biological Effectiveness (RBE)
- Thus, **physics dose and RBE-weighted (biological) dose are much different!**
- To better predict **biological dose**, need to know types (Z,A), angles, energies and amounts of secondaries → cross sections needed, particularly (double) differential (E,Ω)
- Experimental cross section measurements in  $10^2$  MeV range are sometimes in disagreement, old, or have large errors... especially at large angles! (see slides 13-14)

**More cross section measurements are needed!**

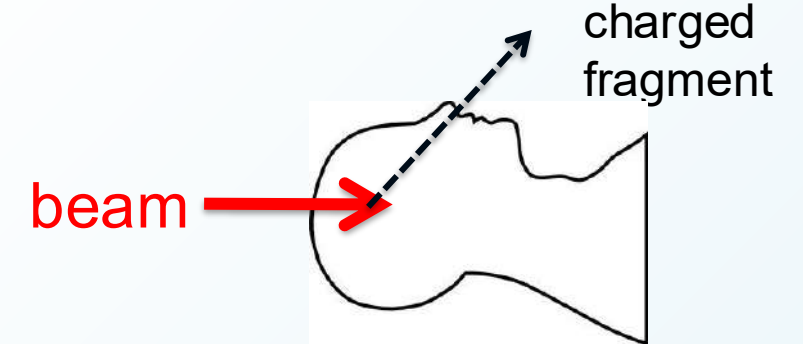
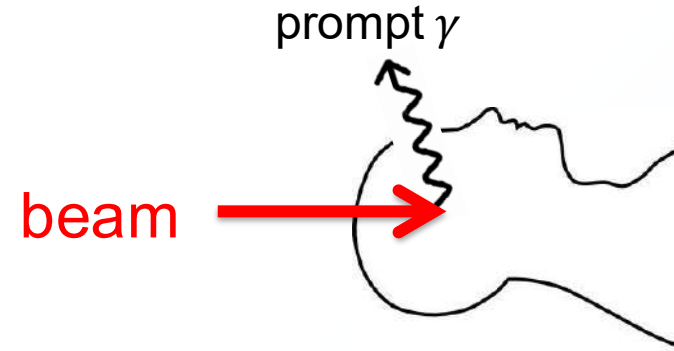
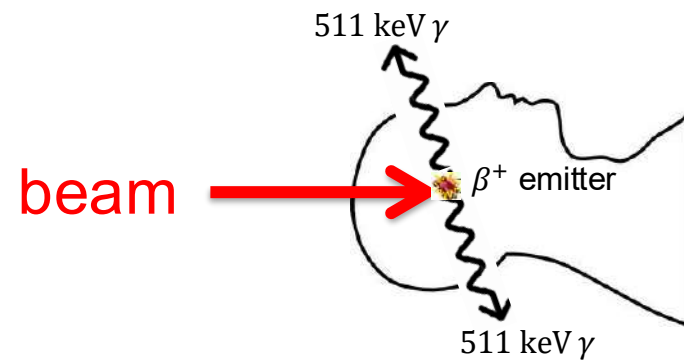
**Recent progress for He:**

Horst F, et al.. Phys Rev C. (2019). 99:014603.

See also "Experimental data of nuclear fragmentation for validating Monte Carlo codes: Present availability and lacks", G. Battistoni, S. Muraro, A. C. Kraan, in: Monte Carlo in Heavy Charged Particle Therapy, Edition1, 2024

# Motivation: particle therapy range monitoring

New cross section measurements could also be extremely useful for **range monitoring**



- Still many uncertainties, particularly regarding charged fragment production
- Some charged fragment measurements for range monitoring done, but only a few angles and energies
- **MC models unreliable at large angles, missing data...**
- New cross section measurements very useful!
- See for instance:

K. Gwosch et. al, Phys. Med. Biol. 58 (2013) 3755–3773

Agodi C, et al flux. Phys. Med. Biol. 57 (2012)5667.

A. Rucinski . Med. Biol.63(2018) 055018.

From: Muraro, Battistoni, Kraan, Front. Phys, 2020 Sec. Medical Physics and Imaging, volume 8 - 2020

TABLE 3 | Summary of measurements in the context of range monitoring studies.

Incident beam	Energy [MeV/u]	Target	Technique	Measurement	Refs.
P	160	PMMA	Prompt $\gamma$	Energy spectra and yields at 90°	Smeets et al. [143]
P	230	Water	Prompt $\gamma$	Energy spectra and yields at 90°	Verburg et al. [151, 152]
P	48	4 samples with varying amount of O, C, H	Prompt $\gamma$	Energy spectra and yields at 90°	Poif et al. [153]
$^{12}\text{C}$	73, 95, and 305	PMMA and water	Prompt $\gamma$	Time-of-flight and energy spectra at 90°	Testa et al. [154–156]
$^{12}\text{C}$	220	Polymethyl methacrylate	Prompt $\gamma$	Energy spectra and yields at 90°	Vanstalle et al. [157]
$^{12}\text{C}$	95 and 310	PMMA and water	Prompt $\gamma$	Energy spectra and yields at 90°	Pinto et al. [144]
$^{12}\text{C}$	80	PMMA	Prompt $\gamma$	Energy spectra and yields at 90°	Agodi et al. [158]
$^4\text{He}$ , $^{12}\text{C}$ , $^{16}\text{O}$	100 to 300	PMMA	Prompt $\gamma$	Yields at 60°, 90°, and 120°	Mattei et al. [159]
$^{12}\text{C}$	80	PMMA	Fast charged hadrons	Proton yields at 60° and 90°	Agodi et al. [160]
$^{12}\text{C}$	220	PMMA	Fast charged hadrons	Fragments with Z = 1 at 90°	Piersanti et al. [76], Mattei et al. [161]
$^4\text{He}$ , $^{12}\text{C}$	120–220	PMMA	Fast charged hadrons	Secondary protons at 90°	Rucinski et al. [162]
$^{16}\text{O}$	–	PMMA	Fast charged hadrons	Yields of fragments with Z = 1 as function of energy and production position at 60° and 90°	Rucinski et al. [163]
$^{12}\text{C}$	400	Composite target	Fast charged hadrons	Secondary fragments for angles 34° to 81°	Alexandrov et al. [164, 165]
p, $^{12}\text{C}$	40–220(p), 65–430(C)	Graphite and beryllium oxide	$\beta^+$	Cross section measurements of $^{10}\text{C}$ , $^{11}\text{C}$ , and $^{15}\text{O}$	Horst et al. [136]
p, $^{12}\text{C}$	110, 140, 175 (p), 212, 260, and 343 (C)	PMMA	$\beta^+$	Absolute activity distributions and total production cross sections of $^{10}\text{C}$ , $^{11}\text{C}$ , and $^{15}\text{O}$	Pshenichnov et al. [166]
P	55	Water, carbon, phosphorus, nd calcium	$\beta^+$	Number of short lived $\beta^+$ emitters	Dendooven et al. [139]
P	10 to 70	Polyethylene and water	$\beta^+$	Cross sections of 4 specific reaction channels for production of $^{11}\text{C}$ , $^{15}\text{O}$ , $^{13}\text{N}$	Akagi et al. [167]
P	10 to 70	Polyethylene	$\beta^+$	Cross sections of specific reaction channels for production of $^{11}\text{C}$ and $^{10}\text{C}$	Matsushita et al. [133]

# Motivation: radioprotection in space...

## The 5 Hazards of Human Spaceflight

1

### Space Radiation

Invisible to the human eye, radiation increases cancer risk, damages the central nervous system, and can alter cognitive function, reduce motor function, and prompt behavioral changes.

2

### Isolation and Confinement

Sleep loss, circadian desynchronization, and work overload may lead to performance reductions, adverse health outcomes, and compromised mission objectives.

3

### Distance from Earth

Planning and self-sufficiency are essential keys to a successful mission. Communication delays, the possibility of equipment failures and medical emergencies are some situations the astronauts must be capable of confronting.

4

### Gravity (or lack thereof)

Astronauts encounter a variance of gravity during missions. On Mars, astronauts would need to live and work in three-eighths of Earth's gravitational pull for up to two years.

5

### Hostile/Closed Environments

The ecosystem inside a vehicle plays a big role in everyday astronaut life. Important habitability factors include temperature, pressure, lighting, noise, and quantity of space. It's essential that astronauts stay healthy and happy in such an environment.



# Motivation: radioprotection in space...

See Presentation by Norbury et al, Nuclear data needs for protection from space radiation, FOOT-MAECI-MOFFITS meeting, May 2025

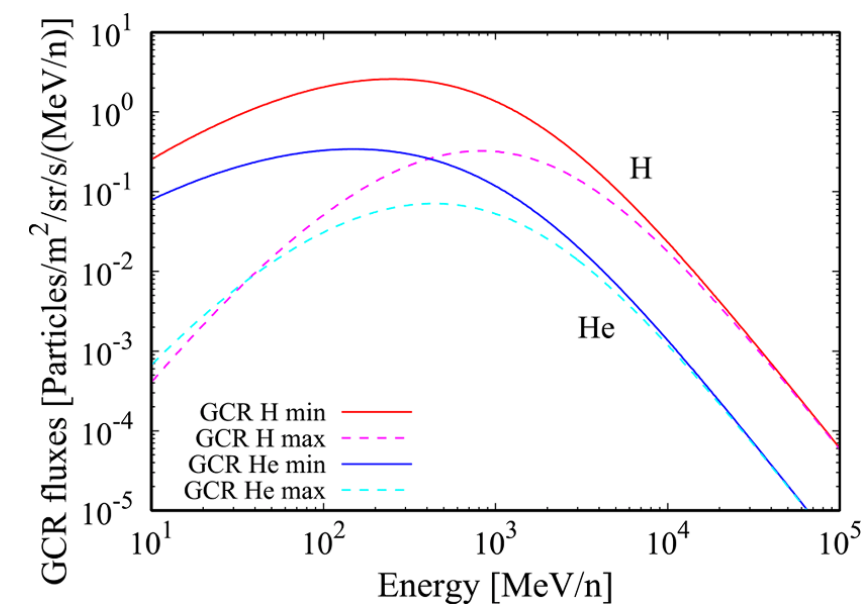
## Galactic Cosmic Rays (GCR)



Crab Nebula

Image courtesy of NASA

- Highly penetrating, complex mixed field including protons and heavier nuclei
- Protons (85%), He ions (12%)
- High charge and energy (HZE) ions (1%) (lower flux but biologically significant)
- Energies from MeV to tens of TeV/n
- Chronic low-dose rate exposure that varies with solar cycle
- **Difficult to shield** due to energy and complexity of field
- Biophysical properties of HZE particles differ vastly from terrestrial radiation with adverse biological affects contributing to health risks
- From supernova shock waves



Masayuki et al,  
Journal of  
radiological  
protection. 40. 947-  
961. 10.1088/1361-  
6498/abb120.

# Motivation: radioprotection in space...

## Geomagnetically trapped radiation

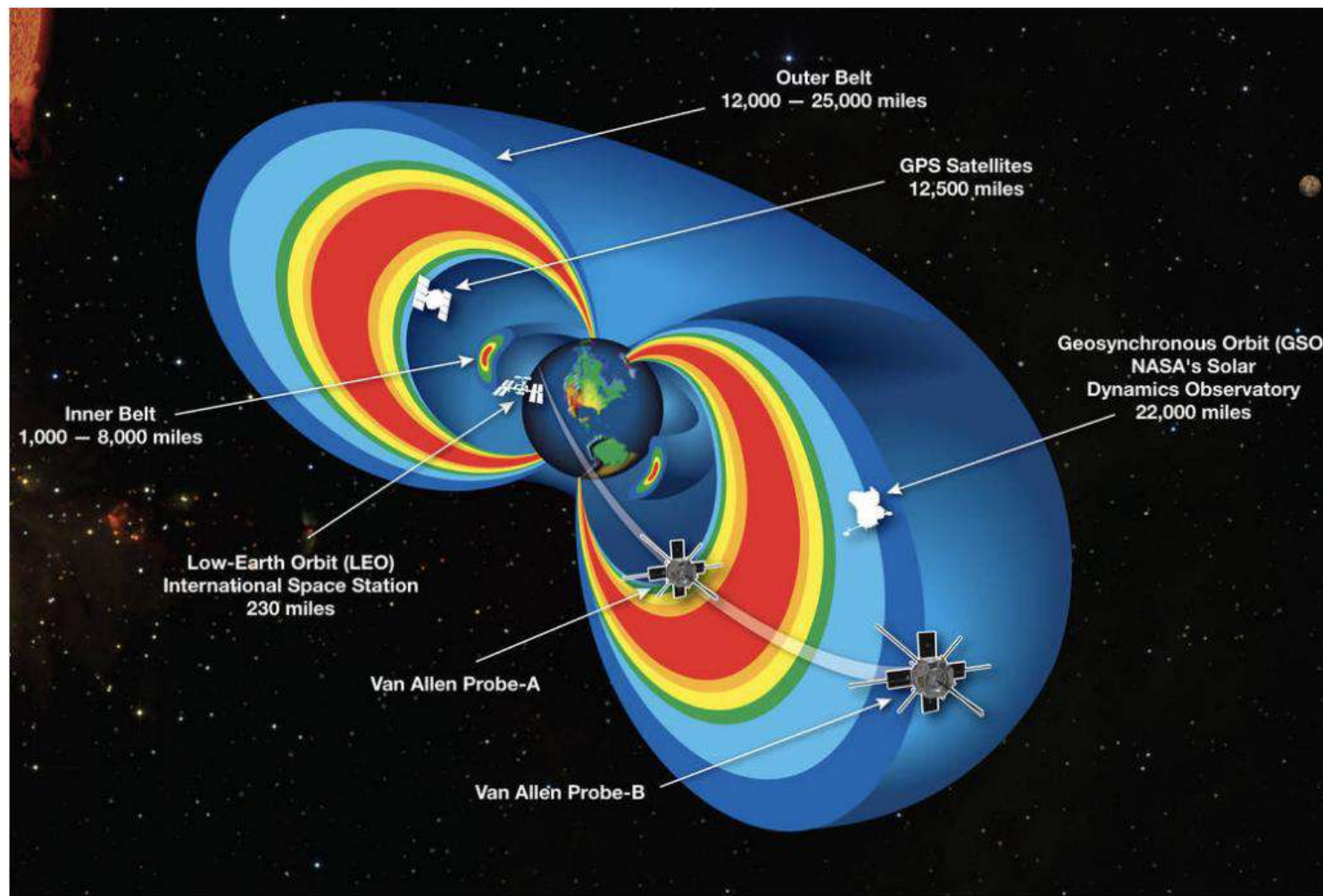


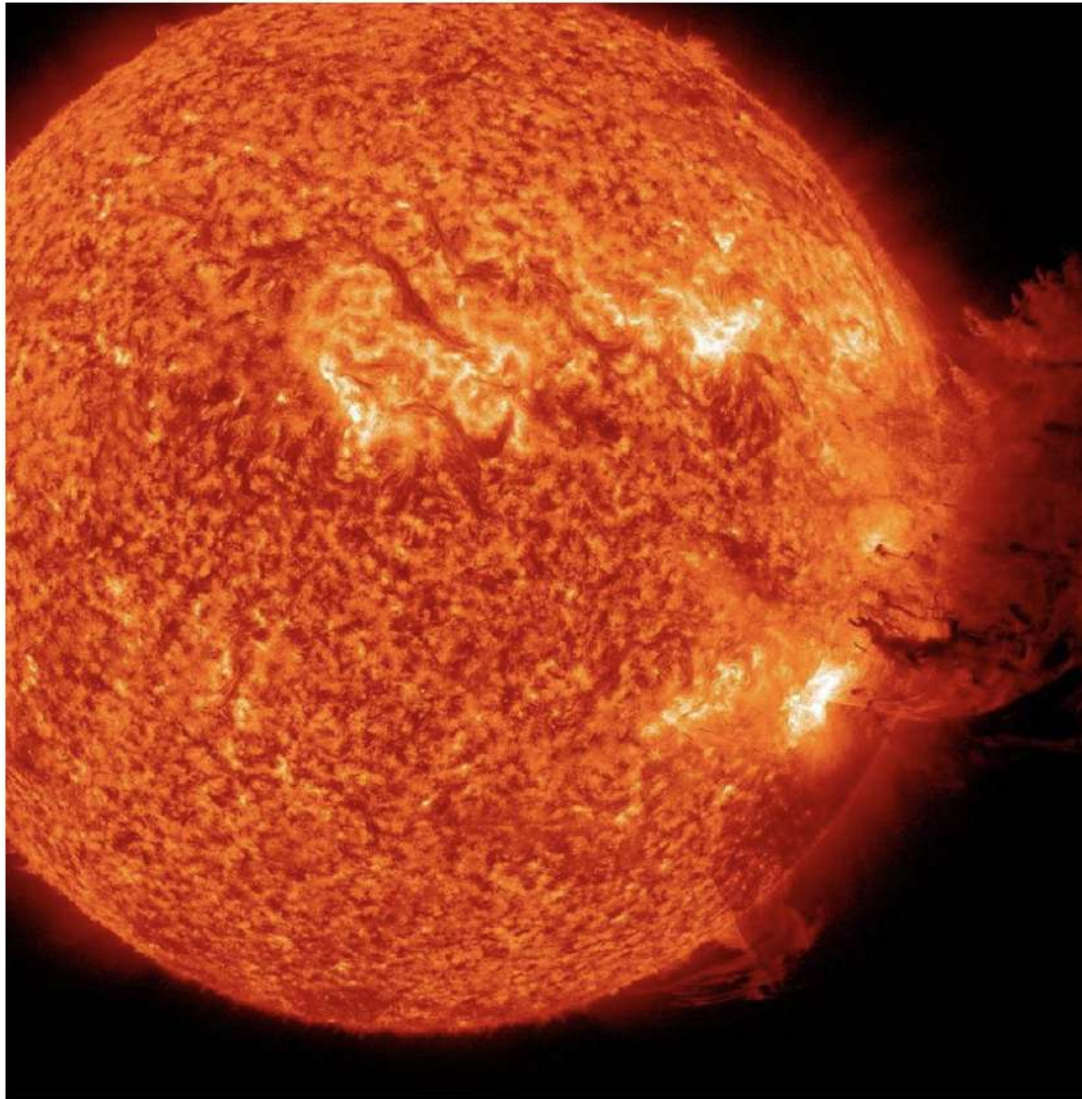
Image courtesy of NASA

- Low energy protons (< 250 MeV) and electrons (< 7 MeV)
- Inner Belt: mostly protons and electrons
- Outer belts: composed of electrons
- Continuous exposure at altitude up to 40,000 km
- **Can be shielded;** mainly relevant to ISS

See Presentation by Norbury et al, Nuclear data needs for protection from space radiation, FOOT-MAECI-MOFFITS meeting, May 2025

# Motivation: radioprotection in space...

## Solar Particle Events (SPE)



7 June 2011

Image courtesy of NASA

- Medium (keV to 100s MeV) to high energy protons ( $< 1$  GeV) from coronal mass ejection
- Intermittent exposure with peak activity during solar max so kind of predictable
- **Can be effectively shielded** to prevent severe acute radiation syndrome
- Storm shelters minimize exposure risk

See Presentation by Norbury et al, Nuclear data needs for protection from space radiation, FOOT-MAECI-MOFFITS meeting, May 2025

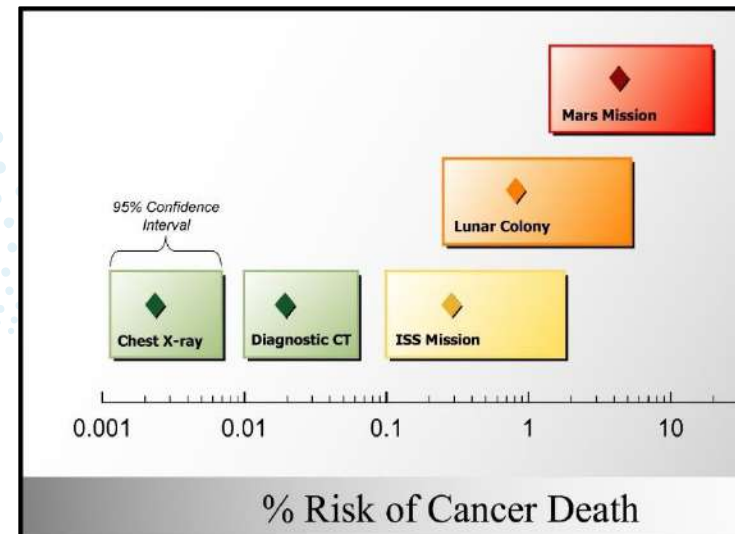
# Motivation: radioprotection in space...

- Radiation in space is one of the obstacles for space exploration

Source	Nuclei	Energy
Galactic cosmic rays	mostly p	MeV-TeV
Solar particles	p, $\alpha$	MeV-GeV
Magnetically trapped particles	p	< 100 MeV

- Dose equivalent in space is high

Where	dose equivalent
On earth	$\sim 7 \mu\text{Sv/day}$
Chest x-ray	$- 0.1 \text{ mSv}$
Brain CT	$\sim 1.6 \text{ mSv}$
Space	$0.5-2 \text{ mS/day}$
Mars	$0.64 \text{ mSv/day}$



For optimal shielding and accurate (physics and biology) modeling of interactions with human tissue, need MC predictions! Especially differential and double differential cross section measurements needed!

- Mainly light ions (p, He) with higher energies than particle therapy

# Particle therapy and radiation protection have common needs!

## Common needs:

- Uncertainty quantification
- Cross section measurements overlap
  - Similar types (double-differential)
  - Similar projectiles (H, He, C, O)
  - Similar projectile energies
  - Similar targets
  - Similar fragments (light ions)
- Nuclear model improvements
- Transport code improvements with improved nuclear models

## But also differences

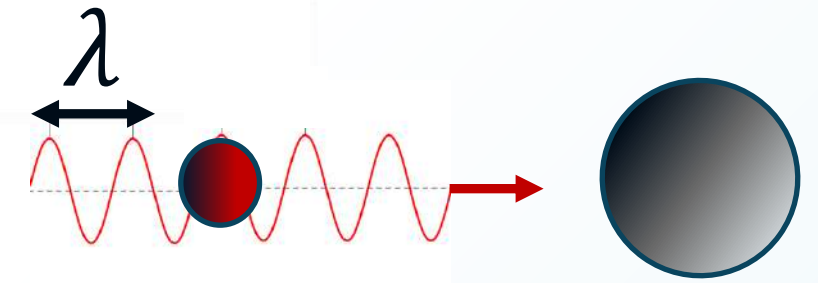
	Ion Therapy	Space Radiation
Energy	10s - 100s MeV/n	10s MeV/n – 50 GeV/n
Projectiles	H, He, C, O	H – Ni
Targets - human body	H, C, O, N, Ca, P, S, K, Na, Cl, Mg	H, C, O, N, Ca, P, S, K, Na, Cl, Mg
Targets - materials		C, Al, Cu, Ti

See Presentation by Norbury et al, Nuclear data needs for protection from space radiation, FOOT-MAECI-MOFFITS meeting, May 2025

- FOOT program: cross sections up to ~800 MeV/u
- So far: measurements up to 400 MeV/u



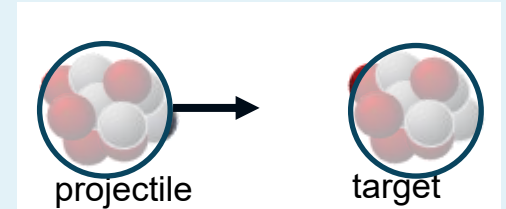
# How about Monte Carlo model predictions?



## Low energies

The semi-classical approximation : at kinetic energies below  $\sim 10$  MeV/A

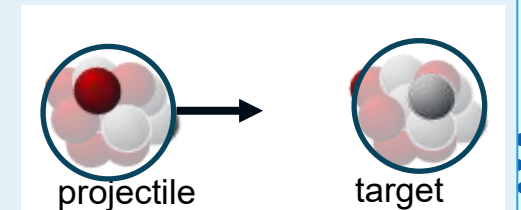
- $\lambda = h/p$  of incident particle is higher than the nuclear size  $\rightarrow$  nucleons are bound, entire nucleus acts as a single unit, and the interaction is between nuclei (scattering, fusion)



## High energies

The single particle approach: at energies well above 1000 MeV/A:

- $\lambda = h/p$  of incident particle is smaller than the nuclear size and much smaller than the mean free path  $\lambda_N$  inside the nucleus  $\rightarrow$  nucleons in the colliding nucleus are like single (nearly free) particles in vacuum, no nuclear structure
- Perturbative region (if high  $p$  transfer), At very large energies: Quark Gluon Plasma



## Intermediate energies

Particle therapy and space radioprotection regime: from  $\sim 10$  to 1000 MeV/A

- No full first principle calculations possible, no perturbative approximations
- Several models exist with different agreement with data: phenomenological models, like Quantum Molecular Dynamic and intranuclear cascade approaches.
- **Essential ingredient to benchmark and validate models for particle therapy and radioprotection in space: cross sections!**

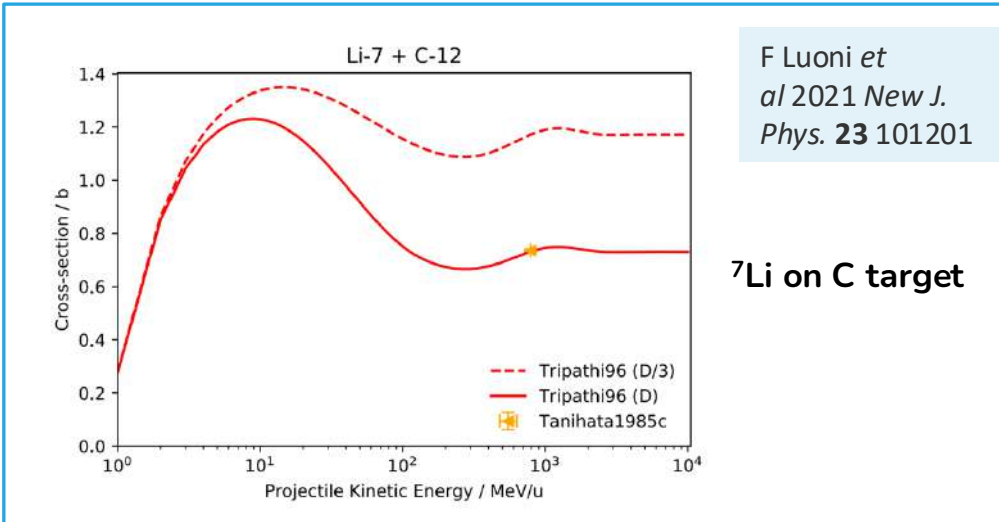


# Experimental data of nuclear fragmentation

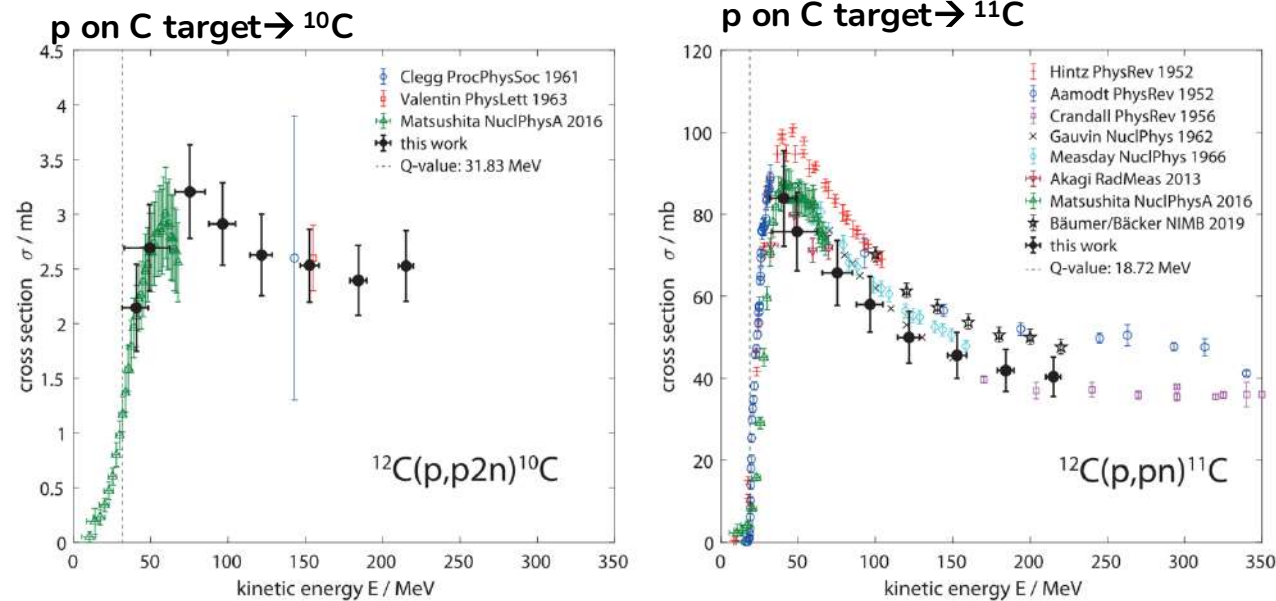
Available data are not yet fully satisfactory

- Some measurements are quite old
- Some data disagree with each other
- Some data are lacking

But recently **new data** are coming!

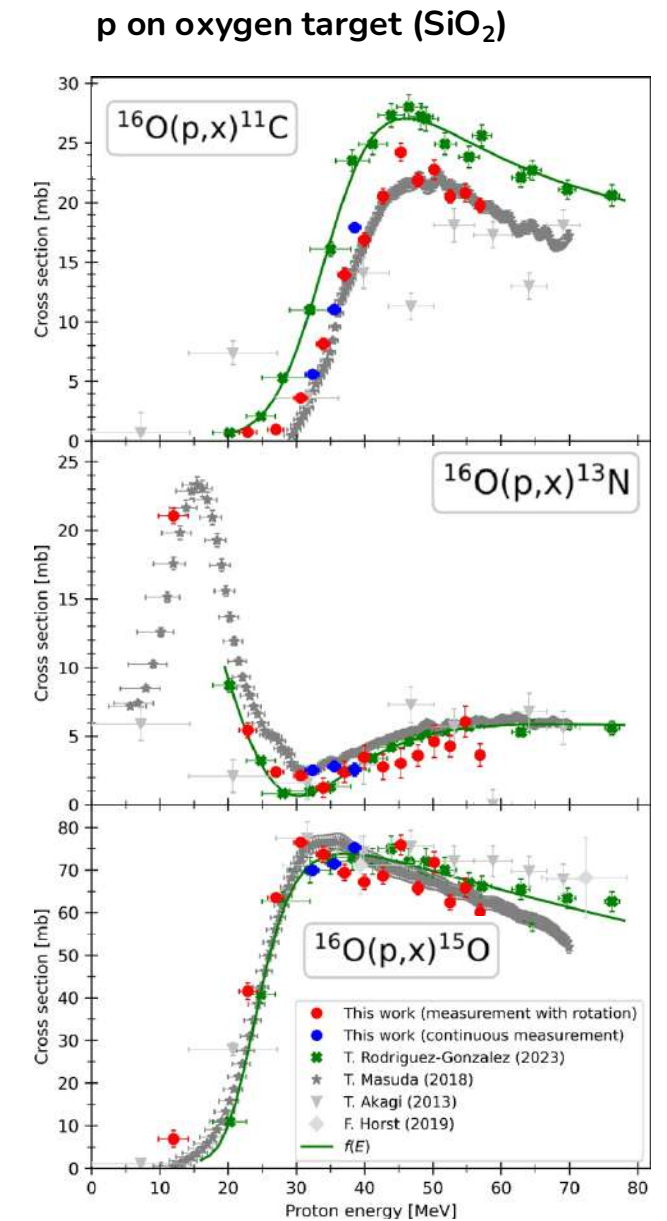
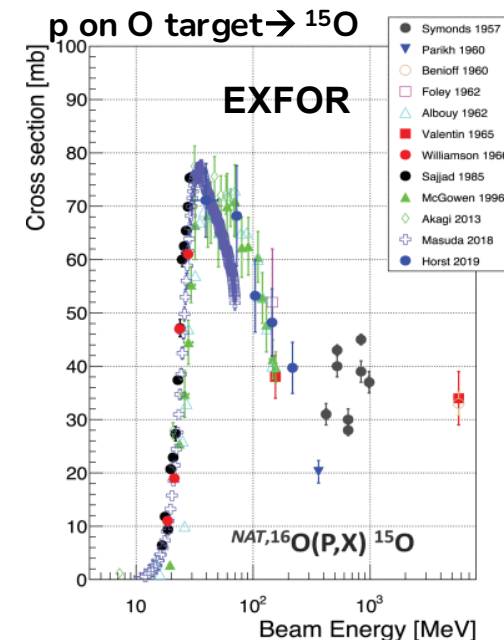


From: F. Horst *et al*, *Phys. Med. Biol.* **64** (2019) 205012 (16pp)



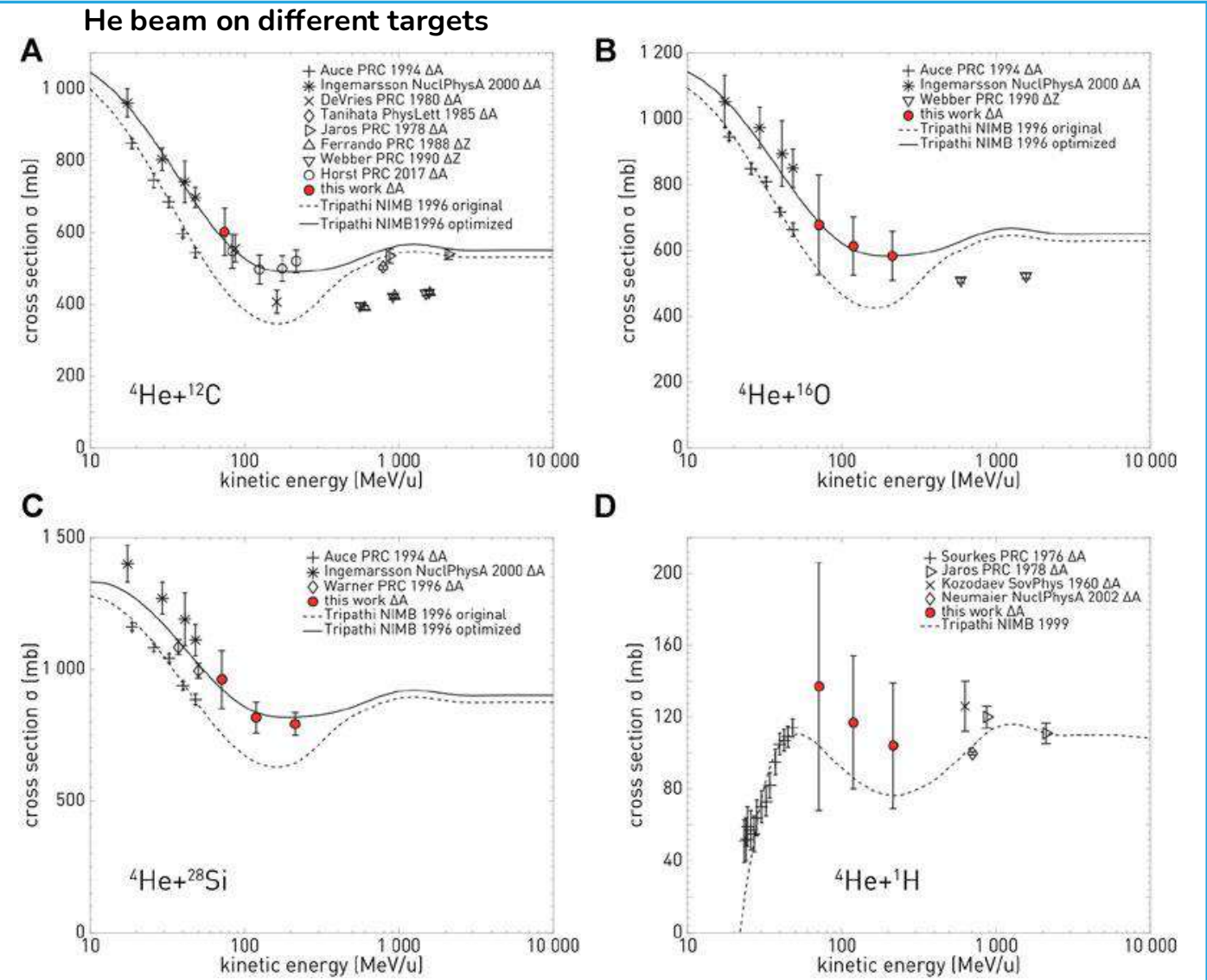
Cross sections for the production of <sup>10</sup>C and <sup>11</sup>C target fragments by protons on carbon targets as a function of energy,

A. C. Kraan and A. Del Guerra, "Technological Developments and Future Perspectives in Particle Therapy: A Topical Review," in *IEEE-TRPMS*, vol. 8, no. 5, pp. 453-481, 2024



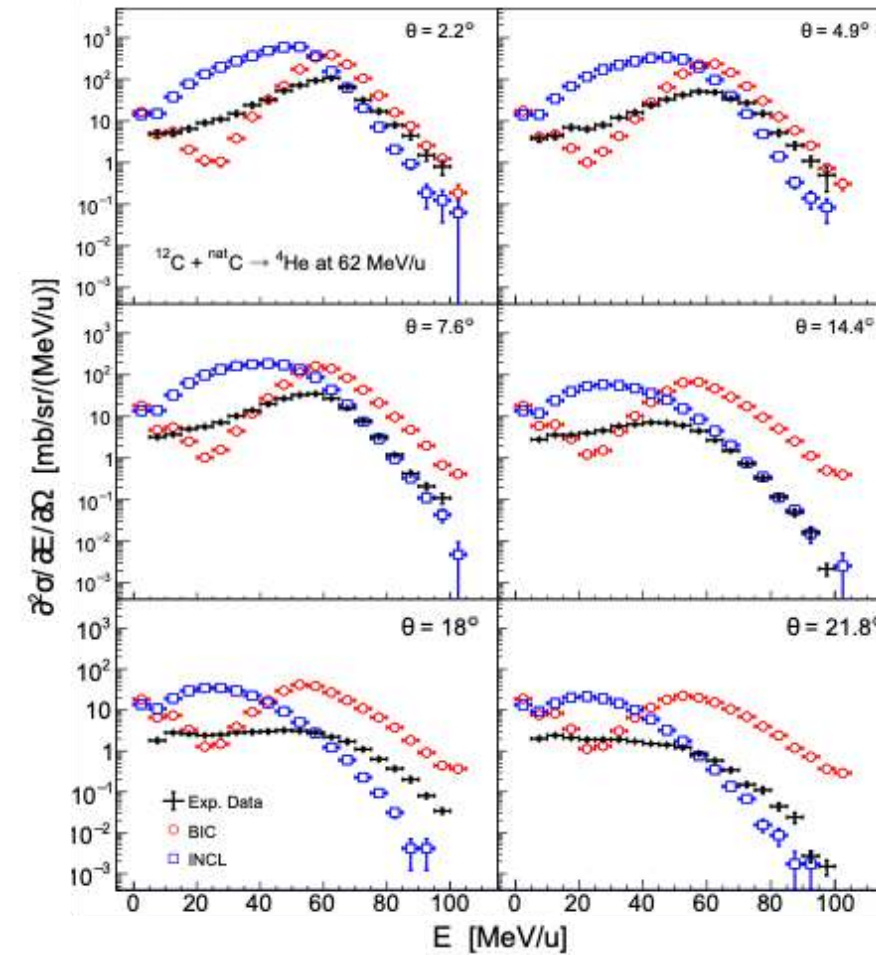
Matulewicz, J., Skwira-Chalot, I., Kusy, S. *et al*. Measurement of cross section of proton-induced reactions on oxygen with silicon dioxide target. *Eur. Phys. J. A* **60**, 203 (2024).

# Experimental data of nuclear fragmentation



Horst F, et al. Measurements of He charge and mass changing cross sections on H, C, O, and Si targets in the energy range 70-220 MeV/u for radiation transport calculations in ion-beam therapy. *Phys Rev C*. (2019). 99:014603. doi:10.1103/PhysRevC.99.014603

P. Arce et al (Geant coll), Medical Physics, 48(1):19, 2021.



Double-differential cross sections at different angles of  $\alpha$ -particle production interaction of 62 MeV/u  ${}^{12}\text{C}$  beam with a thin C target, as a function of the  $\alpha$ -particle kinetic energy. Experimental data from De Napoli et al

See also N. Sakhno et al, ACTA PHYSICA POLONICA A No. 5 Vol. 146 (2024).

protons on different targets

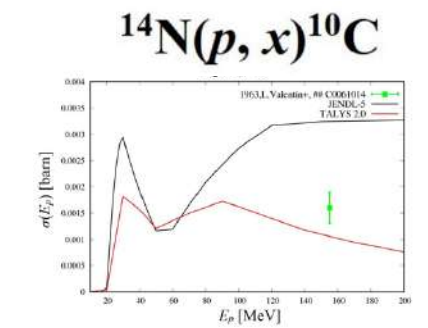


Fig. 4. Calculation results for the  ${}^{14}\text{N}(p, x){}^{10}\text{C}$  nuclear reaction.

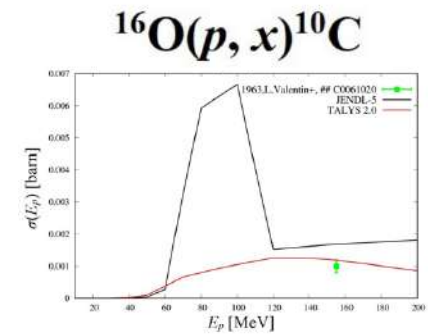
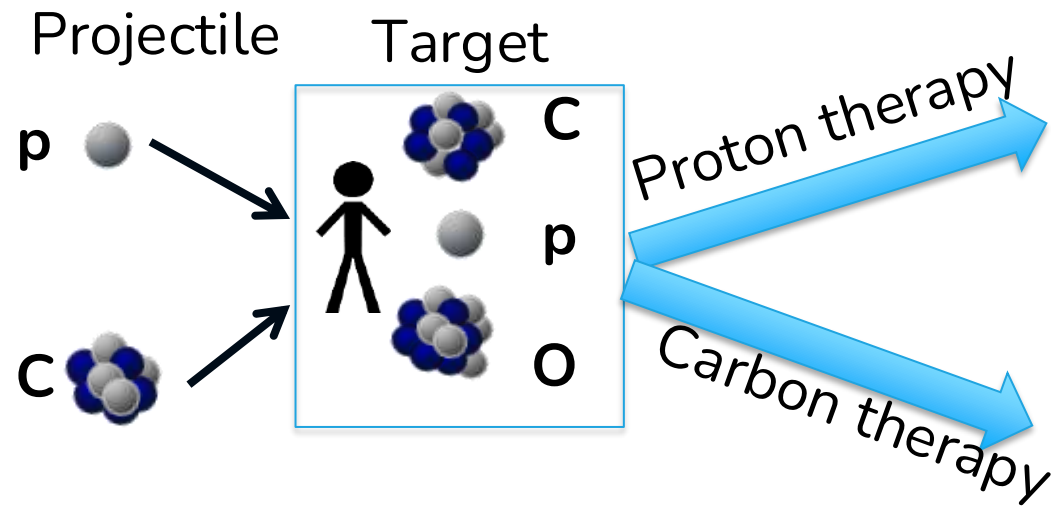


Fig. 5. Calculation results for the  ${}^{16}\text{O}(p, x){}^{10}\text{C}$  nuclear reaction.

**More cross section measurements are needed for validating MC codes!**

# Target and projectile fragmentation

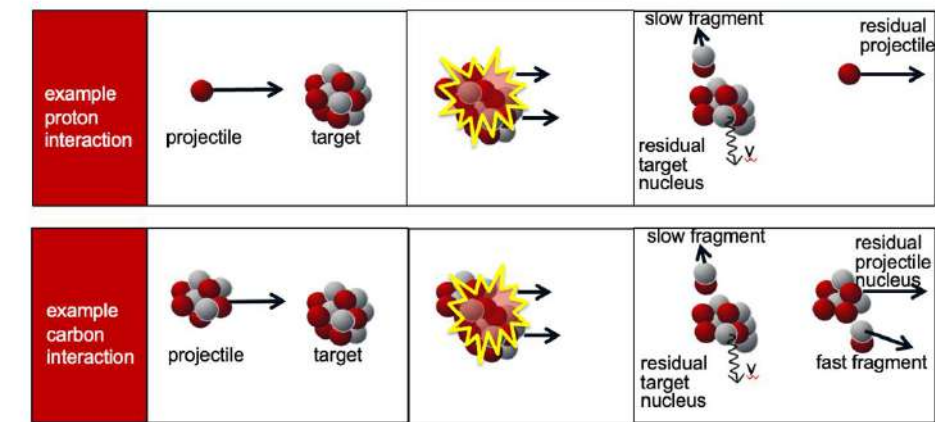
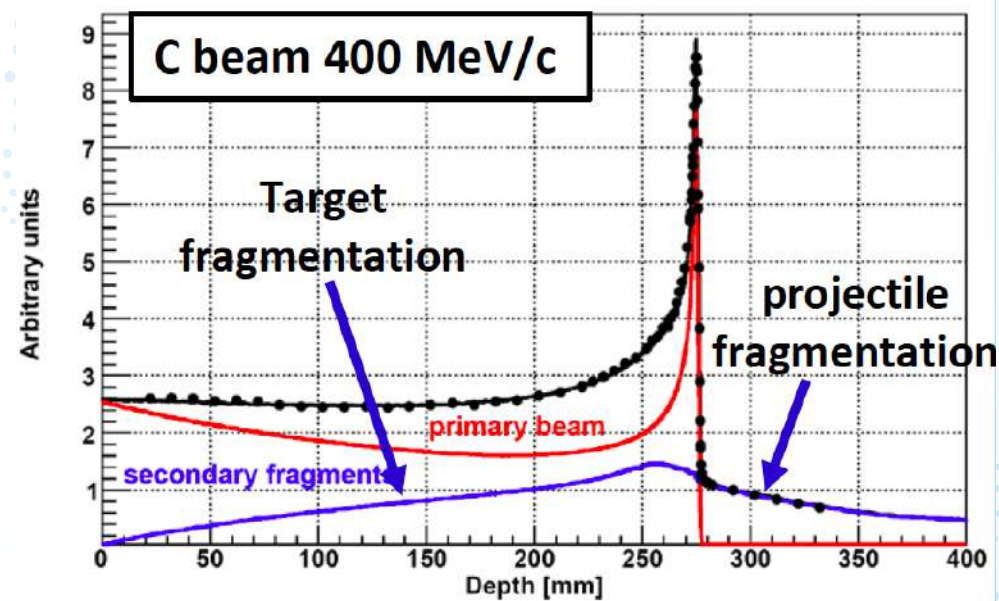


Who fragments? Range

$p+p \rightarrow$  no  
 $p+C,O \rightarrow$  target Short ( $\mu\text{m}$ )

$C+p \rightarrow$  projectile Long ( $>$  few cm)  
 $C+C,O \rightarrow$  both Both

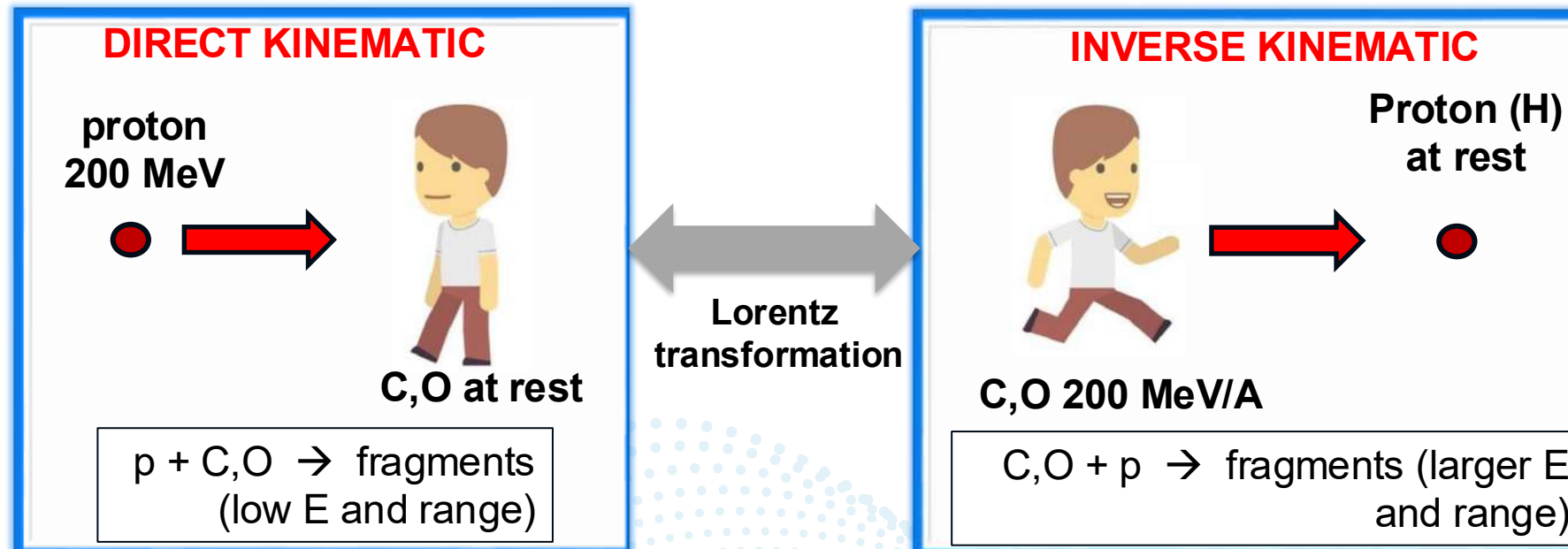
- Long range fragments can be measured directly
- But how to measure short range fragments?
  - Difficult to directly detect them, would need very thin target
  - Such a very thin target produces very few events (+background).
  - Other techniques: difficult/expensive



# FOOT strategy: inverse kinematics

**Problem with target fragmentation:**

target can be as thick as a few mm  $\gg$  range of fragments, which is of order  $\sim$  few  $\mu\text{m}$ )

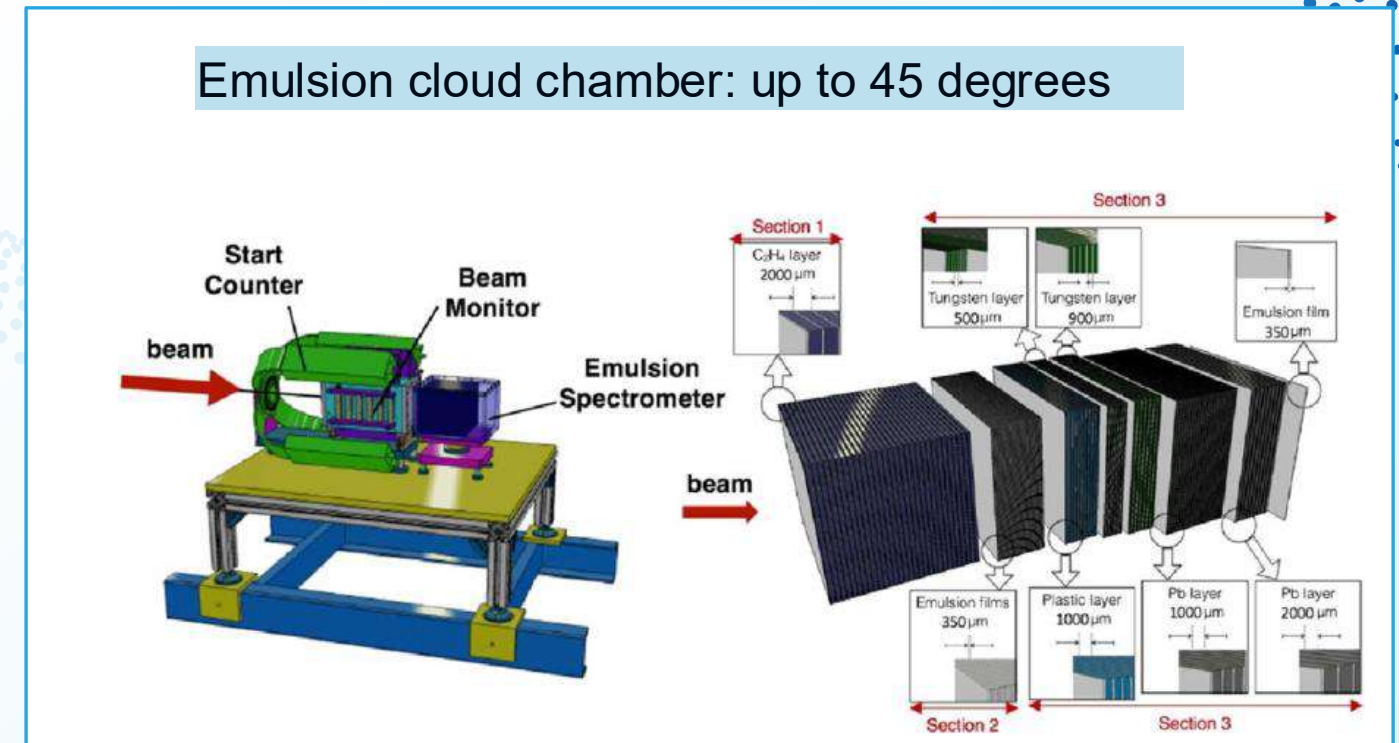
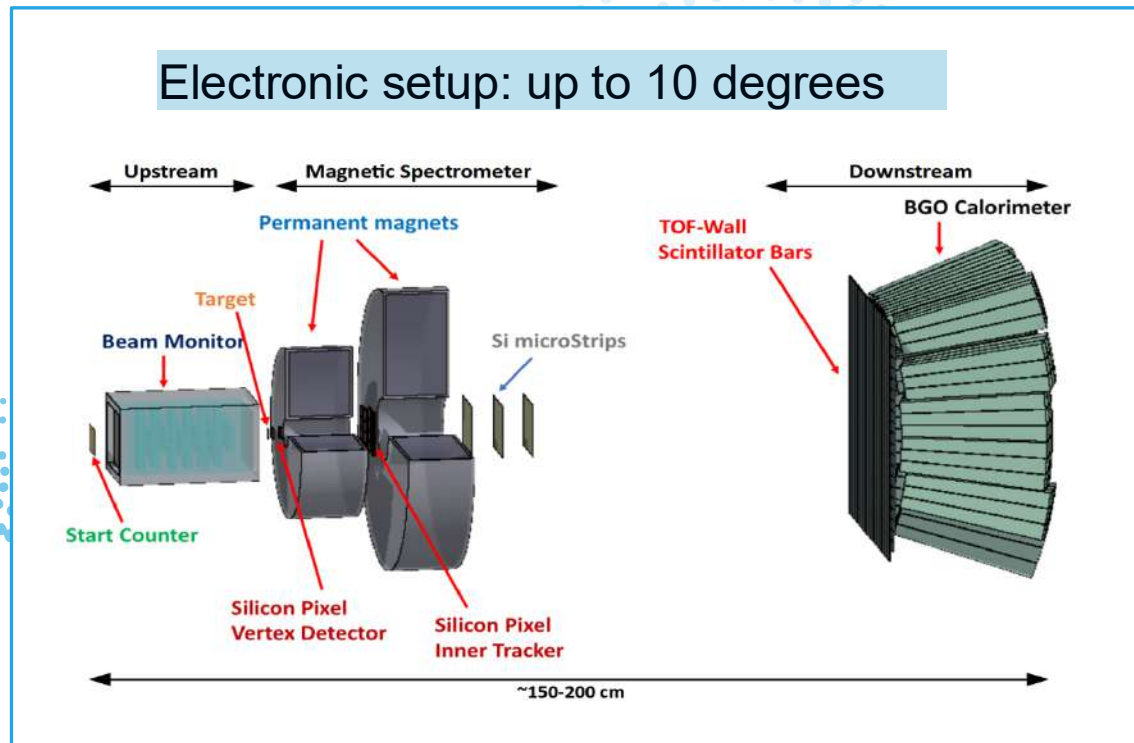


$$\frac{d\sigma}{dE_{kin}}(H) = \frac{1}{4} \left( \frac{d\sigma}{dE_{kin}}(\text{C}_2\text{H}_4) - 2 \frac{d\sigma}{dE_{kin}}(\text{C}) \right)$$

Webber et al, Phys Rev C (1990) 41(2); 520  
Dudouet et al, Phys Rev C (2013) 88(2):064615

# FOOT physics program

- Measure cross sections (double differential, in E and angle) → measure **A, Z, angle and E of particles**
- Beams of light ions ( $Z \leq 8$ ) with energies of order of a few  $10^2$  MeV/u. Available at very few centers in Europe, including
  - CNAO (National Center of Oncological Hadrontherapy) in Pavia
  - HIT (Heidelberger Ionenstrahl-Therapiezentrum) in Heidelberg
  - GSI (Helmholtzzentrum für Schwerionenforschung) in Darmstadt.
- Target: tissue like targets: C, polyethylene
- FOOT data taking typically in treatment room → **need a moveable and compact system**
- Two complementary setups:
  - Electronic detectors setup ( $Z \geq 2$ ), up to 10 degrees
  - Emulsion Cloud Chamber ( $Z \leq 3$ ), up to 70 degrees

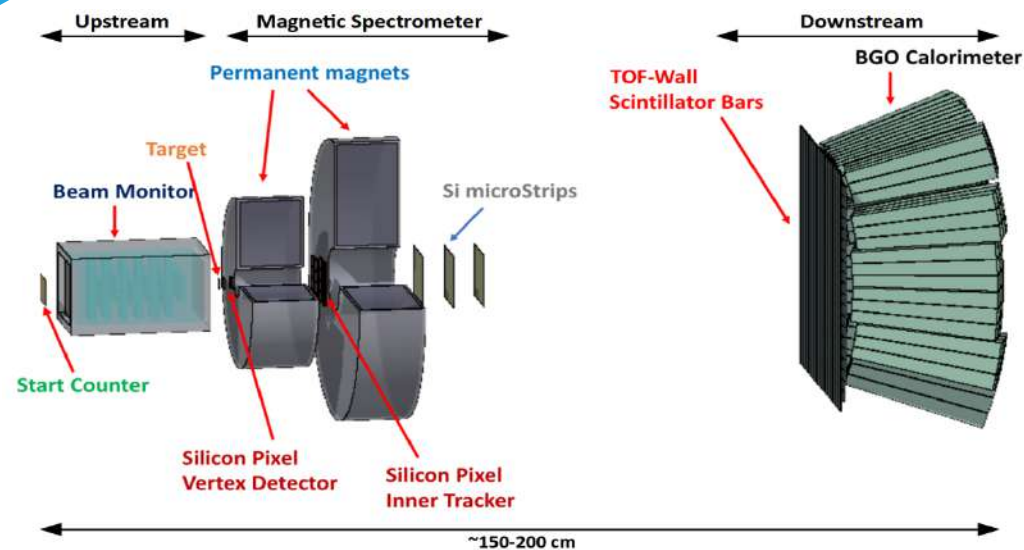


# FOOT physics program

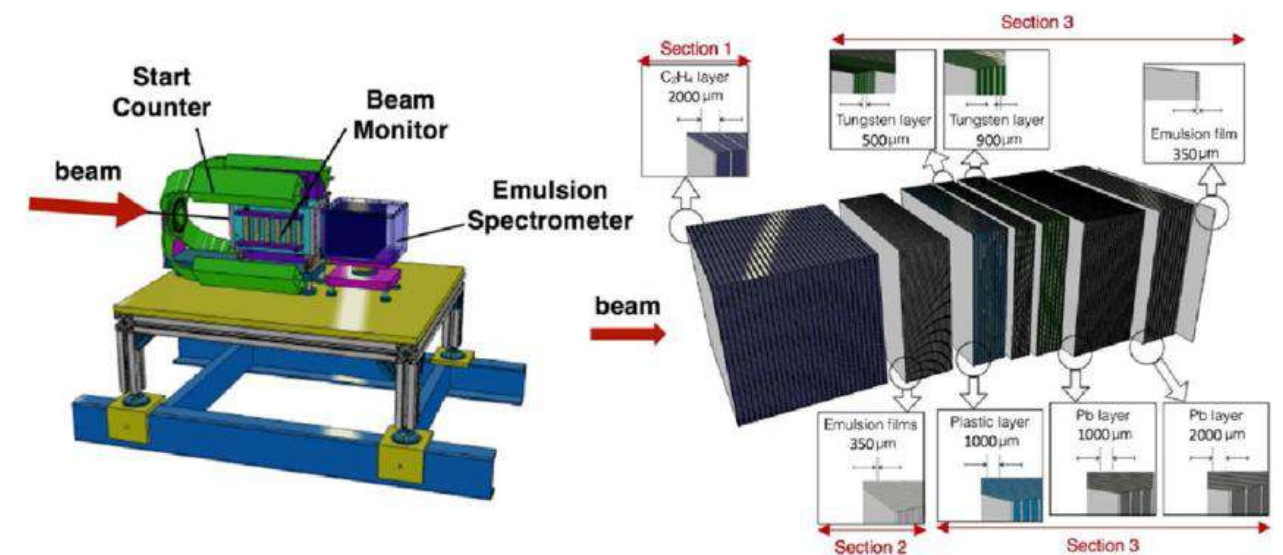
- Measure cross sections (double differential, in E and angle) → measure **A, Z, angle and E of particles**
- Beams of light ions ( $Z \leq 8$ ) with energies of order of a few  $10^2$  MeV/u. Available at very few centers in Europe, including
  - CNAO (National Center of Oncological Hadrontherapy) in Pavia
  - HIT (Heidelberger Ionenstrahl-Therapiezentrum) in Heidelberg
  - GSI (Helmholtzzentrum für Schwerionenforschung) in Darmstadt.
- Target: tissue like targets: C, polyethylene
- FOOT data taking typically in treatment room → **need a moveable and compact system**
- Two complementary setups:
  - Electronic detectors setup ( $Z \geq 2$ ), up to 10 degrees
  - Emulsion Cloud Chamber ( $Z \leq 3$ ), up to 70 degrees

TODAY

## Electronic setup: up to 10 degrees



## Emulsion cloud chamber: up to 45 degrees

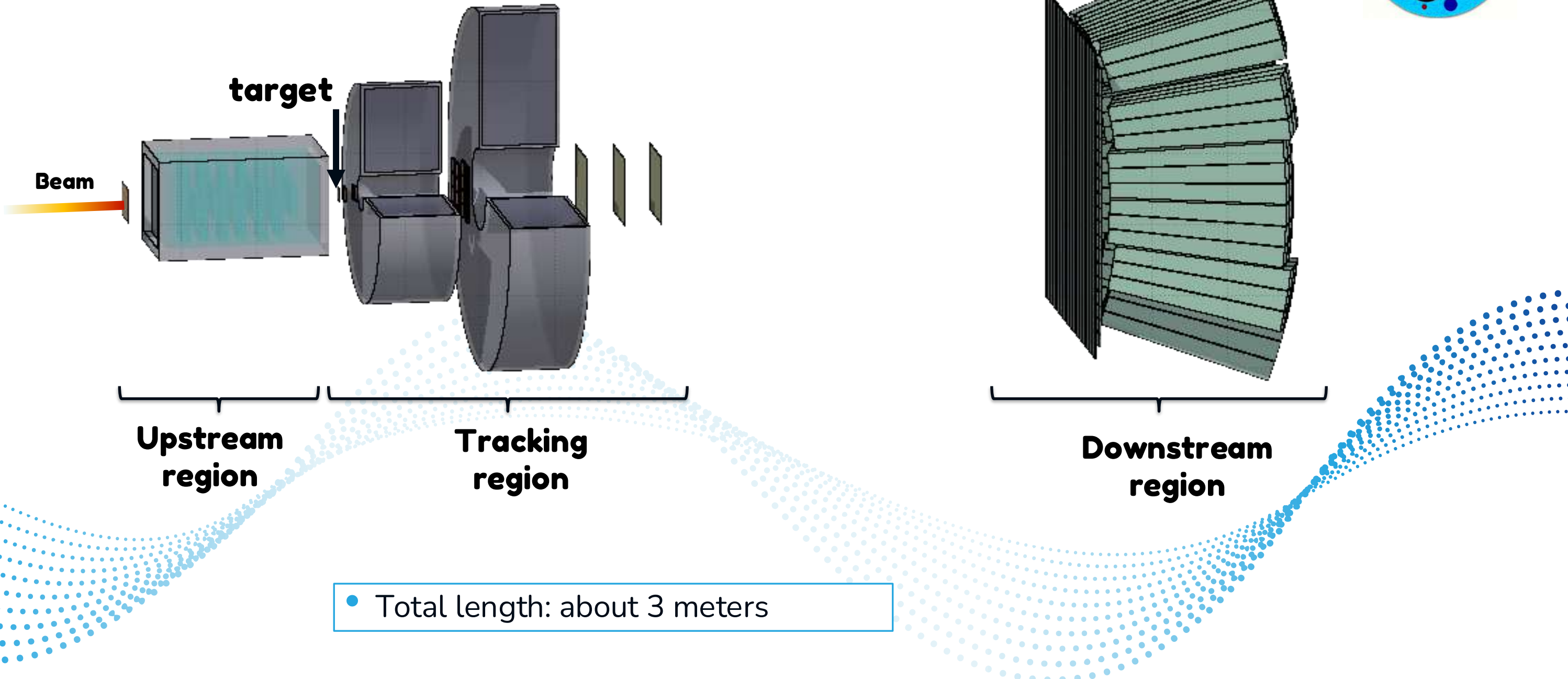


# The detector

Electronic setup



# FOOT detector (electronic setup)



• Total length: about 3 meters

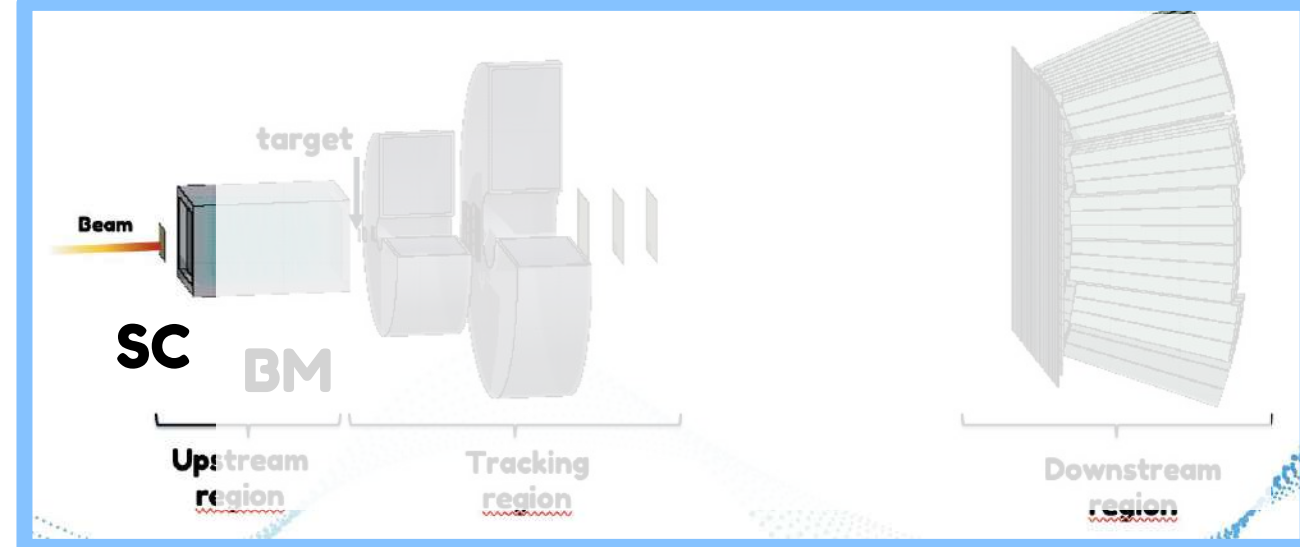
# FOOT Start Counter detector

## Start Counter (SC):

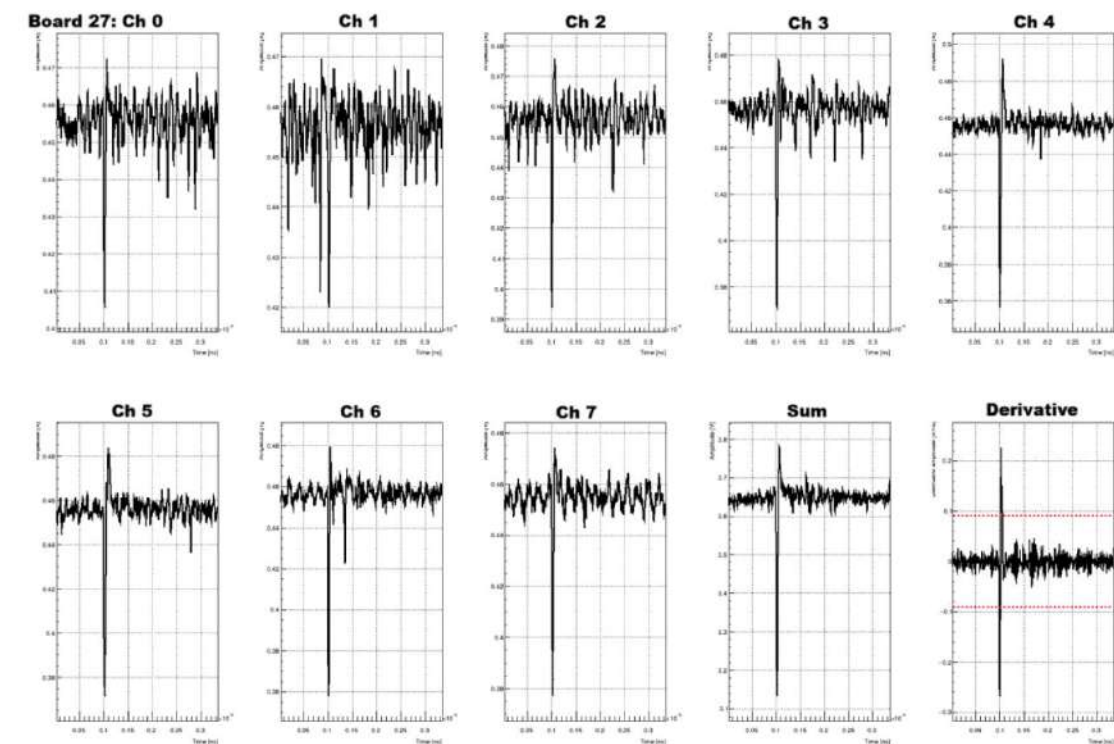
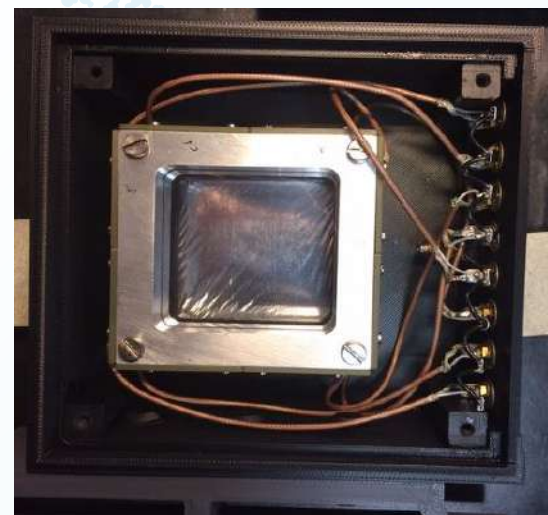
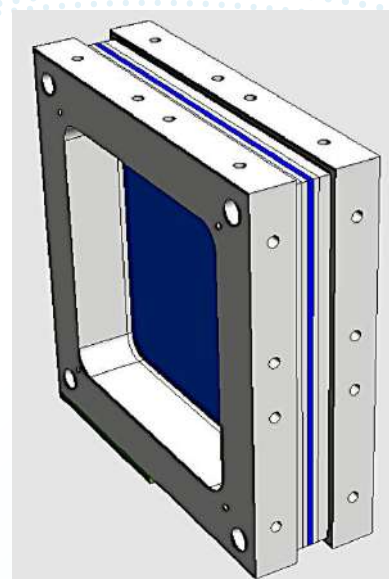
- First detector encountered by beam
- 250  $\mu\text{m}$  thick plastic scintillator
- EJ 228, Eljen Technology
- 5x5  $\text{cm}^2$  active area
- 48 SiPMs (ASD-NUV3S 3x3 $\text{mm}^2$ ), 8 channels readout
- Closed with a thin layer of 4  $\mu\text{m}$  aluminized mylar
- DAQ system developed at PSI for MEG2
- Channels connected to custom board WaveDREAM
- SC signals from 8 channels summed and the resulting WF is analyzed with a CFD algorithm  $\rightarrow T_{sc}$

- **Trigger**
- **First time stamp for TOF**

G. Traini, A. Alexandrov, B. Alpat,  
Il Nuovo Cimento (2020).



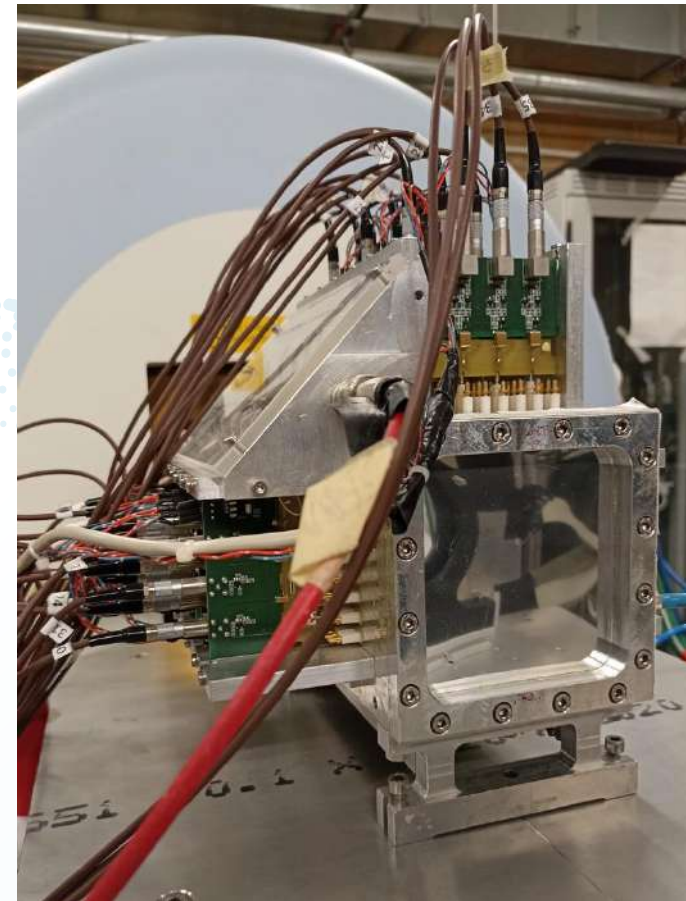
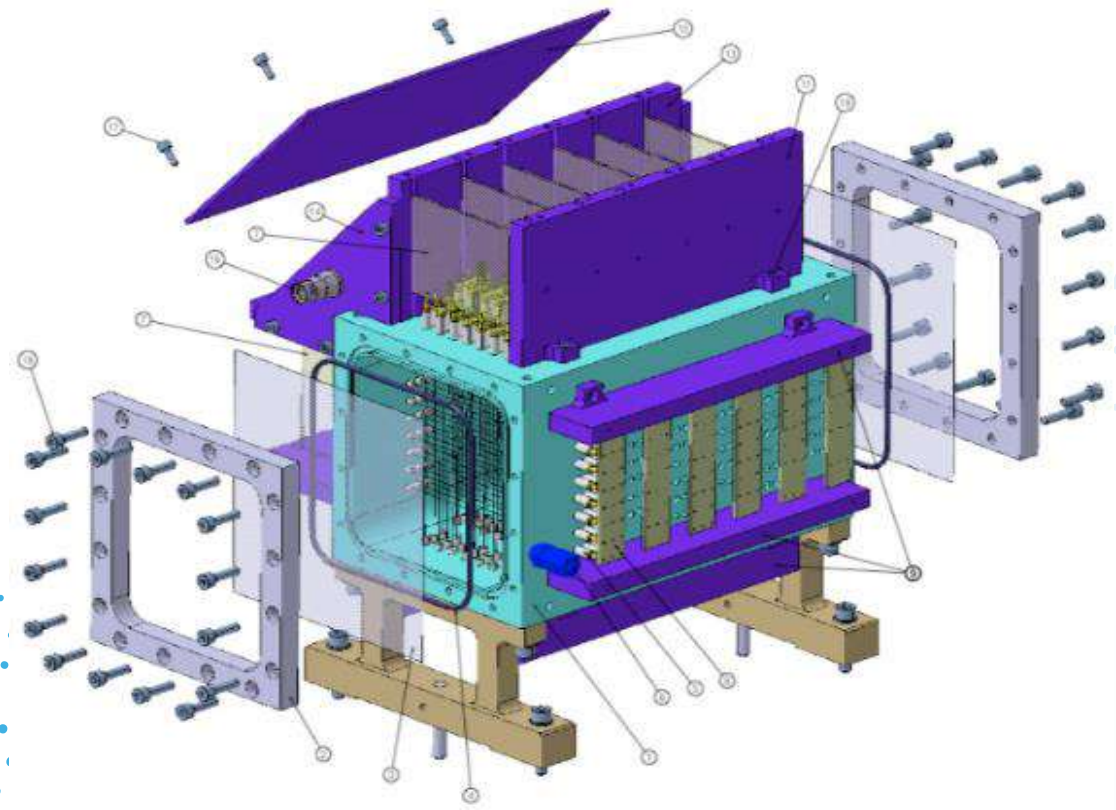
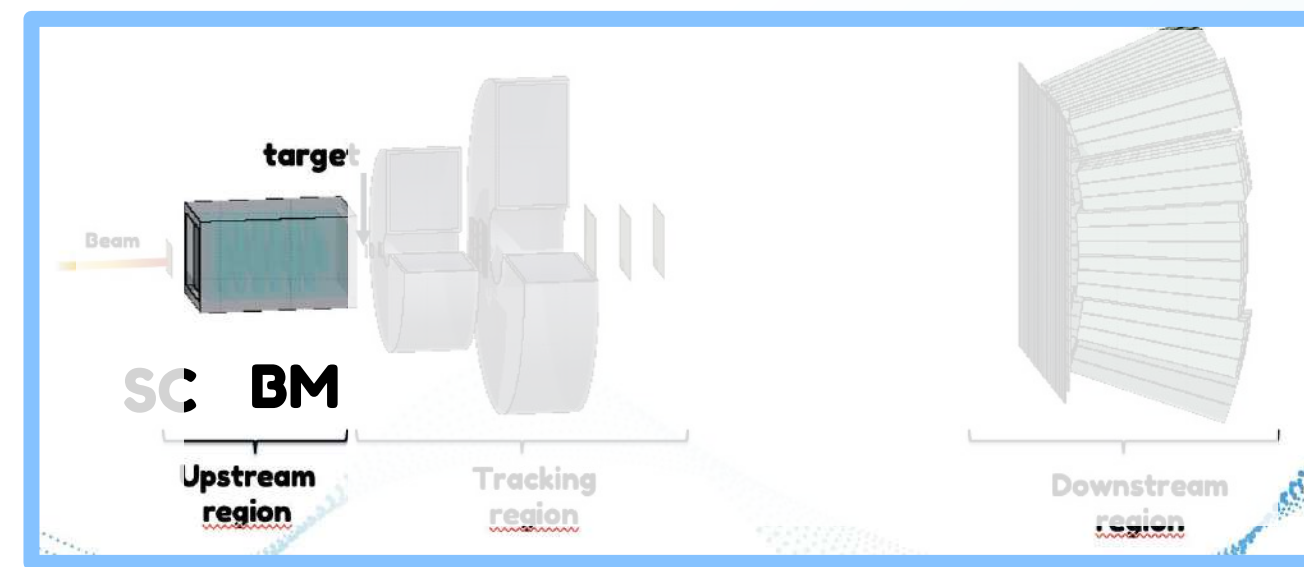
Galli, Francesconi,  
NIM A 936 (2019) 39



# FOOT detector: upstream region

Pre-target region: beam characterization

## Beam monitor (BM)



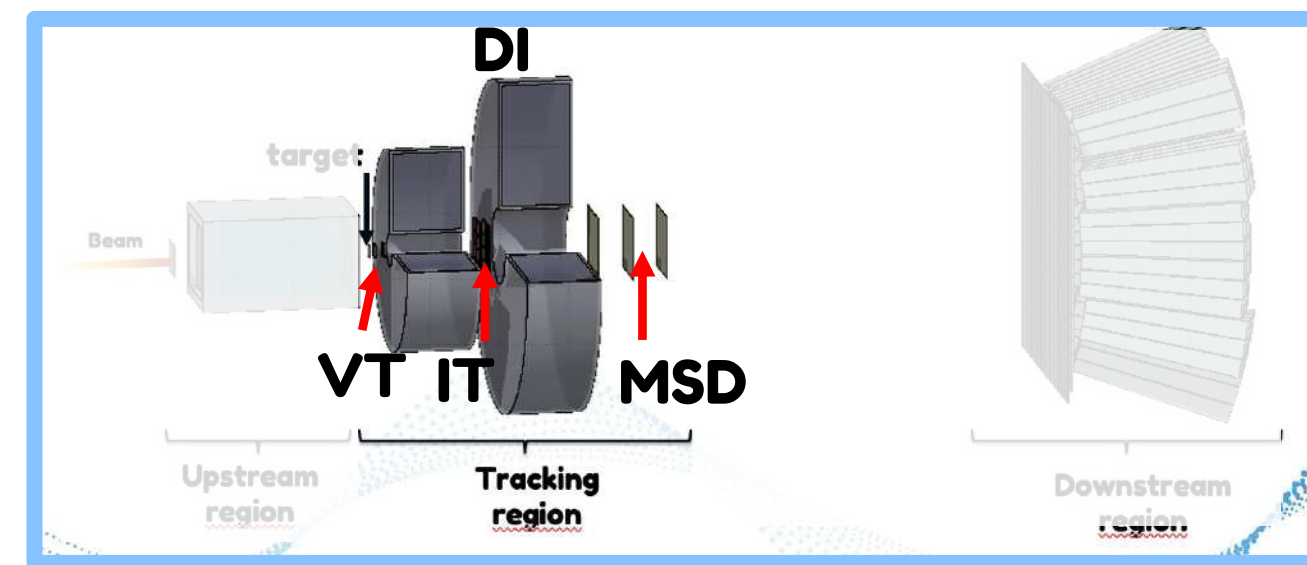
- Drift chamber
- Gas: Ar/CO<sub>2</sub> (80/20%)
- 12 layers, 3 cells each

- Beam momentum
- Direction

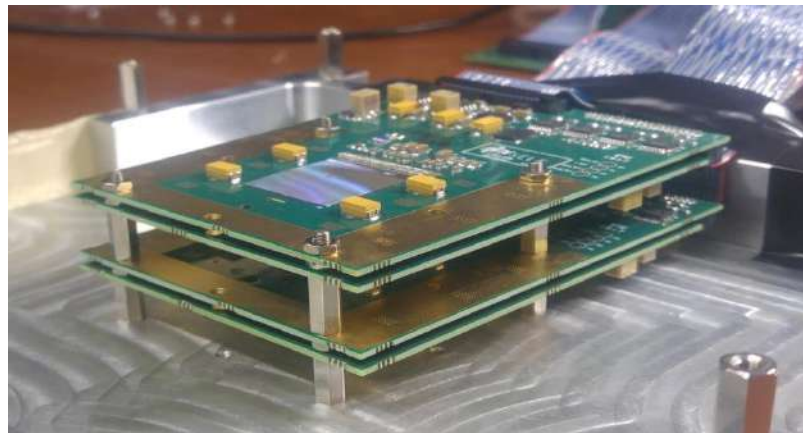
Dong et al., NIMA, 986, 2021, 164756

# FOOT detector: tracking region

Tracking region → **Fragment tracking and momentum**



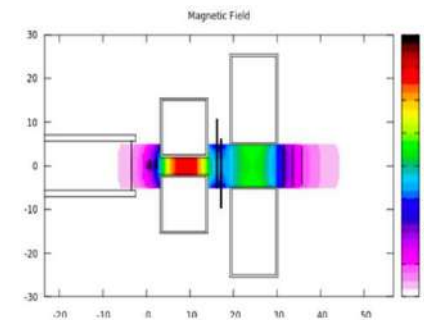
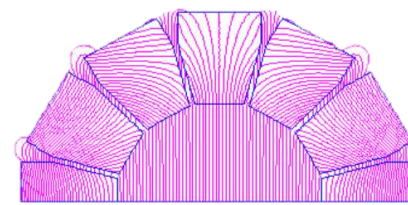
## Vertex (VT) & Inner Tracker (IT)



- VT: 4 layers Si pixel ( $20 \times 20 \mu\text{m}^2$ ),  $2 \times 2 \text{ cm}^2$  active area
- IT: 2 layers Si pixel ( $20 \times 20 \mu\text{m}^2$ ),  $8 \times 8 \text{ cm}^2$  total active area

→ **Fragment tracking**

## Dipole magnets (DI)



- 2 permanent Hallbach magnets
- B field in y axis (max 0.9 and 1.4 T)

→ **Particle curvature**

## Micro Strip Detector (MSD)



- 3 couples of orthogonal layers
- $9 \times 9 \text{ cm}^2$  active area
- $150 \mu\text{m}$  thickness
- $50 \mu\text{m}$  strip implantation pitch

→ **Fragment tracking**

# FOOT TOF-Wall detector

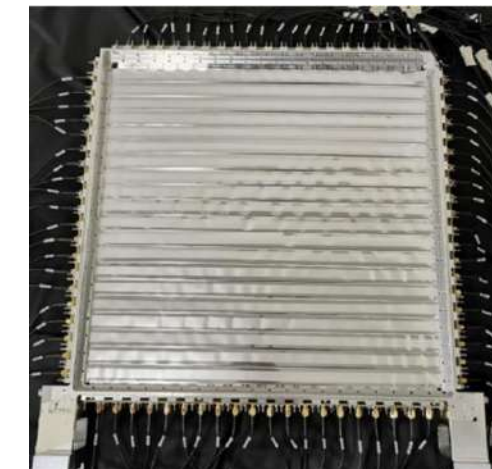
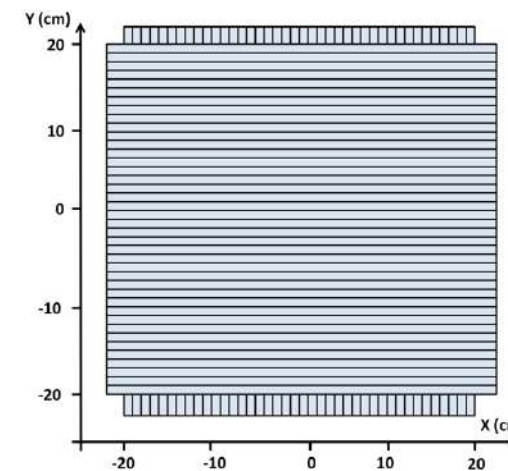
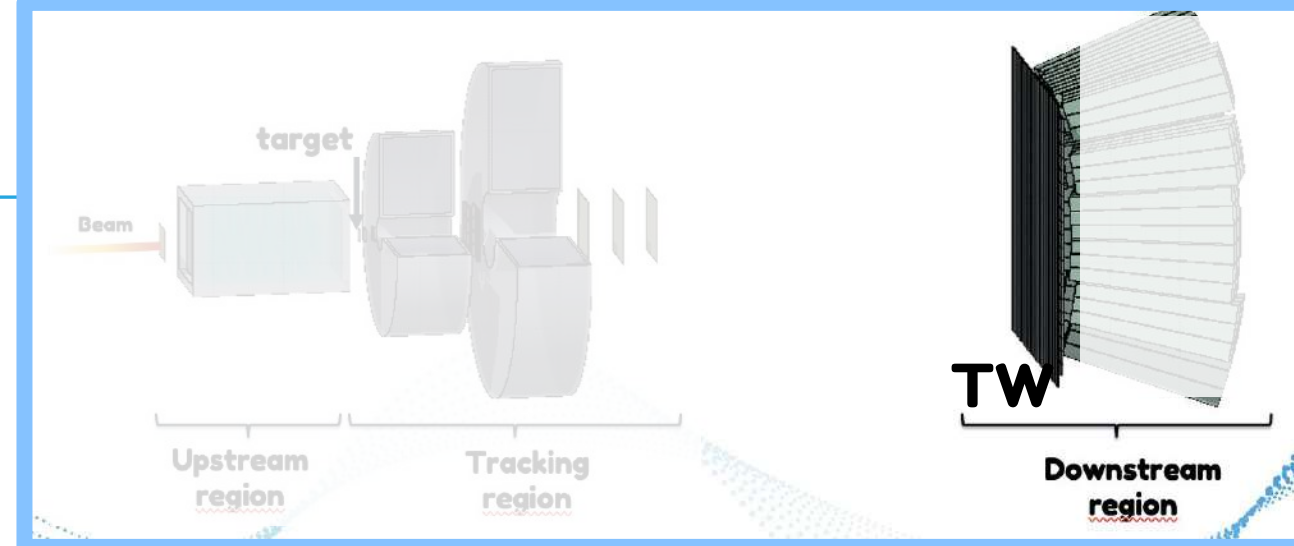
## TOF-wall (TW): $\Delta E$ and second time stamp for TOF

- 2 orthogonal layers of bars: 20+20 bars



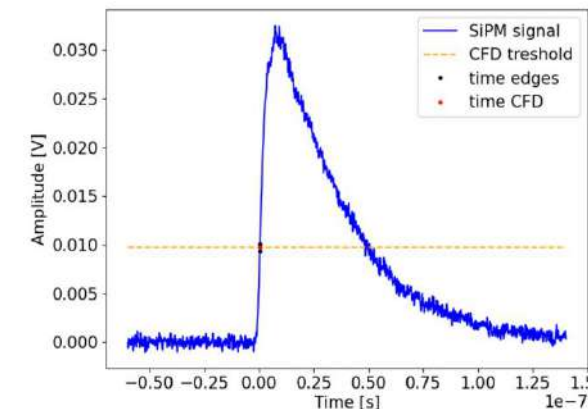
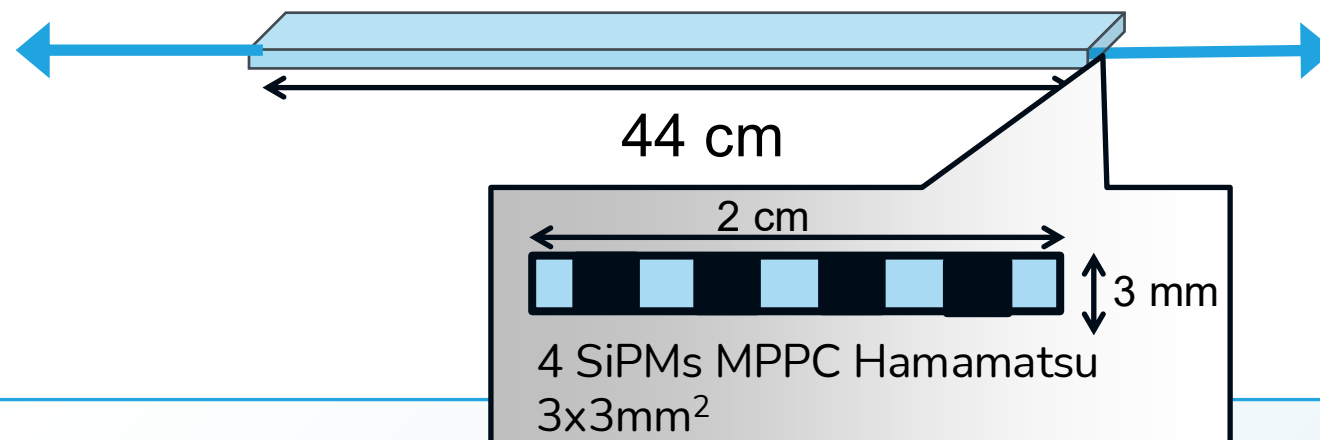
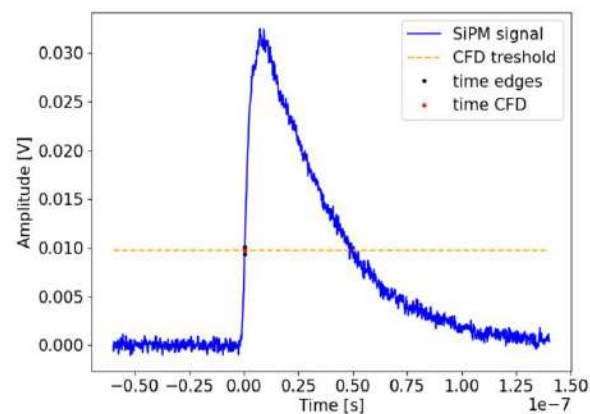
**Bar:** plastic scintillator EJ200, Eljen technology

- 44 cm long, 3 mm thick, 2 cm wide
- Each bar side: 4 SiPMs MPPC Hamamatsu 3x3mm<sup>2</sup>
- DAQ system developed at PSI for MEG2
- Channels from each bar connected to custom board WaveDREAM
- CFD algorithm to determine time



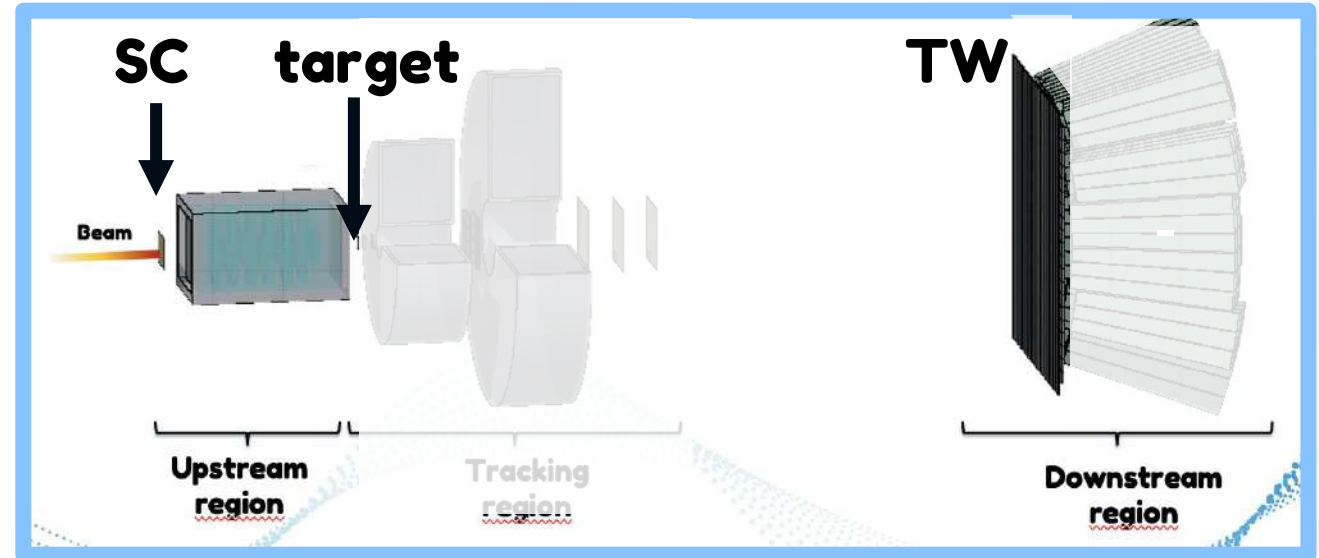
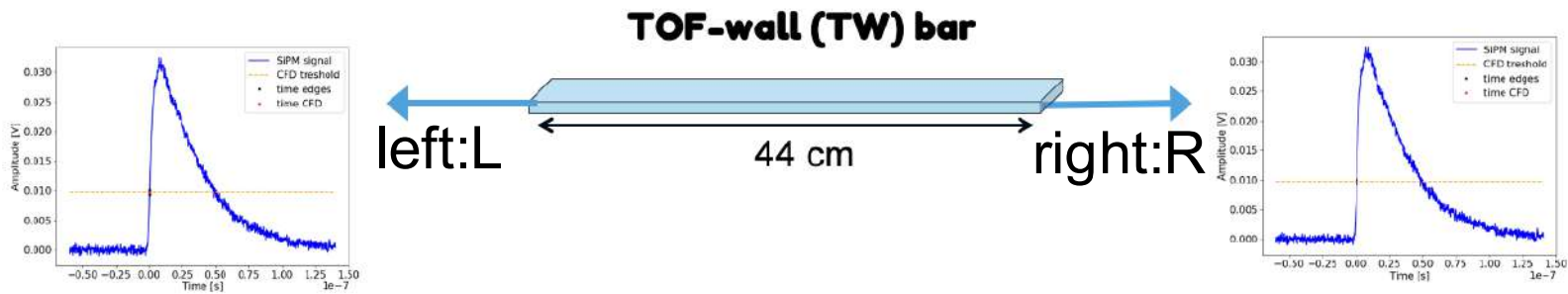
M. Morrocchi, et al, IEEE Trans Nuc Sc 68.5 (2020), pp. 1161–1168

## TOF-wall (TW) bar



# Tof Wall data processing and charge identification

## Data processing:



### Raw charge

- Bar: obtain  $Q_L$  and  $Q_R$ : waveform integrated
- Total charge in bar:  $Q_{bar} = \sqrt{Q_L Q_R}$
- Calibration by using MC simulations  $\rightarrow \Delta E$

### Raw Time-Of-Flight

- $T_{TWbar} = \frac{T_L + T_R}{2}$
- $TOF_{raw} = T_{TWbar} - T_{SC}$
- Correct for time between SC and target  $\rightarrow TOF$

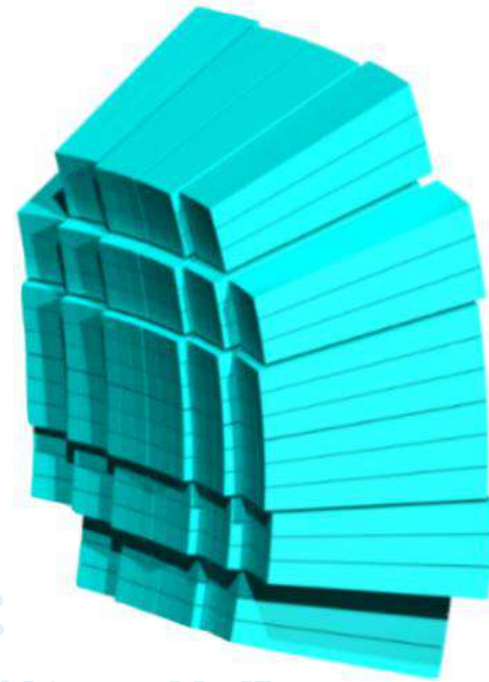
Z by Bethe-Bloch equation

$$\begin{array}{ccc}
 \Delta E & \text{fragment charge } Z & TOF \\
 \downarrow & \downarrow & \downarrow \\
 \left\langle \frac{dE}{dx} \right\rangle_{coll} & = K \frac{\rho_t Z_t}{A_t} \frac{Z^2}{\beta^2} \left[ \frac{1}{2} \log \left( \frac{2m_e c^2 \beta^2 \gamma^2 W_{max}}{I_t^2} \right) - \beta^2 - \frac{\delta}{2} - \frac{C}{Z} \right] & 
 \end{array}$$

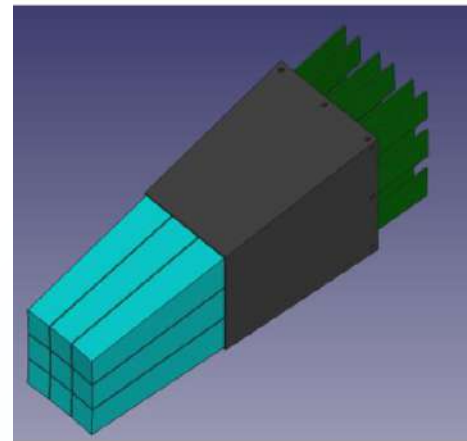
# FOOT detector: downstream region

## Calorimeter (CAL)

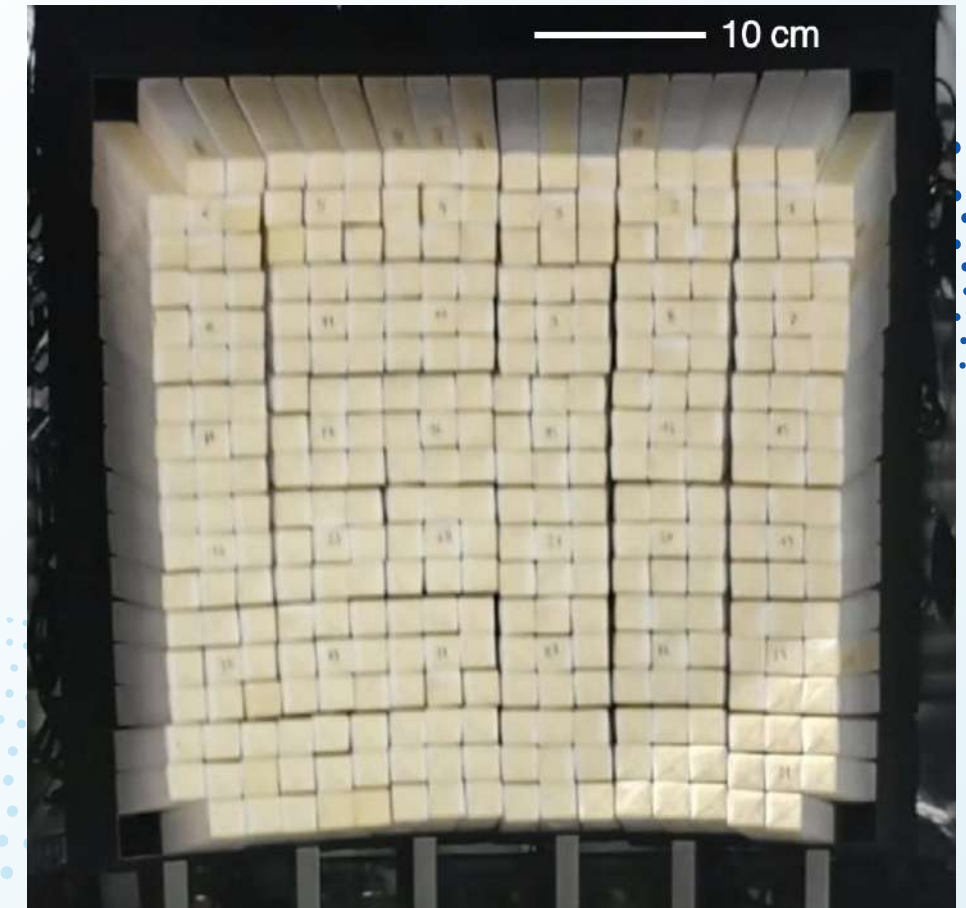
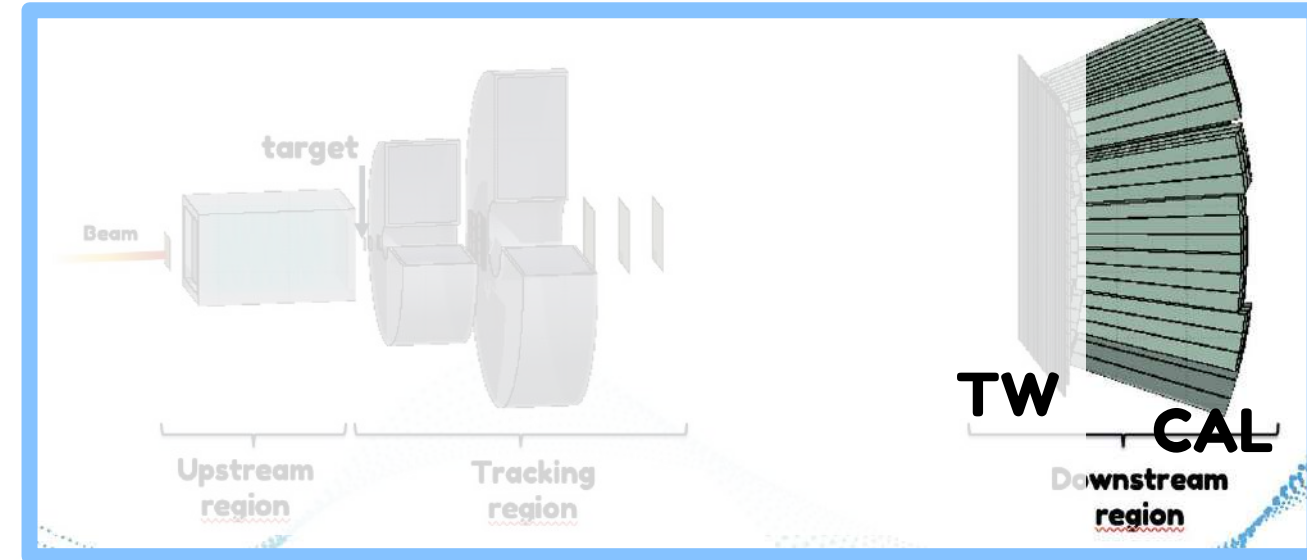
- BGO – inorganic scintillator
- 288 crystals – 330 kg
- 25 SiPMs/crystal
- 1 crystal – 1 channel readout



- Kinetic energy
- Fragment identification (mass)



10



# Mass identification

- **Mass A** reconstruction: 3 ways

- TOF & Tracker:

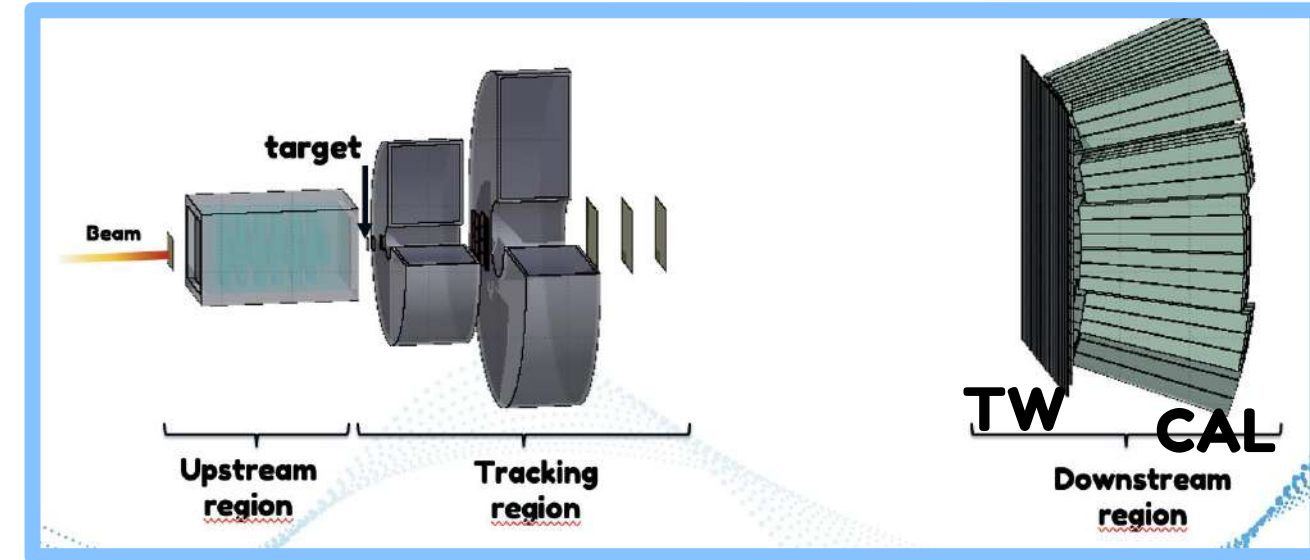
$$p = mc\beta\gamma$$

- TOF & Calorimeter:

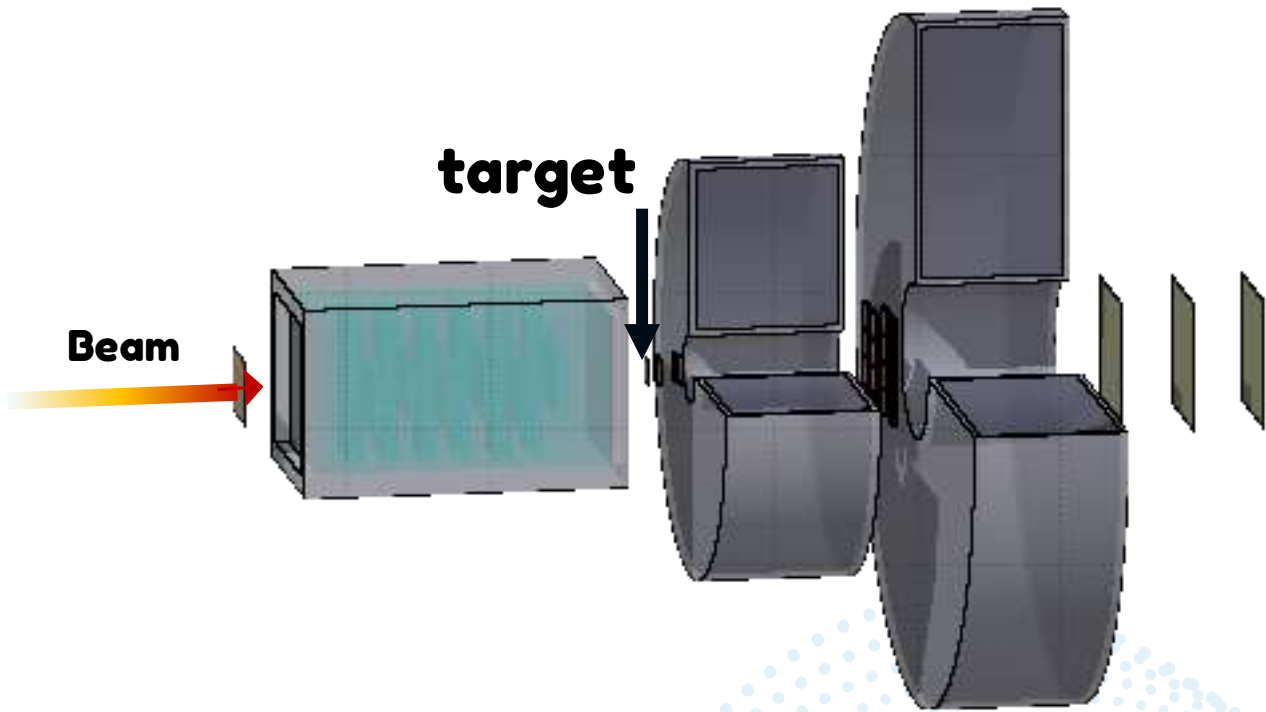
$$E_{\text{kin}} = mc^2(\gamma - 1)$$

- Tracker & Calorimeter

$$E_{\text{kin}} = \sqrt{p^2c^2 + m^2c^4} - mc^2$$

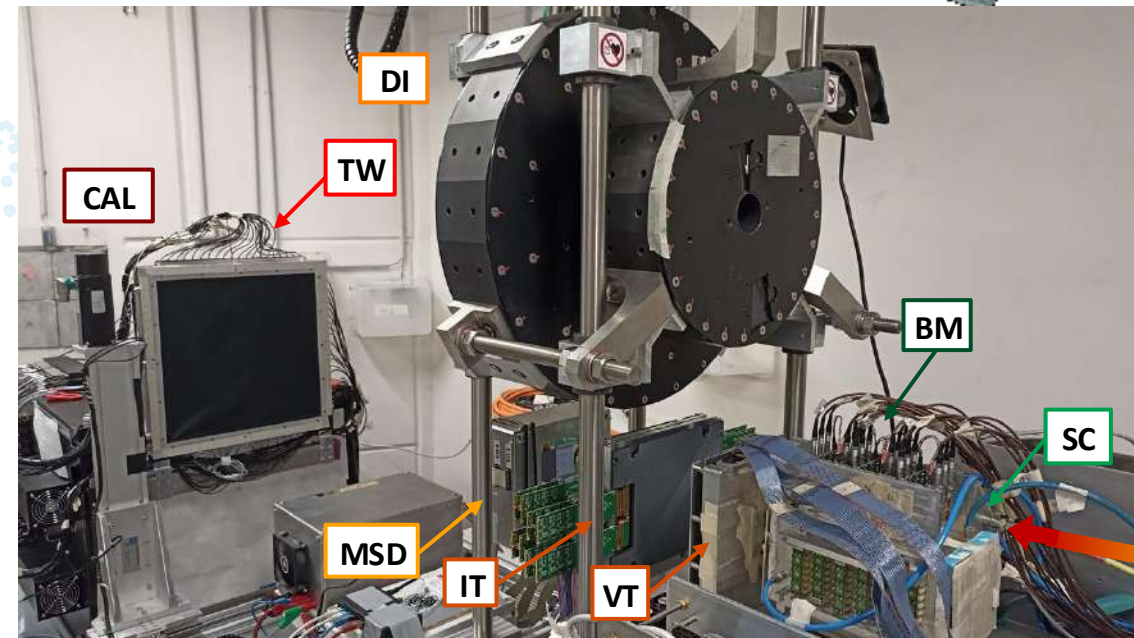


# FOOT detector: status 2026 of electronic setup



## Status March 2026

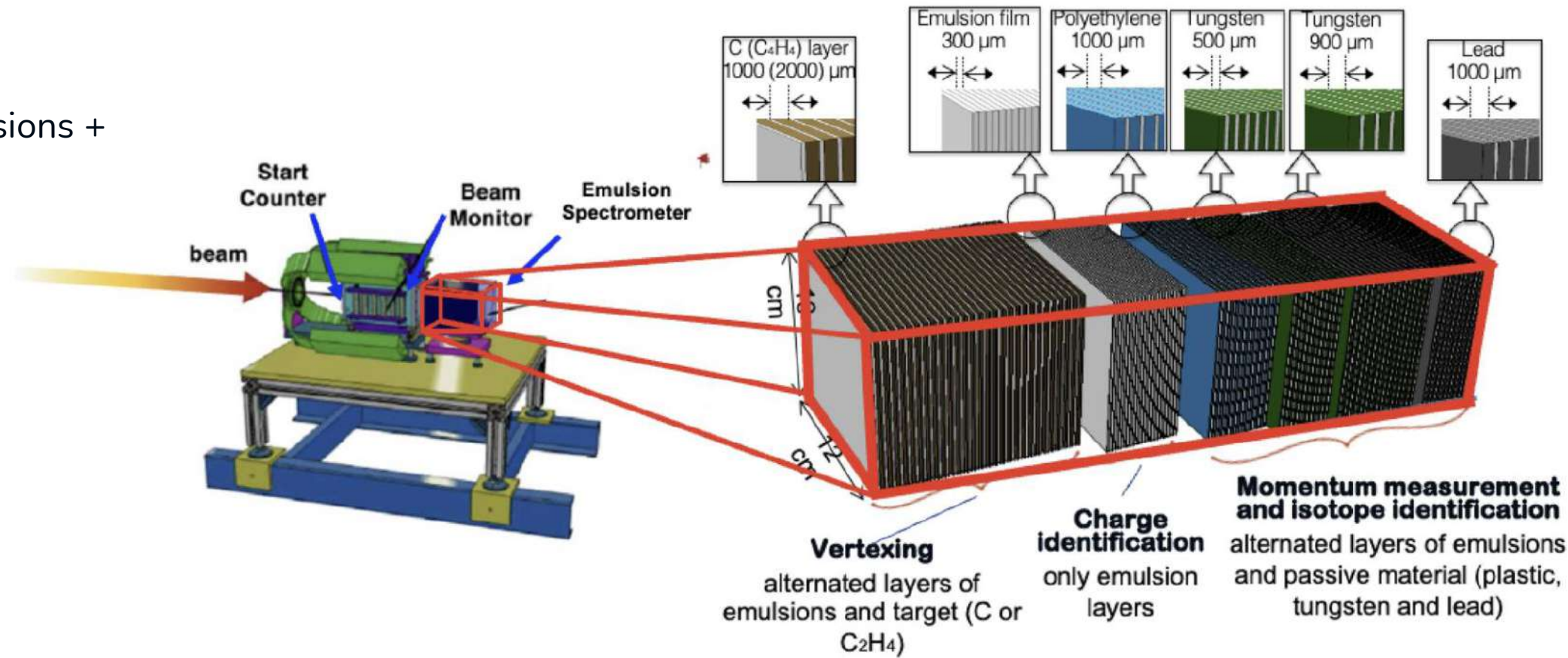
- Start counter: ready and fully tested
- Beam monitor: ready and fully tested
- Magnets: ready and tested
- VTX: ready, being tested
- Inner tracker: test phase
- Microstrip detectors: in advanced test phase
- ToF-Wall: ready and fully tested
- Calorimeter: ready, in advanced test phase



# FOOT detector: emulsion spectrometer

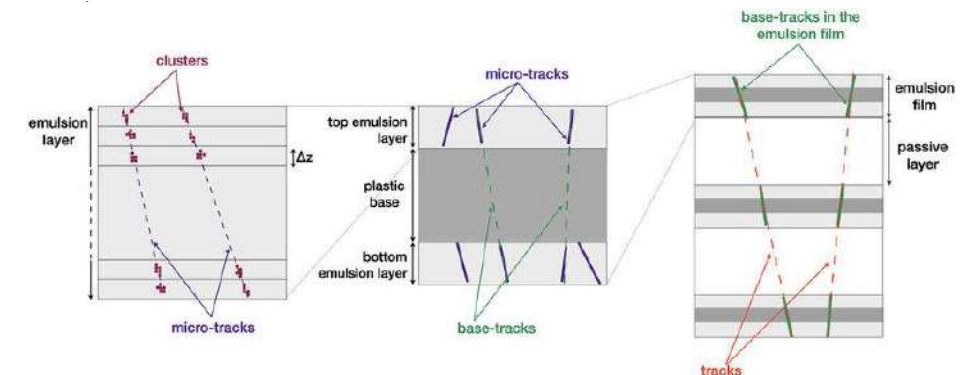


- “Light” fragments  $Z \leq 3$
- Angular coverage of  $45^\circ$
- Sections:
  - **Vertexing:** emulsions + target
  - **Charge id:** emulsion layers
  - **Momentum and isotope id:** emulsions + passive material
- Different beam energies with single irradiation



**Status March 2026**

Ready, fully tested, and acquiring data



# Recent measurements and results

A decorative graphic consisting of multiple parallel, wavy lines of small blue dots. The dots are arranged in a pattern that resembles a sine wave or a series of overlapping curves, creating a sense of motion and depth. The background is a solid, medium blue color.

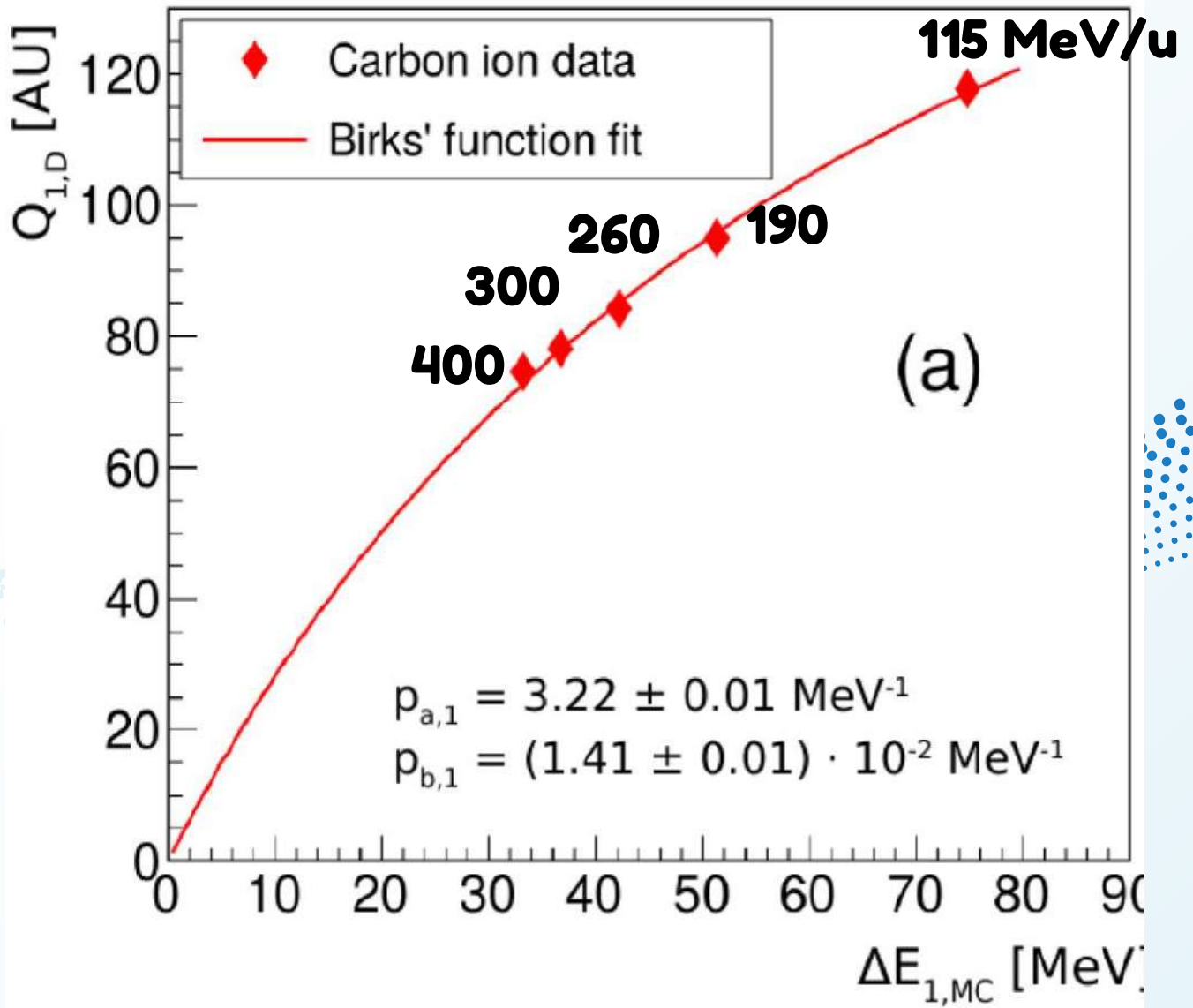
# TOF-Wall energy calibration

- Each bar was calibrated by equalizing raw charge with FLUKA Monte Carlo simulations
- Non-linear relationship between energy deposit and detected charge in a bar (**quenching**)
- Not a perfect fit with Birks'

$$\frac{dL}{dx} = \frac{S \frac{dE}{dx}}{1 + kB \frac{dE}{dx}}$$

- **What happens if we look at the whole spectrum produced in target fragmentation?**

**Carbon ions of various energies, shot directly on scintillator bar**



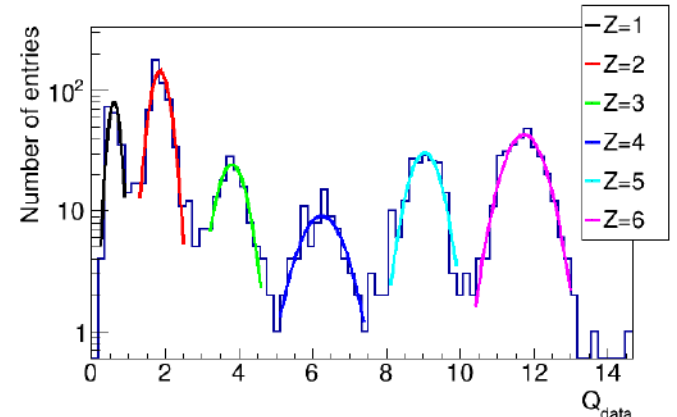
# TOF-Wall energy calibration

- Calibration by equalizing raw charge with FLUKA Monte Carlo simulations
- Non-linear relationship between energy deposit and detected charge in a bar (**quenching**)
- Not a perfect fit with Birks'

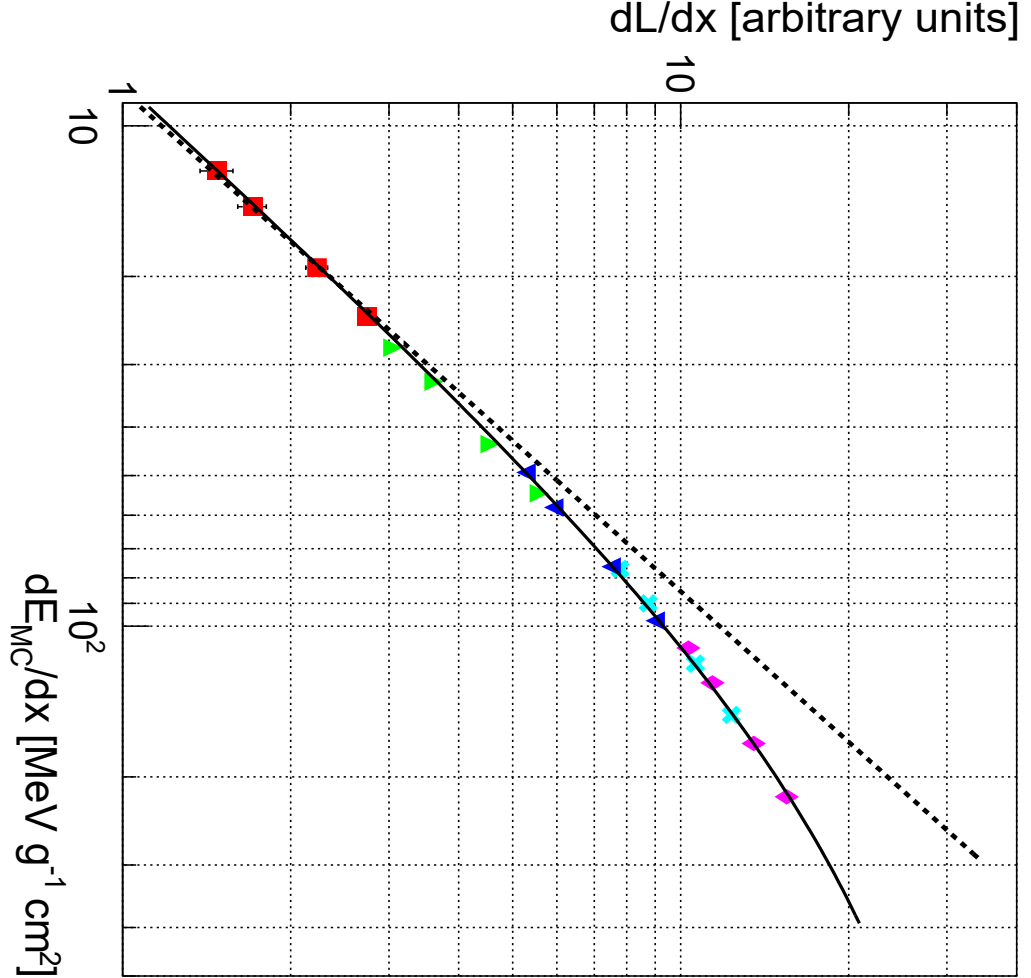
$$\frac{dL}{dx} = \frac{S \frac{dE}{dx}}{1 + kB \frac{dE}{dx}}$$

• **What happens if we look at the whole spectrum produced in target fragmentation?**

- Used 5 peaks x 4 energies



**Carbon ions of various energies, shot on C target**



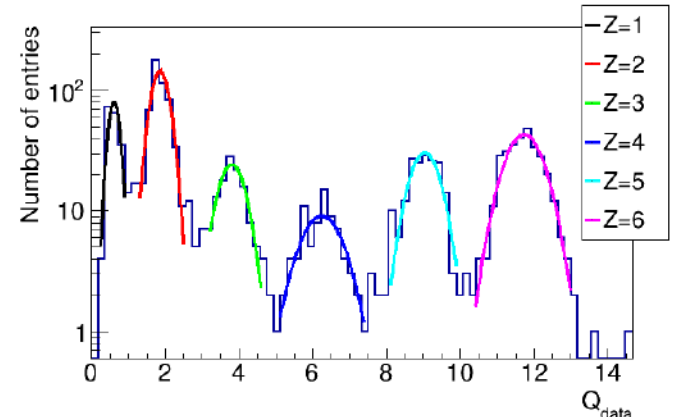
# TOF-Wall energy calibration

- Calibration by equalizing raw charge with FLUKA Monte Carlo simulations
- Non-linear relationship between energy deposit and detected charge in a bar (**quenching**)
- Not a perfect fit with Birks'

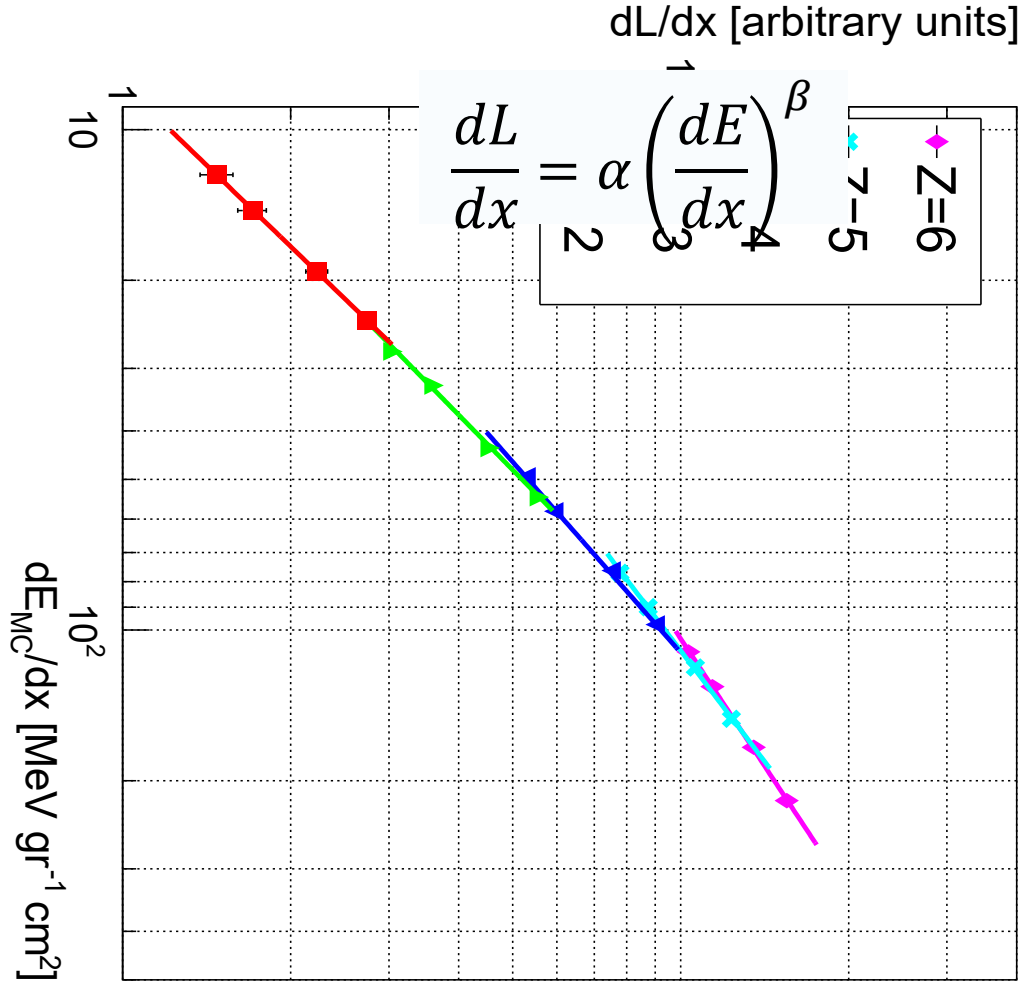
$$\frac{dL}{dx} = \frac{S \frac{dE}{dx}}{1 + kB \frac{dE}{dx}}$$

• **What happens if we look at the whole spectrum produced in target fragmentation?**

- Used 5 peaks x 4 energies



**Carbon ions of various energies, shot on C target**



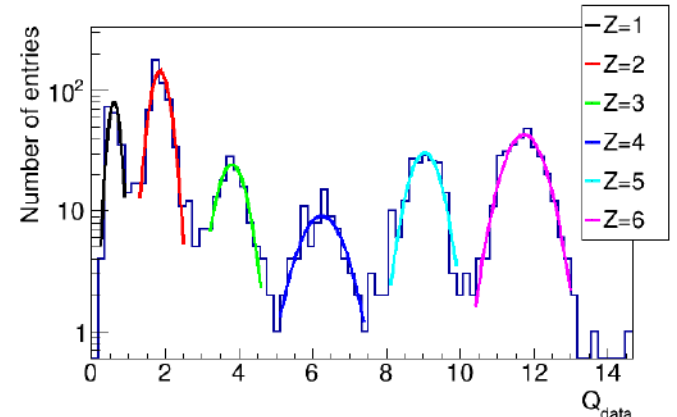
# TOF-Wall energy calibration

- Calibration by equalizing raw charge with FLUKA Monte Carlo simulations
- Non-linear relationship between energy deposit and detected charge in a bar (**quenching**)
- Not a perfect fit with Birks'

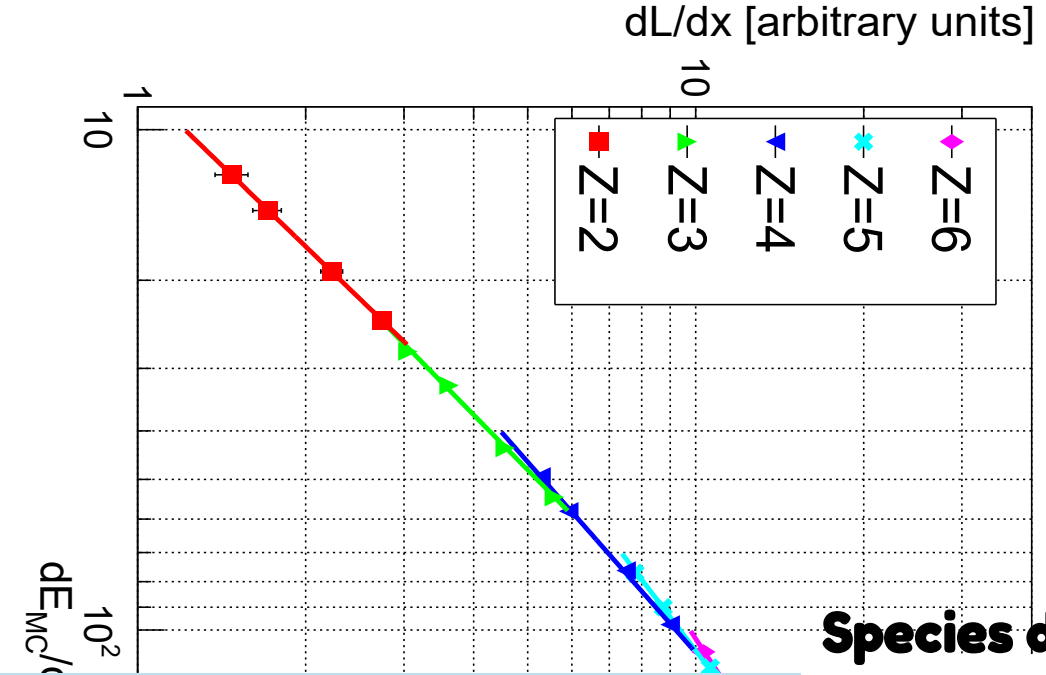
$$\frac{dL}{dx} = \frac{S \frac{dE}{dx}}{1 + kB \frac{dE}{dx}}$$

• **What happens if we look at the whole spectrum produced in target fragmentation?**

- Used 5 peaks x 4 energies

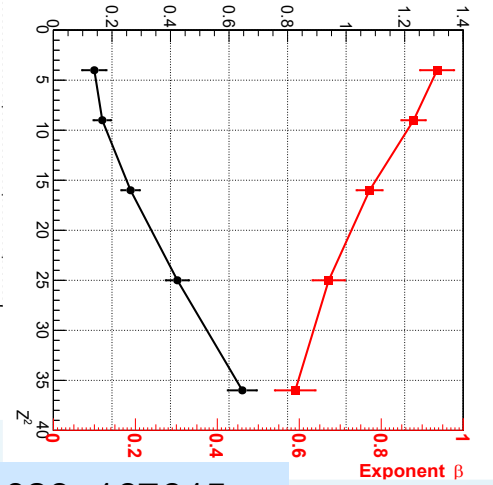


**Carbon ions of various energies, shot on C target**



**Species dependency:**

- Amplitude  $\alpha$ : increases for larger Z,
- Exponent  $\beta$ : decreases for larger Z, because of more significant quenching in core for high Z particles (?)
- See Matsufuji et al, NIMA437, 1999



See Kraan, et al, NIMA 1045, 2023, 167615

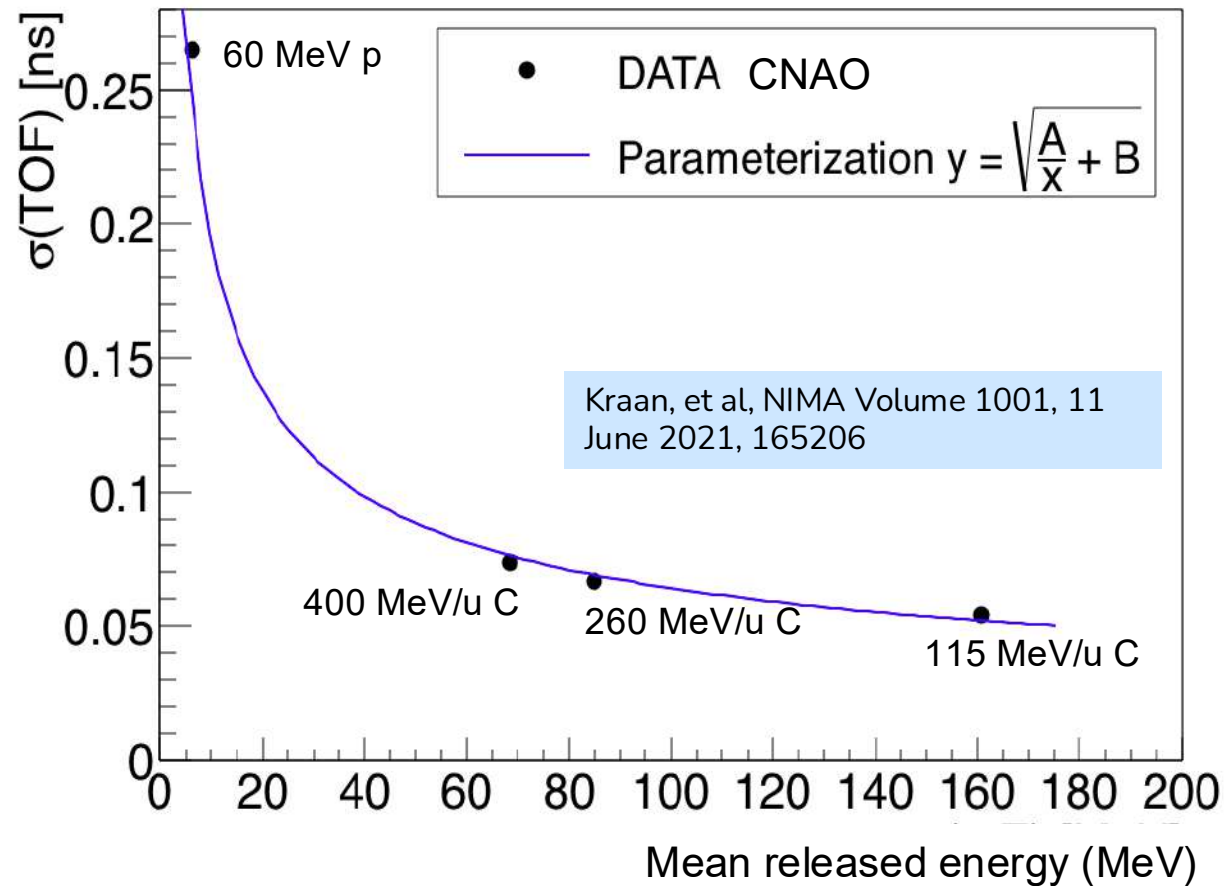
# TOF and Delta-E Resolution

Shot directly on bars, no target

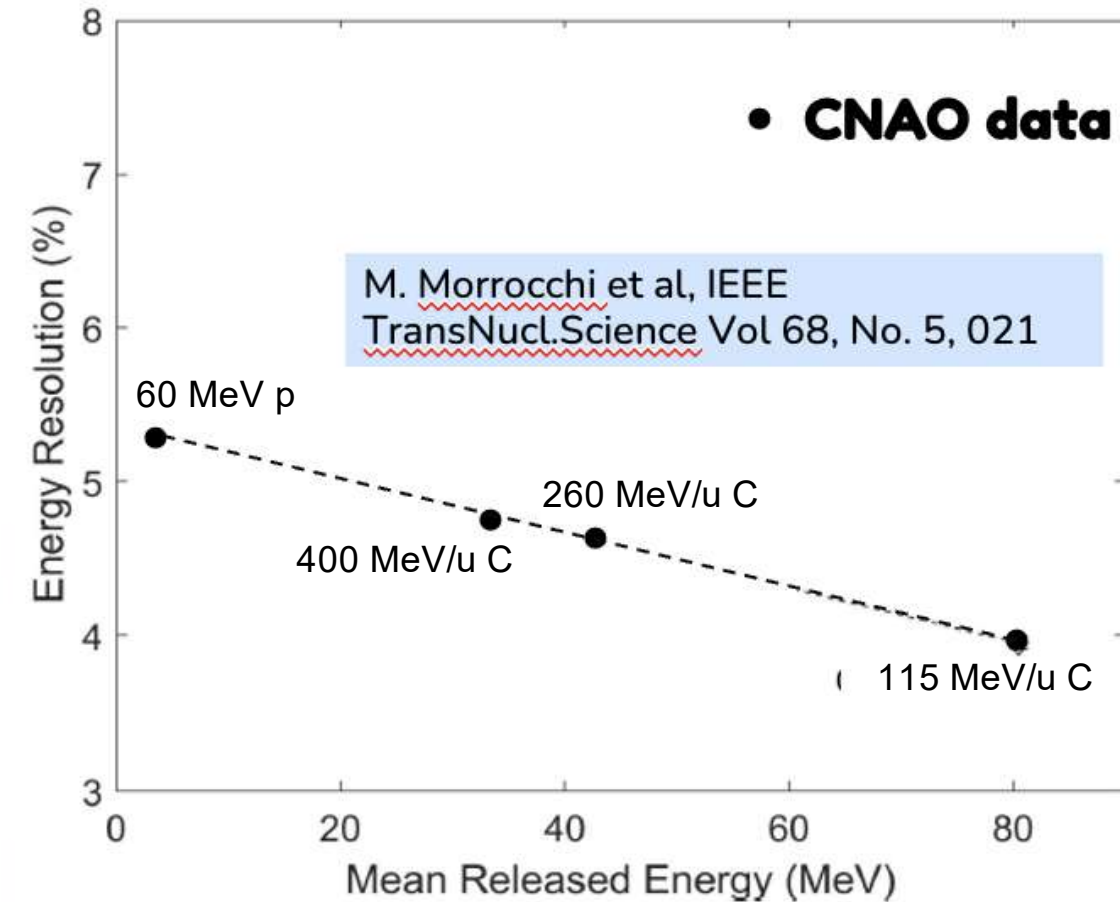


CNAO=Centro Nazionale di Adroterapia Oncologica

TOF Wall time resolution



TOF Wall energy resolution



Resolution	Protons	Carbon ions
Time-of-flight TOF	265 ps	54 -75 ps

	60 MeV Protons	Carbon ions
Resolution (%)	5.7%	4.0% - 4.7%

# Z identification: resolutions

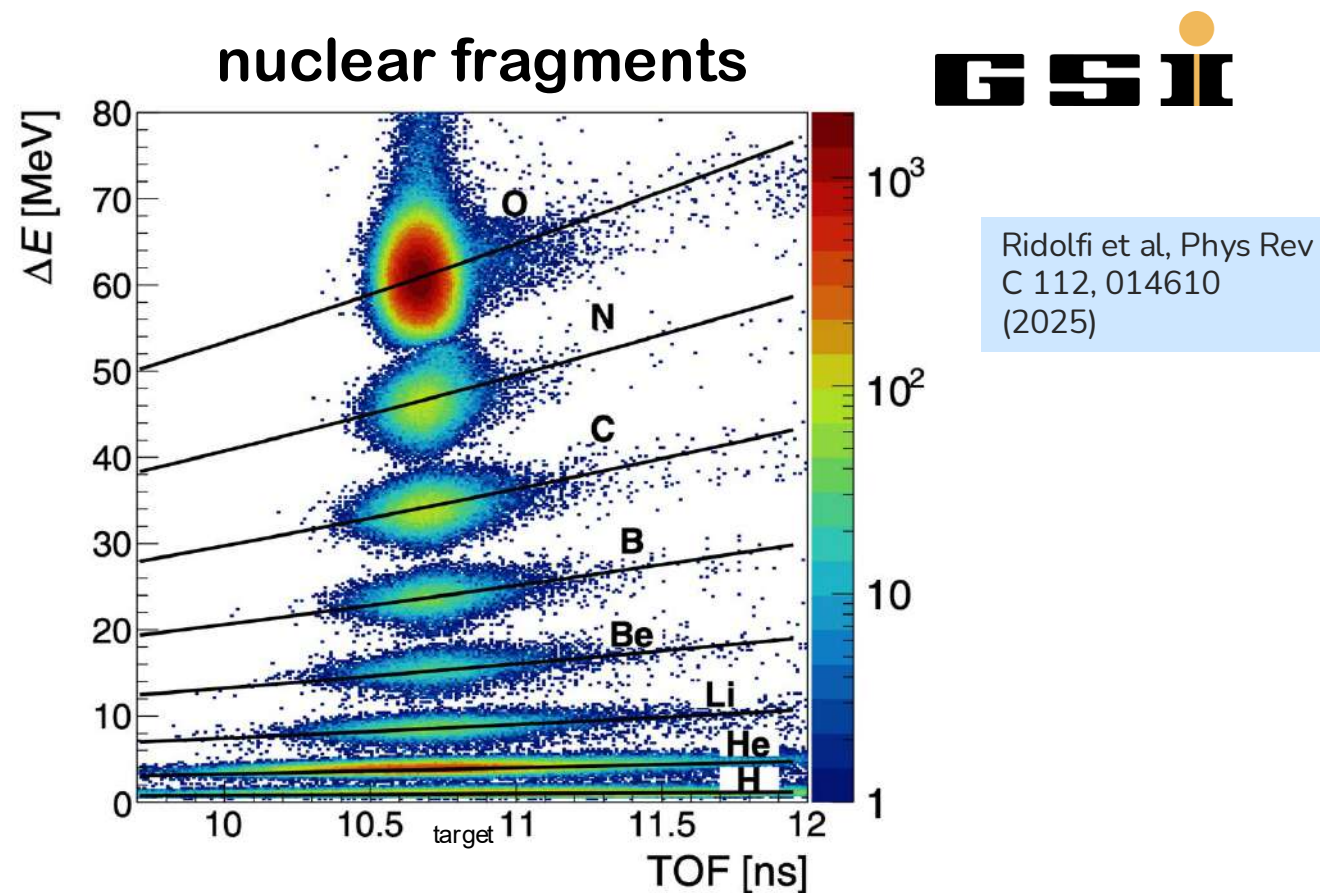
**Resolutions** determined **without target (different data takings)**

Facility	Particle	Beam energy [MeV/u]	$\mu(Z)$	$\sigma(Z)$	$R_Z[\%]$
CNAO	p	60	0.96	0.06	6.10
HIT	He	100	2.03	0.06	2.72
HIT	He	140	2.04	0.07	3.44
HIT	He	200	2.06	0.09	4.36
HIT	He	220	2.05	0.09	4.51
CNAO	$^{12}\text{C}$	115	6.17	0.15	2.51
CNAO	$^{12}\text{C}$	260	6.01	0.21	3.52
CNAO	$^{12}\text{C}$	400	6.07	0.24	3.85
GSI	$^{16}\text{O}$	400	8.07	0.22	2.67

# Z identification with TOF and Delta-E

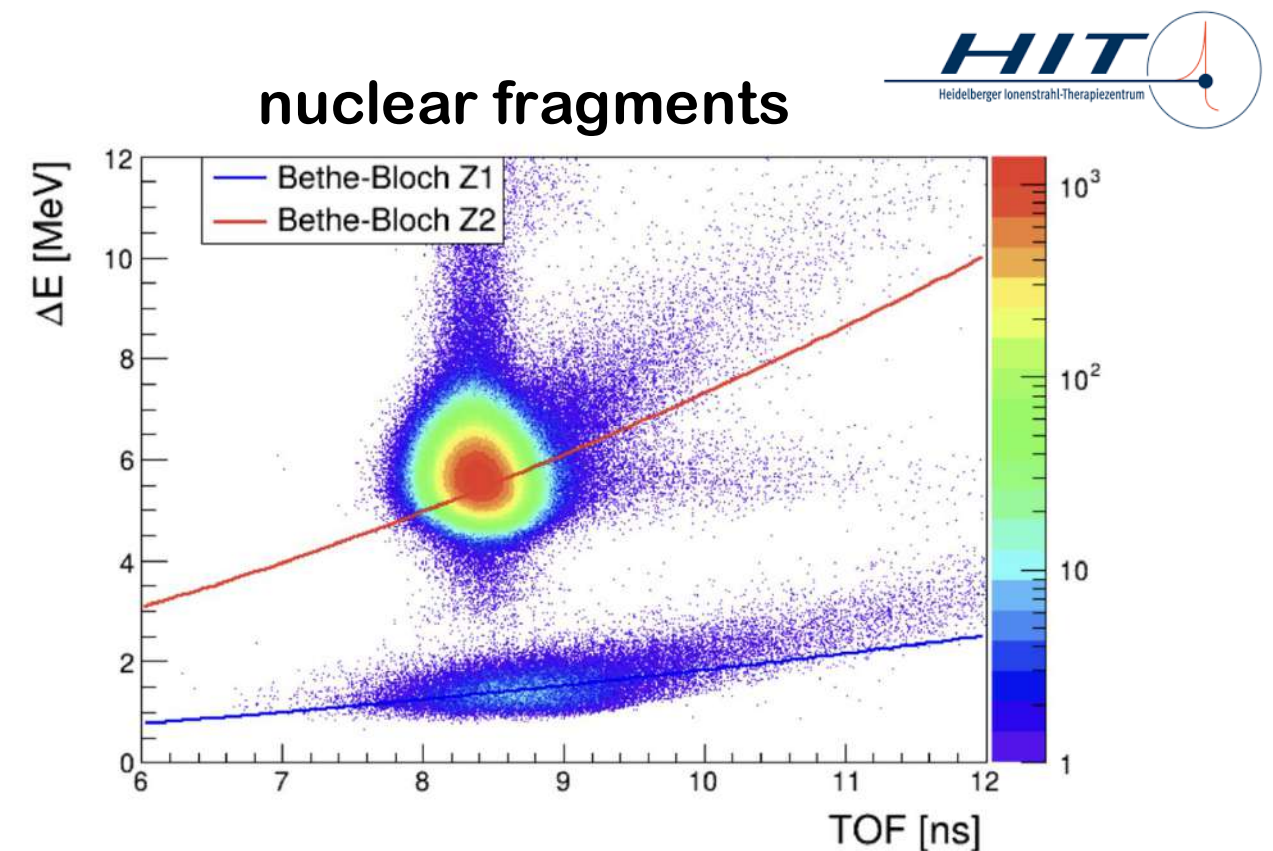
Example of charge spectrum for 400 MeV/u  
**oxygen ions on graphite target** at **GSI**  
Helmholtzzentrum für Schwerionenforschung

- Partial setup: no magnet, no calorimeter



Example of charge spectrum for 200 MeV/u  
**helium ions on graphite target** at Heidelberger  
Ionenstrahl-Therapiezentrum **HIT**

- Partial setup: no magnet, part of calorimeter

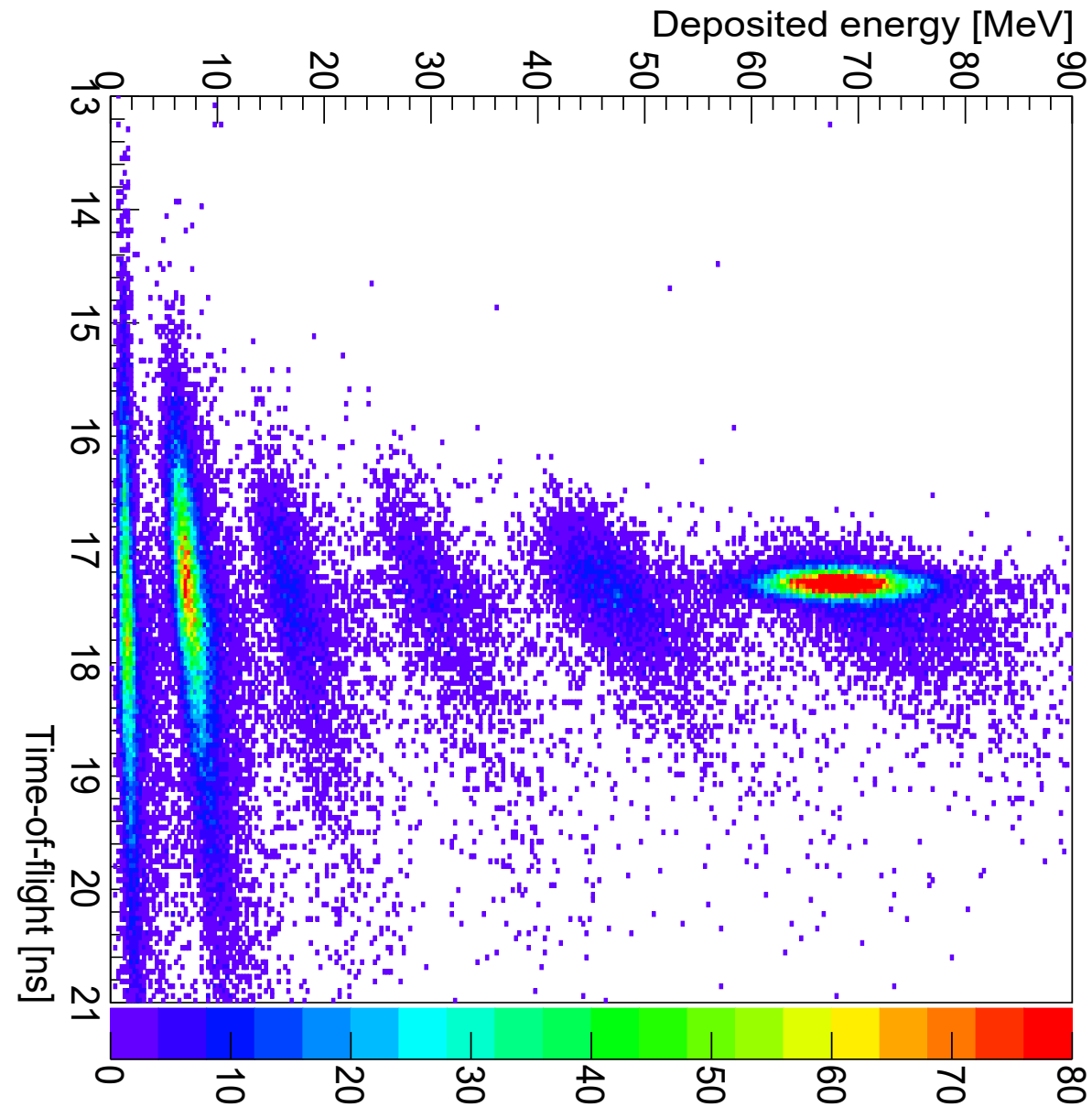


# Z identification with TOF and Delta-E

Example of charge spectrum for  
150 MeV/u **carbon ions** on  
**carbon target** at **CNAO**

- Partial setup: no magnet, no calorimeter

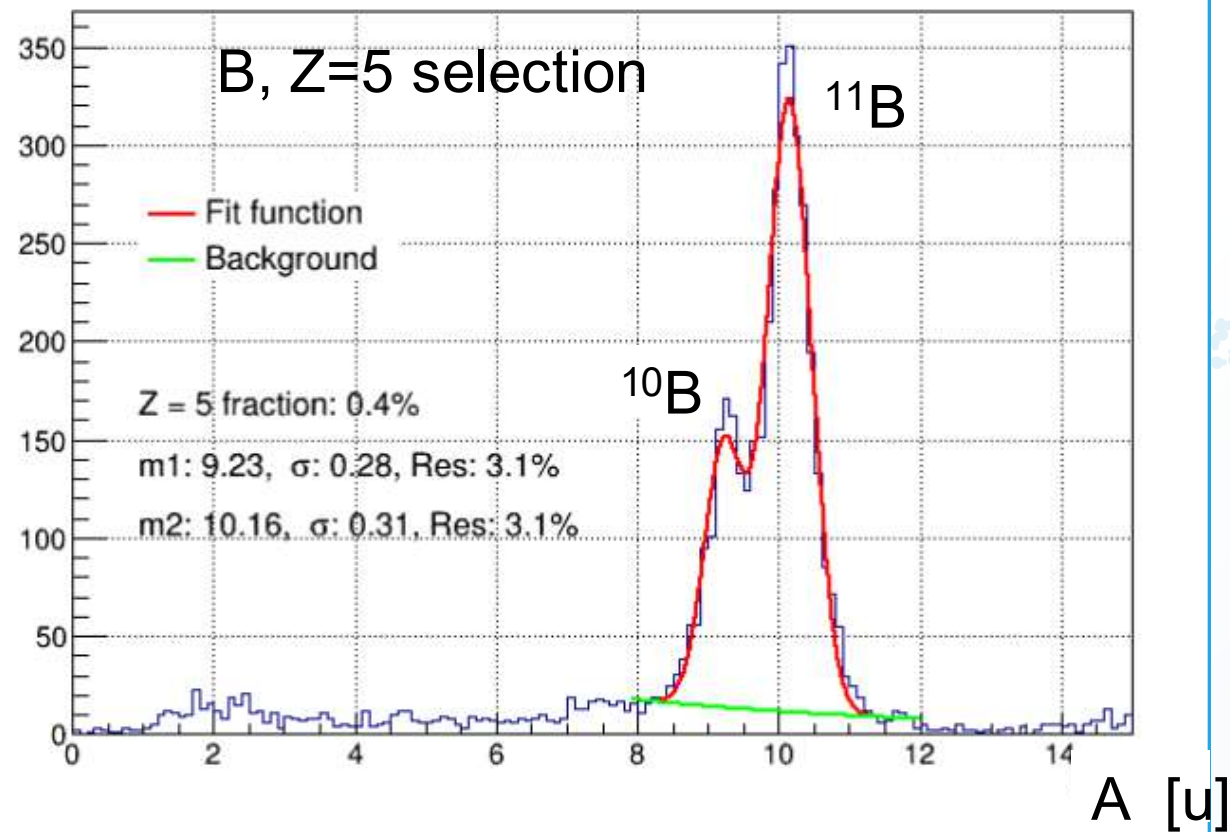
**CNAO**



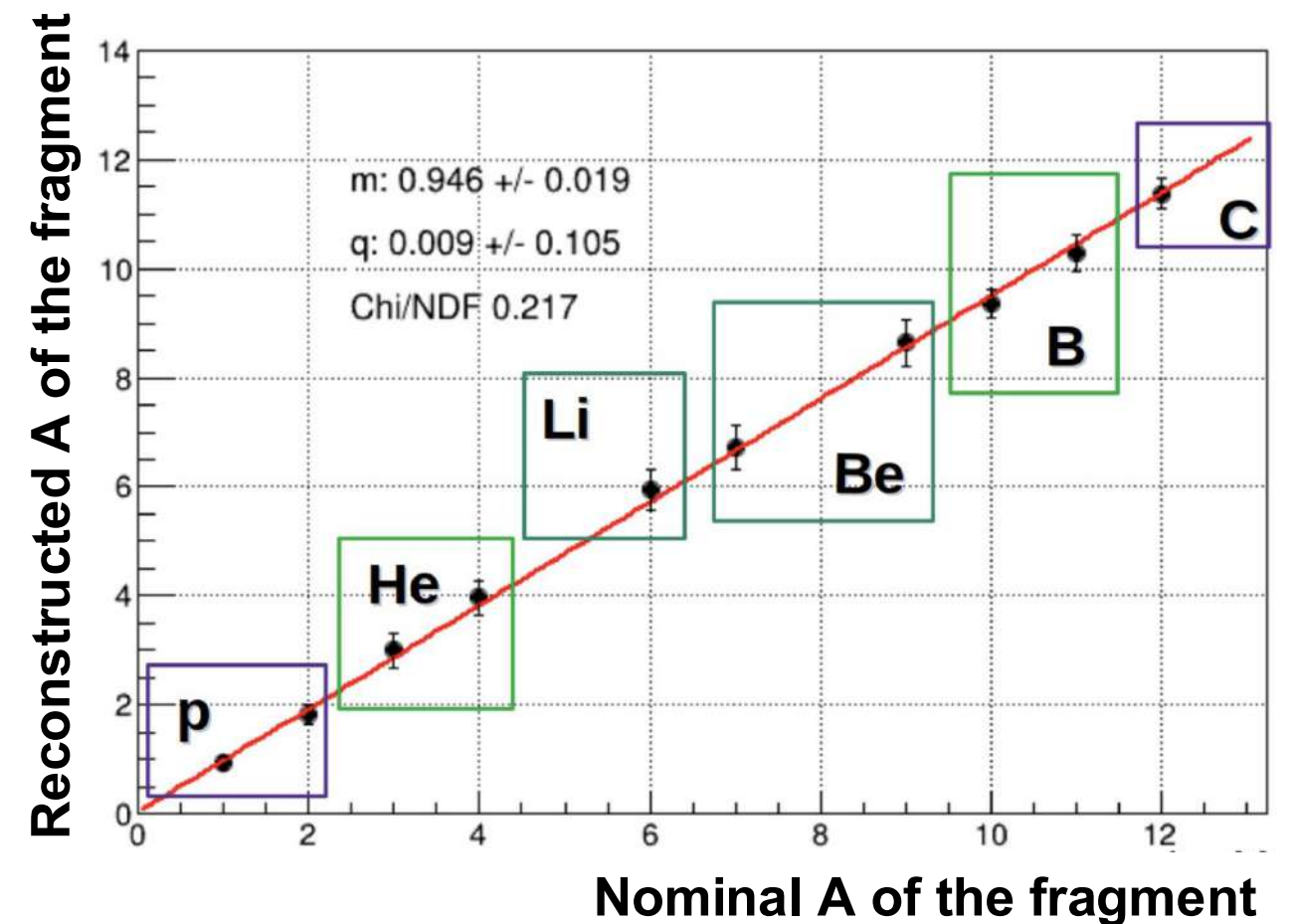
# Isotope identification with Calo & TOF

$$A = \frac{E_{kin}[MeV] \cdot u}{0.931494 MeV \cdot (\gamma - 1)}$$

Reconstructed (FLUKA MC) mass peaks from 200 MeV/u  $^{12}\text{C}$  beam on carbon target, at CNAO

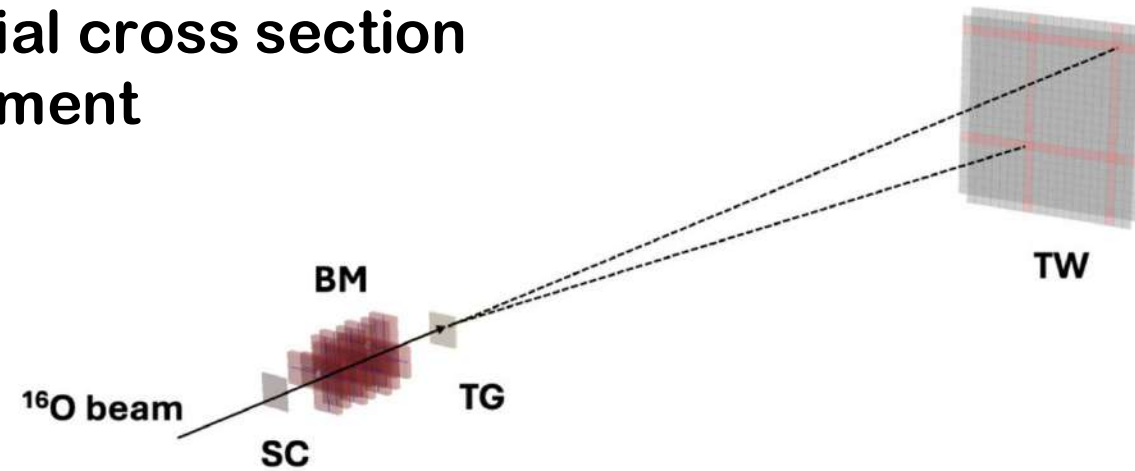


Reconstructed (FLUKA MC) mass vs nominal pass, in 200 MeV/u  $^{12}\text{C}$  beam on carbon target, at CNAO



# Cross section measurements GSI data

## Differential cross section measurement

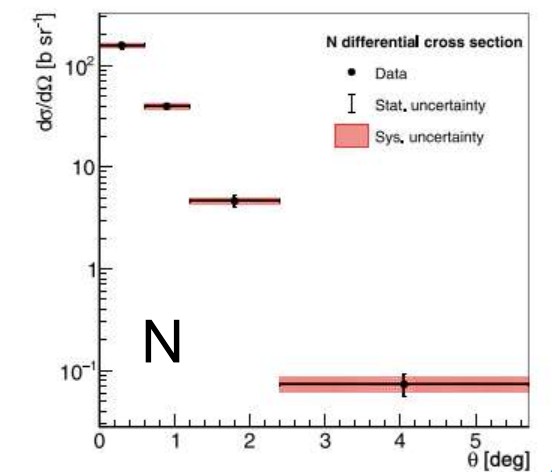
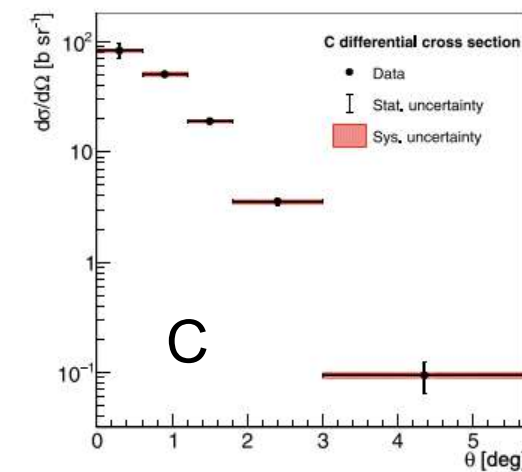
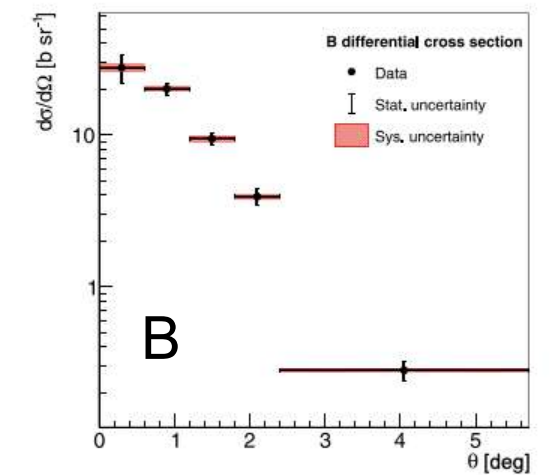
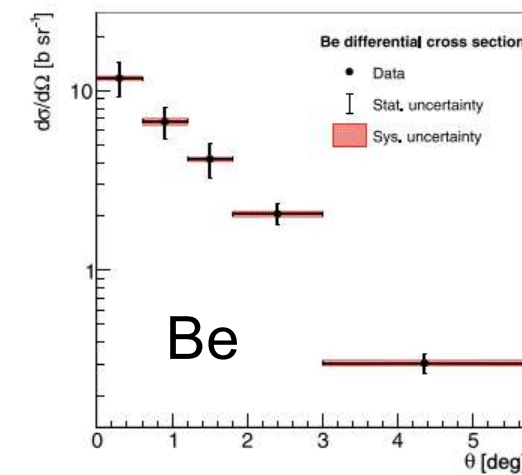
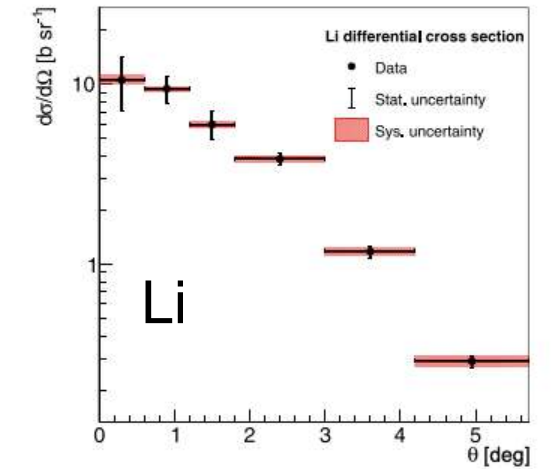
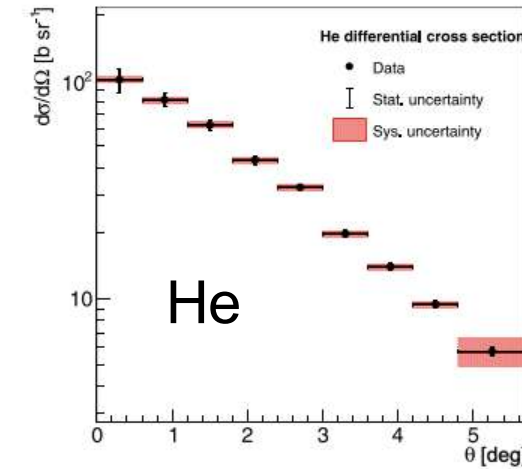


$$\frac{d\sigma}{d\Omega}(Z, \theta) = \frac{Y(Z, \theta)}{N_{\text{prim}} N_{\text{TG}} \varepsilon(Z, \theta) \Delta\Omega}$$

- $Y(Z, \theta)$  = selected number of fragments of a **given charge  $Z$**  measured by TW at a given angle  $\theta$
- $N_{\text{prim}}$  = selected number of primaries impinging on the target
- $\varepsilon(Z, \theta)$  = efficiency for a given charge in a given angle
- $\Delta\Omega$  = solid angle bin width
- $N_{\text{TG}}$  = number of interaction centers in the target per unit surface  

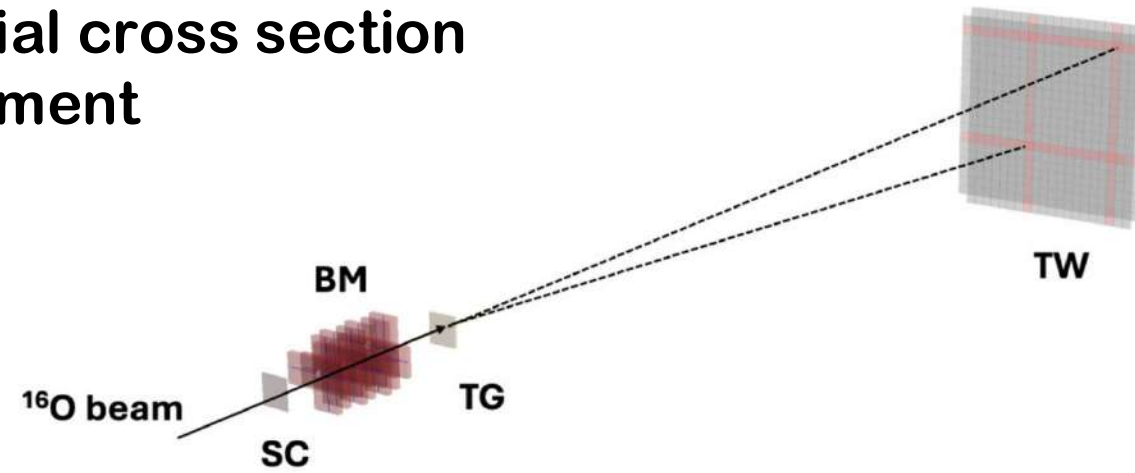
$$N_{\text{TG}} = \frac{\rho d N_A}{A}$$

Ridolfi et al., Phys Rev C 112, 014610 (2025)



# Cross section measurements GSI data

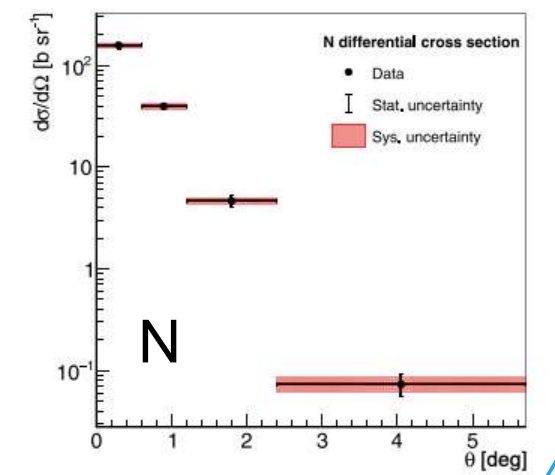
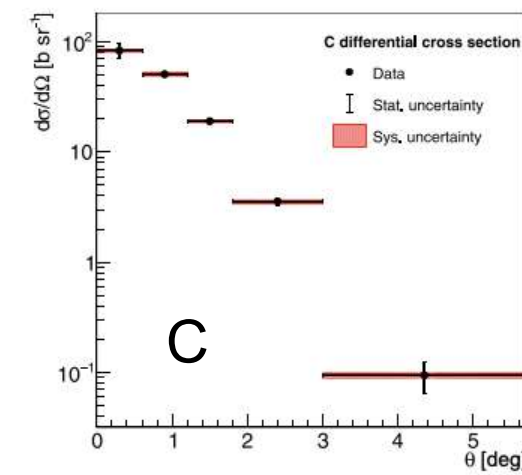
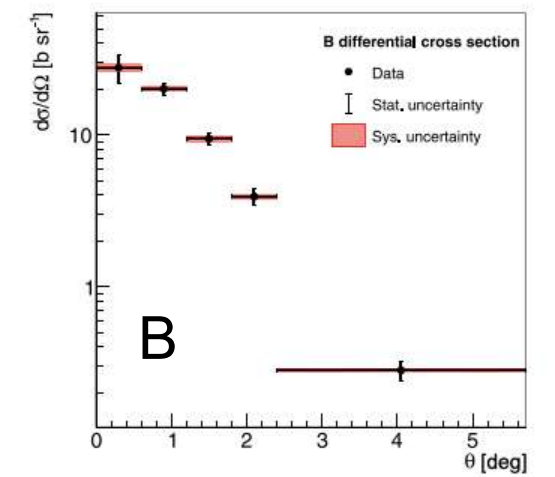
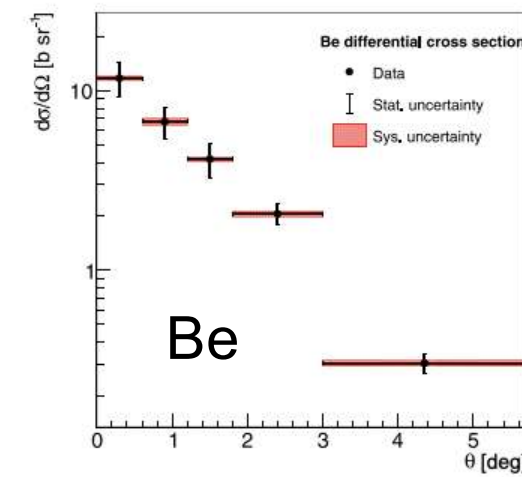
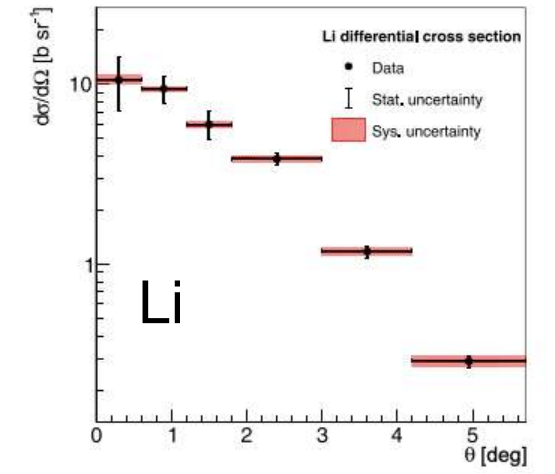
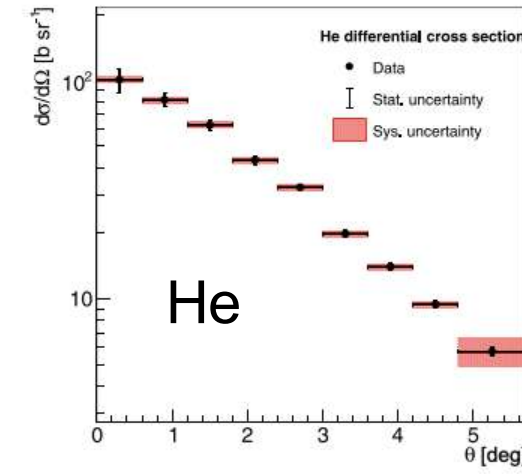
## Differential cross section measurement



Differential cross section for various charge fragments extracted:

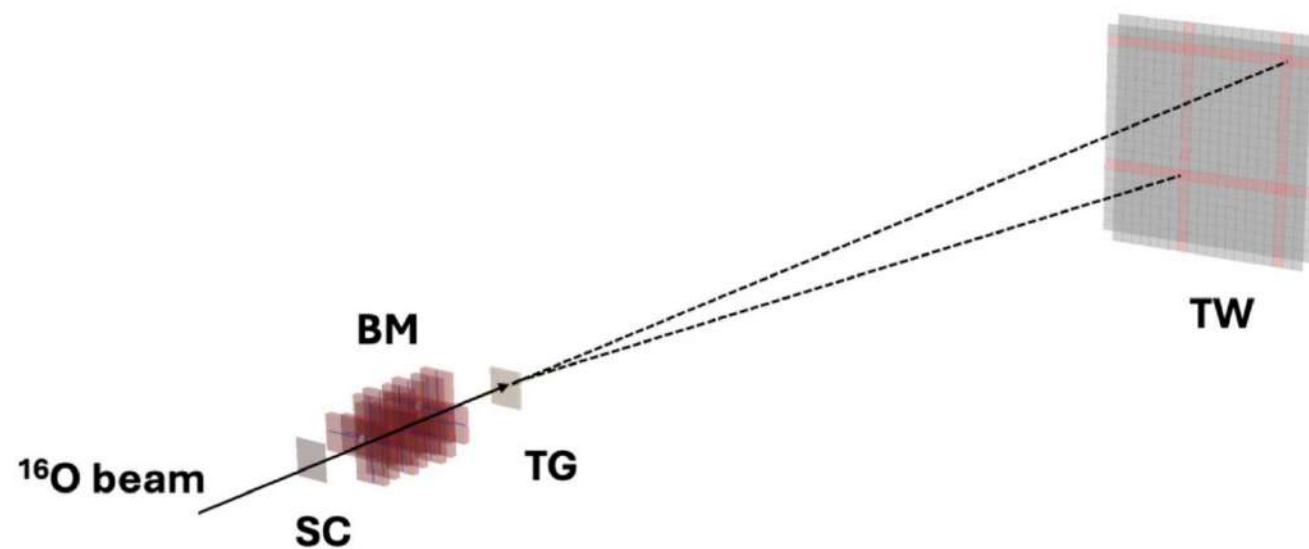
- Measurements up to 5.7 degrees
- Values from about 0.1 up to  $10^2$  b sr<sup>-1</sup>

Ridolfi et al., Phys Rev C 112, 014610 (2025)



# Cross section measurements GSI data

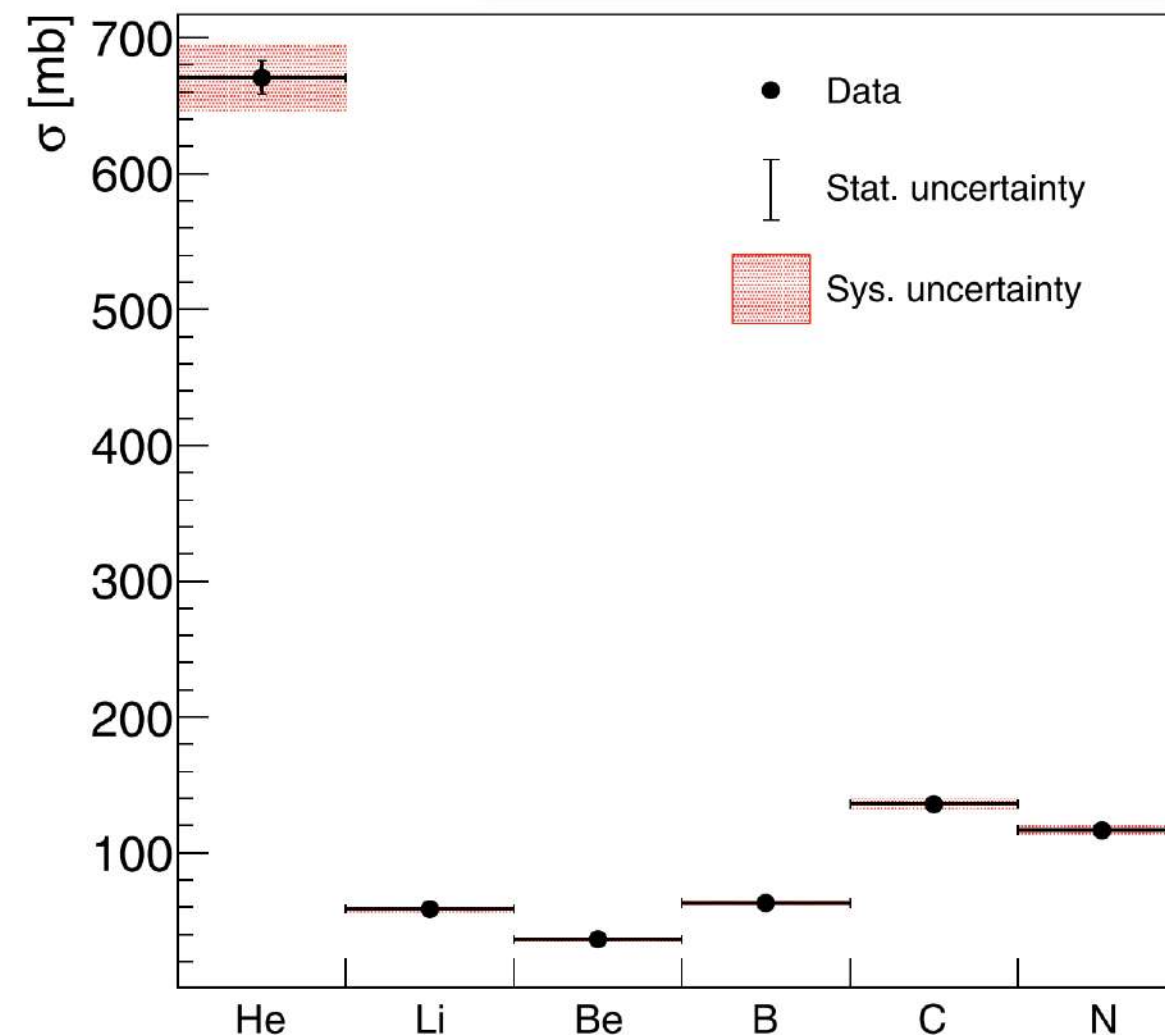
Ridolfi, Phys Rev C 112, 014610 (2025)



## Total cross section measurement 400 MeV/nucleon $^{16}\text{O}$ beam on graphite target

Element	$\sigma \pm \Delta_{\text{stat}} \pm \Delta_{\text{sys}}$ (mb)	$\Delta_{\text{stat}}/\sigma$	$\Delta_{\text{sys}}/\sigma$
He	$671 \pm 12 \pm 25$	1.9%	3.7%
Li	$59 \pm 3 \pm 2$	5.6%	3.5%
Be	$37 \pm 3 \pm 1$	7.8%	3.0%
B	$63 \pm 4 \pm 2$	6%	3%
C	$136 \pm 6 \pm 4$	4.4%	3.1%
N	$117 \pm 6 \pm 4$	5.4%	3.0%

Ridolfi, Phys Rev C 112, 014610 (2025)



Main uncertainties from:

- Statistics
- Systematics: reconstruction, out-of-target fragmentation

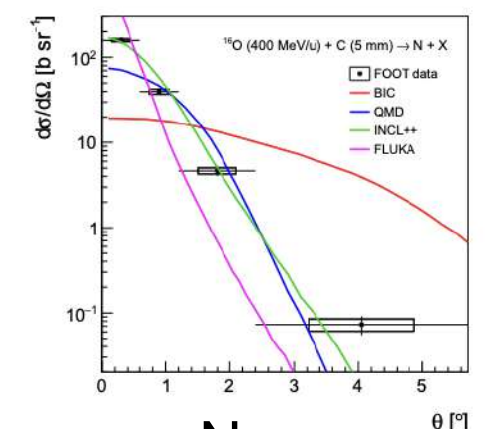
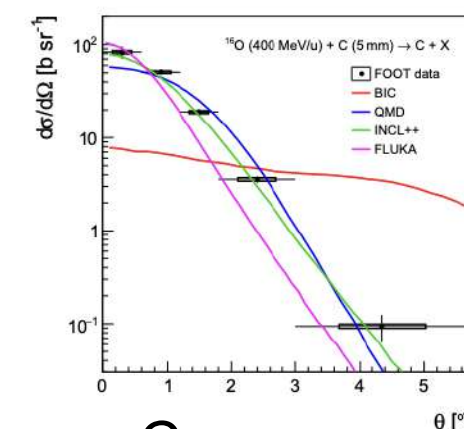
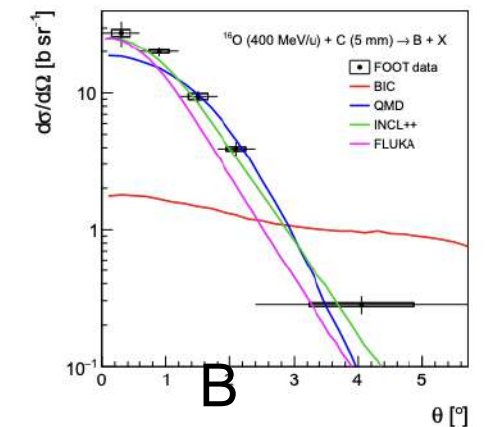
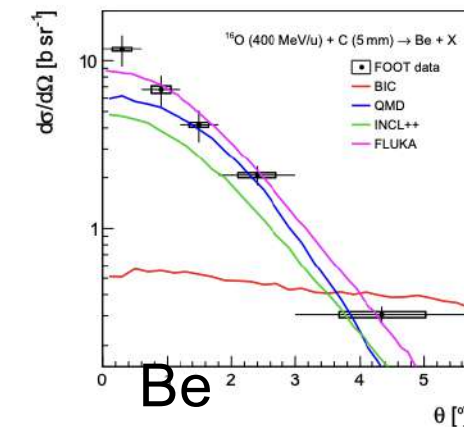
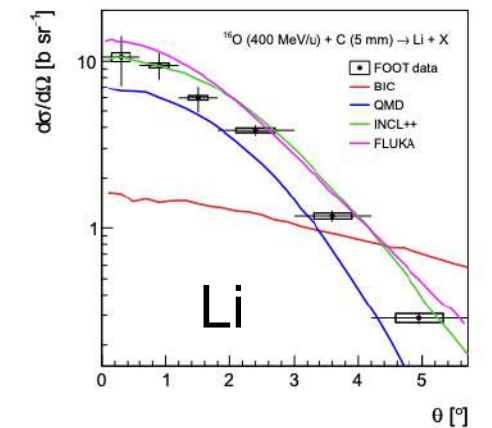
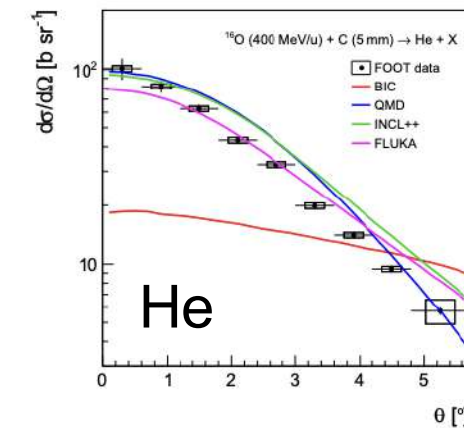
# Comparison with models

Comparison with theoretical predictions from 4 different nuclear interaction models used in MC codes:

- FLUKA MC code
  - relativistic Quantum Molecular Dynamics model: rQMD2.4. (high E, but coupled to PEANUT it's ok for FOOT)
- Geant 4 Binary Ion Cascade (BIC) model: Glauber-Gribov cross sections
- Geant 4 Quantum Molecular Dynamics (QMD): nucleon is treated as wavepacket that evolve according to QMD
- Liège Intranuclear Model (INCL<sup>++</sup>): nuclear reaction is series of dependent nucleon-nucleon collisions in target

Difference lay in:

- distinct physical models, such as different approaches to direct reactions, pre-equilibrium reactions, or compound nucleus reactions.
- Underlying Nuclear Data Libraries may differ
- Benchmarking with data differs



# Comparison with models

Comparison with theoretical predictions from 4 different nuclear interaction models used in MC codes:

- FLUKA MC code



relativistic Quantum Molecular Dynamics model: rQMD2.4. (high E, but coupled to PEANUT it's ok for FOOT)

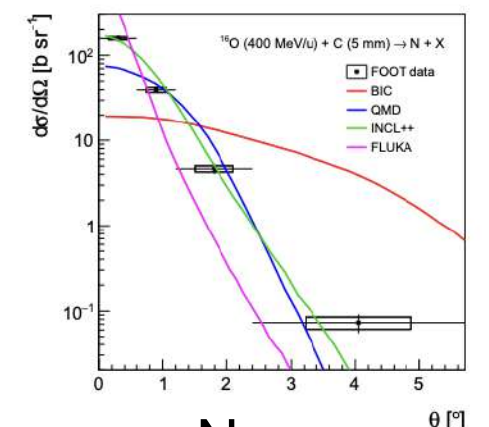
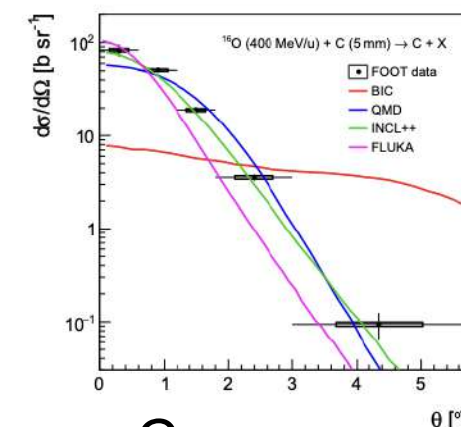
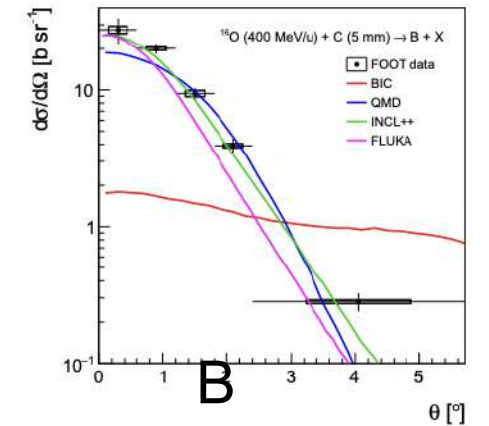
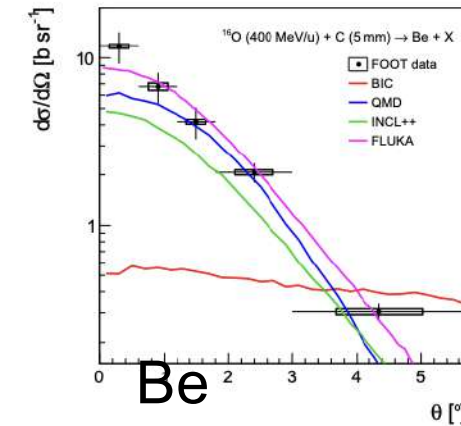
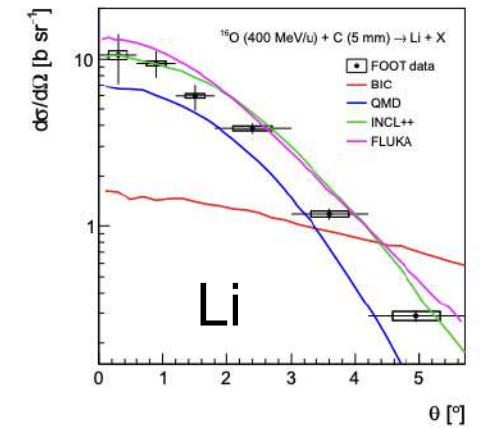
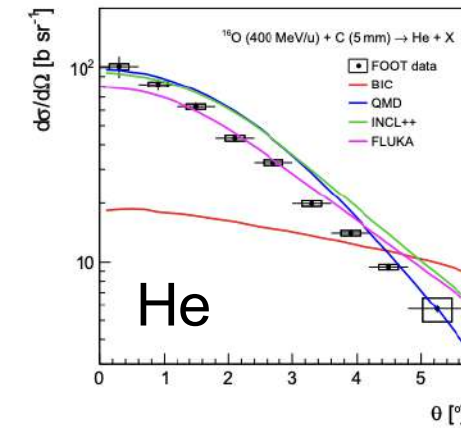
- Geant 4 Binary Ion Cascade (BIC) model: Glauber cov cross sections

- Geant 4 Quantum Molecular Dynamics (QMD): nucleon treated as wavepacket that evolve according to QMD

- Liège Intranuclear Model (INCL<sup>++</sup>): nuclear reaction is series of dependent nucleon-nucleon collisions

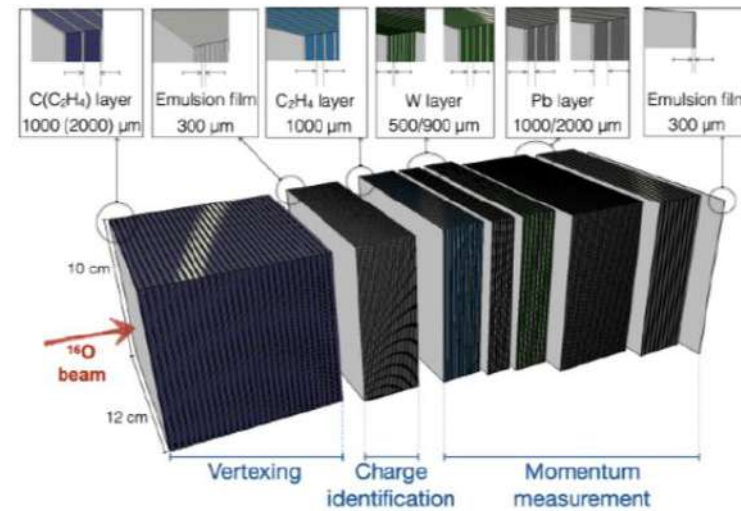
Difference lay in:

- distinct physical models, such as different approaches to direct reactions, pre-equilibrium reactions, or compound nucleus reactions.
- Underlying Nuclear Data Libraries may differ
- Benchmarking with data differs

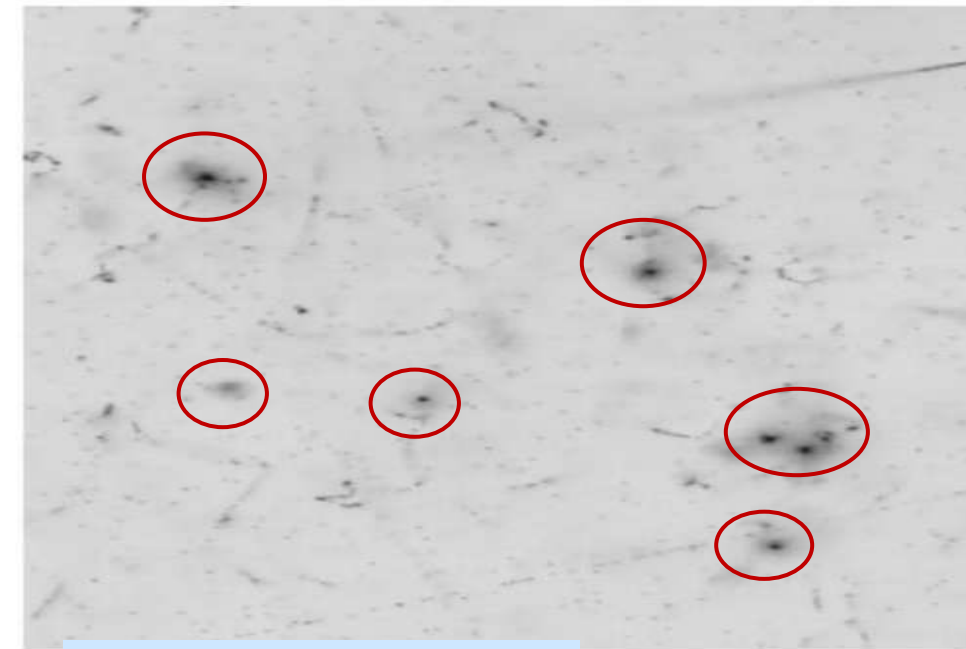


# Emulsion spectrometer

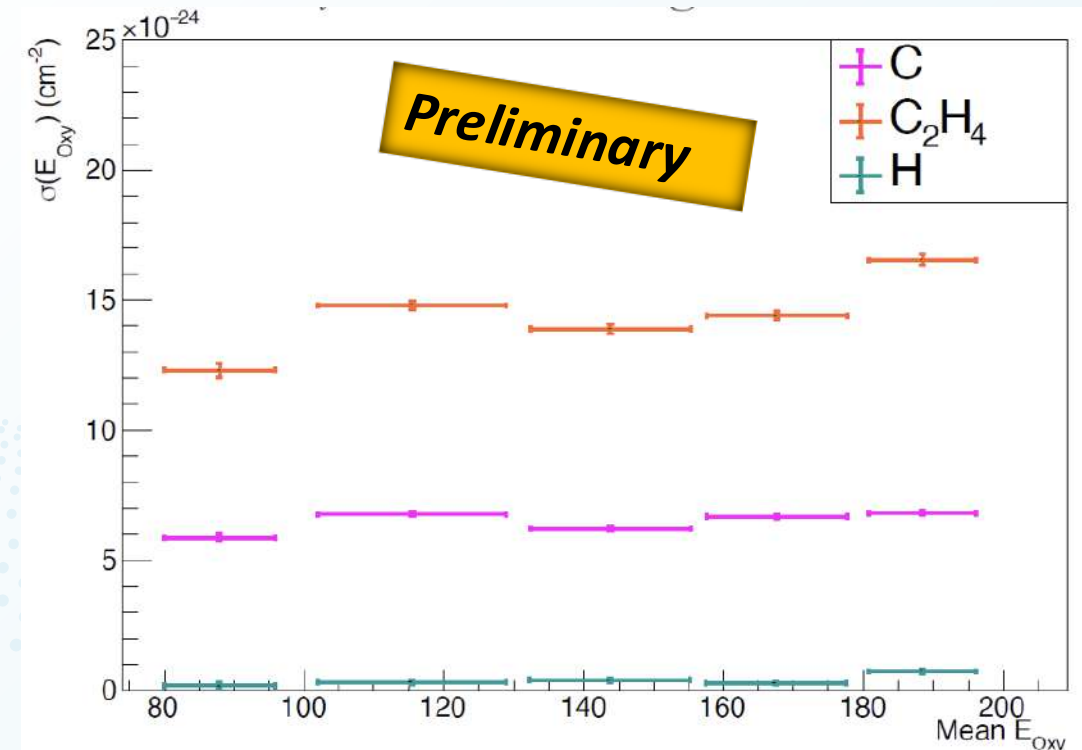
- 200 MeV/u  $^{16}\text{O}$  beam delivered on a carbon or polyethylene target embedded between the emulsion films



- Fragments pass through the detector, leaving a track in the emulsion sensitive gelatine
- After a development process and a thermal treatment, a dedicated analysis allows to reconstruct the tracks and charge of the fragments
- Integrated cross section of oxygen on carbon and polyethylene is estimated. The proton production cross section is computed by a linear combination of the two (inverse kinematic approach)



Oxygen tracks in the emulsion.



Total reaction cross sections on C, C $_2$ H $_4$ , and H as a function of energy.

# Conclusion

- The FOOT experiment has two set-ups for measuring cross sections:
  - Electronic detectors setup ( $Z \geq 2$ ), up to  $\sim 10$  degrees
  - Emulsion Cloud Chamber ( $Z \leq 3$ ), up to  $\sim 70$  degrees
- The FOOT experiment will provide a set of double differential fragmentation cross sections. More accurate modelling of fragment productions  $\rightarrow$  more accurate calculations of biological dose
  - Better treatments!
  - Improving radiation protection in space
- Initial data takings were performed with a subset of detectors
  - Focus here on Tof Wall  $\rightarrow$  resolutions, experimental tests, etc
- Fragment charge can be reconstructed with the FOOT electronic setup
  - Successfully measuring cross sections for fragments and angles with both set-ups
  - Benchmarking with main fragmentation nuclear models
- New! Fragment masses have been reconstructed using Tof-Wall and Start Counter
- More results to come in next years



# FOOT January 2026



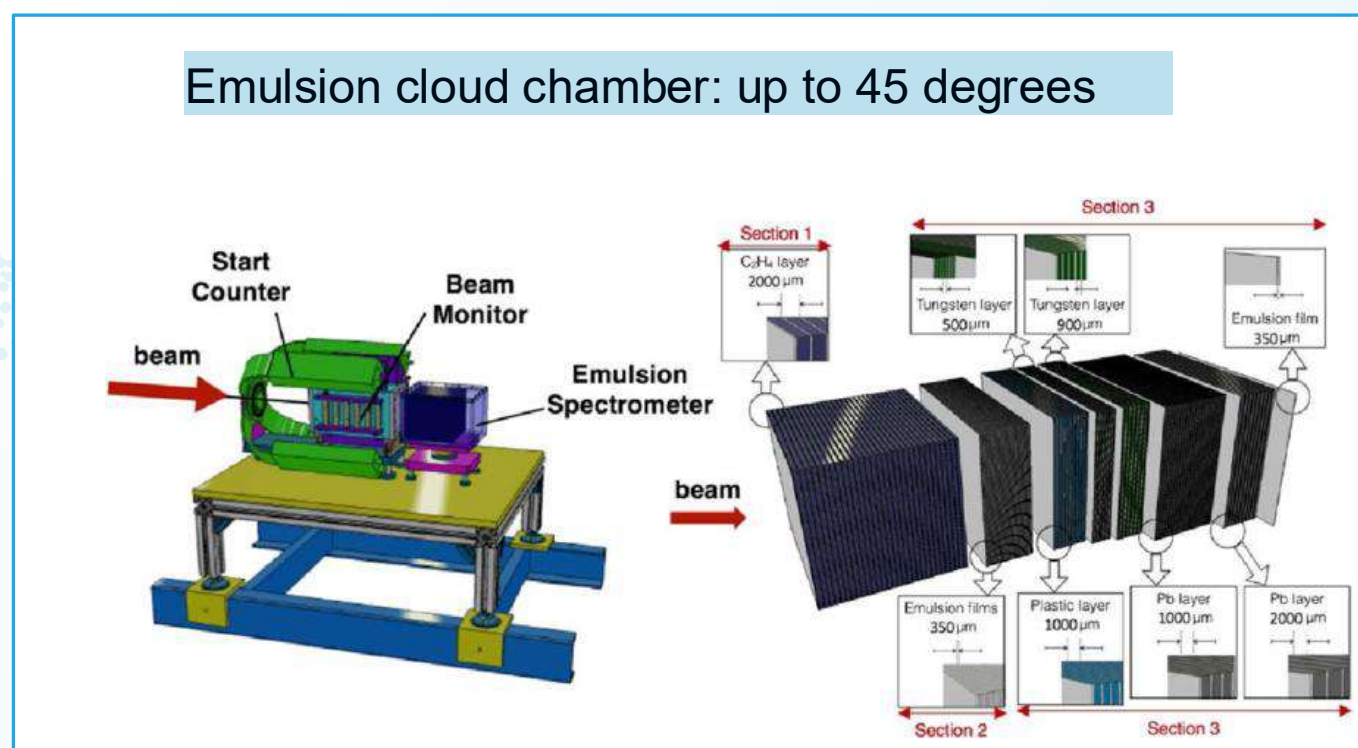
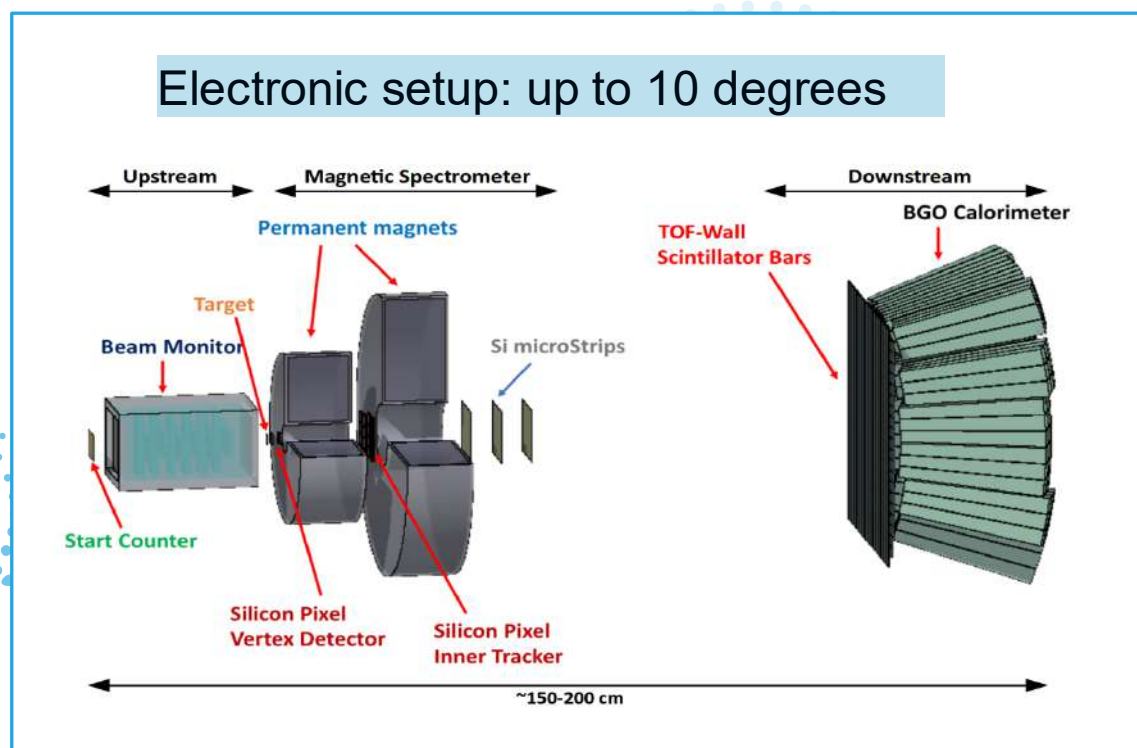
Many thanks to Tomasz Matulewicz for the invitation!

A decorative graphic consisting of multiple parallel, wavy lines of small blue dots. The dots are arranged in a pattern that resembles a sine wave or a series of overlapping curves, creating a sense of movement and depth. The background is a solid, medium blue color.

# FOOT (FragmentatiOn Of target) detector



- Measure for each fragment: Mass A, Charge Z, Polar angle  $\theta$ , Kinetic energy E
- Usable in different accelerator facilities: portable design.
- Light projectile and target nuclei at 200-800 MeV/u (protons, helium, carbon, oxygen)
- Characterize primaries and fragments
- Target: Graphite, Polyethylene (thin, typically 5 mm)
- Measurements both in direct and inverse kinematics
- Two complementary setups: Electronic detectors setup ( $Z \geq 2$ ) and Emulsion Cloud Chamber ( $Z \leq 3$ )

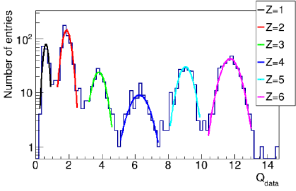


# TOF-Wall energy calibration (interesting physics)

- Non-linear relationship between energy deposit and detected charge in a bar (**quenching**)
- Not a perfect fit with Birks'

$$\frac{dL}{dx} = \frac{S \frac{dE}{dx}}{1 + kB \frac{dE}{dx}}$$

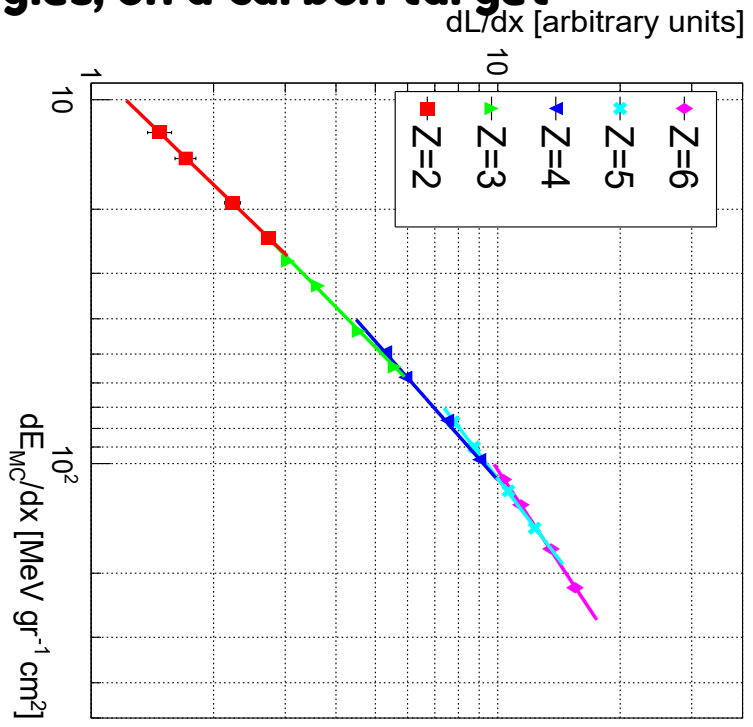
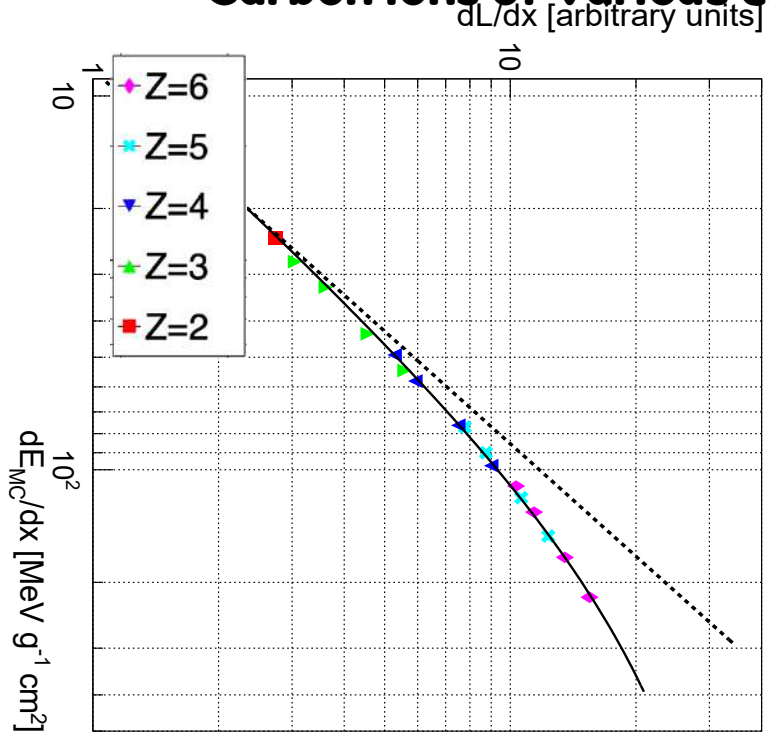
- **What happens if we look at the whole spectrum produced in target fragmentation?**



- **XX MeV** Carbon ions on carbon target
- 4 energies, 5 Z values → 20 points
- Fit with 5 different curves (similar to Matsufuji et al, NIMA437, 1999)

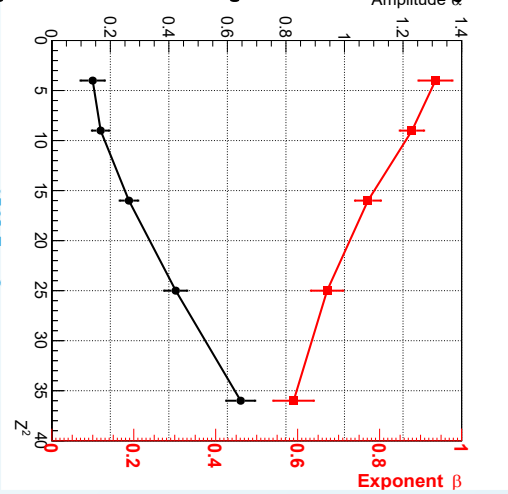
$$\frac{dL}{dx} = \alpha \left( \frac{dE}{dx} \right)^\beta$$

Carbon ions of various energies, on a carbon target



- Amplitude  $\alpha$ : increases for larger Z,
- Exponent  $\beta$ : decreases for larger Z, because of more significant quenching in core for high Z particles (?)

Species dependency:



See Kraan, et al, NIMA 1045, 2023, 167615

# Z identification: resolutions

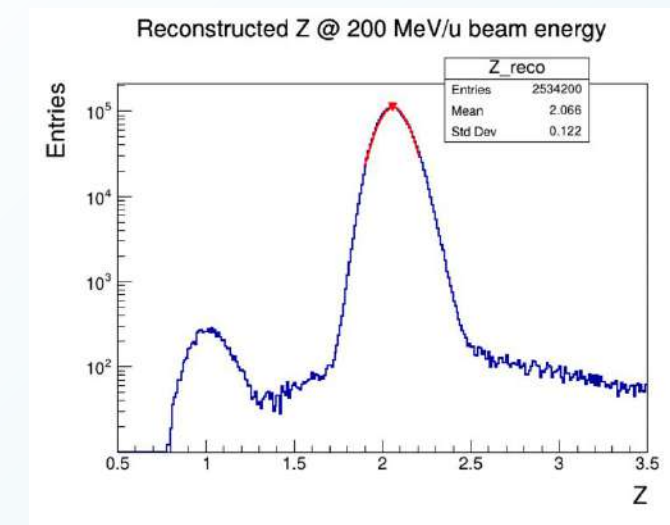
**Resolutions** determined  
**without target**

## Helium Different particles at different data takings):

- TOF resolution: 116 ps (at 100 MeV/u) to 157 ps (220 MeV/u)
- Energy resolution: 5% (at 100 MeV/u) to 8% (at 220 MeV/u)
- Z identification resolution from 2.7% to 4.5%.

Z resolution compared with previous data takings (settings not identical)

Facility	Particle	Beam energy [MeV/u]	$\mu(Z)$	$\sigma(Z)$	$R_Z[\%]$
CNAO	p	60	0.96	0.06	6.10
HIT	He	100	2.03	0.06	2.72
HIT	He	140	2.04	0.07	3.44
HIT	He	200	2.06	0.09	4.36
HIT	He	220	2.05	0.09	4.51
CNAO	$^{12}\text{C}$	115	6.17	0.15	2.51
CNAO	$^{12}\text{C}$	260	6.01	0.21	3.52
CNAO	$^{12}\text{C}$	400	6.07	0.24	3.85
GSI	$^{16}\text{O}$	400	8.07	0.22	2.67



# Mass reconstruction

Charge of the fragment reconstructed using the Bethe-Bloch equation:

$$\left\langle \frac{dE}{dx} \right\rangle_{coll} = K \frac{\rho_t Z_t Z^2}{A_t \beta^2} \left[ \frac{1}{2} \log \left( \frac{2m_e c^2 \beta^2 \gamma^2 W_{max}}{I_t^2} \right) - \beta^2 - \frac{\delta}{2} - \frac{C}{Z} \right]$$

*dE/dx* from **TOF-WALL** or **MICROSTRIP**

**TOF**

Three different methods to reconstruct the mass of the fragments:

$$A_1 = \frac{p}{U\beta\gamma}$$

**TOF+dE/dx** and **TRACKER**

$$A_2 = \frac{E_{kin}}{U(\gamma - 1)}$$

**TOF +dE/dx** and **CALORIMETER**

$$A_3 = \frac{p^2 - E_{kin}^2}{2E_{kin}}$$

**TRACKER** and **CALORIMETER**